Andreia Sofia Ferreira Saruga

Bachelor in Biotechnology

Cyto- and Genotoxicity Assessment of Manufactured Nanomaterials in the A549 Cell Line

A thesis submitted in conformity with the requirements for the degree Master in Biotechnology

Supervisor: Doutora Maria João Silva, Departamento de Genética Humana do Instituto Nacional de Saúde Doutor Ricardo Jorge, I.P.

Co-supervisor: Doutora Maria Henriqueta Louro, Departamento de Genética Humana do Instituto Nacional de Saúde Doutor Ricardo Jorge, I.P.

Jury:

President: Professor Doutor Pedro Miguel Calado Simões

Examiner: Professor Doutor António Sebastião Rodrigues

FACULDADE DE CIÊNCIAS E TECNOLOGIA
UNIVERSIDADE NOVA DE LISBOA

September, 2016

Andreia Sofia Ferreira Saruga

Bachelor in Biotechnology

Cyto- and Genotoxicity Assessment of Manufactured Nanomaterials in the A549 Cell Line

A thesis submitted in conformity with the requirements for the degree Master in Biotechnology

FACULDADE DE CIÊNCIAS E TECNOLOGIA
UNIVERSIDADE NOVA DE LISBOA

September, 2016

Cyto- and Genotoxicity Assessment of Manufactured Nanomaterials in A549 the Cell Line

ACKNOWLEDGMENTS

First of all, I must thank my family, especially my parents, because without them, without their support this journey could not be possible to realize.

I want to thank my supervisors, Drª Maria João Silva for had accepted me in their research group, for all the scientific knowledge transmitted and for revision of this thesis; Drª Henriqueta Louro, for all the help in the lab work, during the processing of the results, statistics analysis and also in the revision of this work. To Professor Pedro Baptista from FCT/UNL for always being available when I contacted him.

I want to show my gratitude to all my friends and everyone who somehow had contributed and helped me during the realization of this work. My friend Joana Torrejais who always tried to support me in the lab even when she was busy and working too.

ABSTRACT

A number of nanomaterials (NMs) have been applied in different fields due to their unique physico-chemical properties. As the use and applications have increased in some industries, serious concerns about their potential impact on the environment and the human health have been raised and have been a challenge for the regulatory authorities.

This work aimed at assessing the toxicity of three classes of NMs, namely cerium dioxide, CeO_2 (NM-212), titanium dioxide, TiO_2 (NM-101 and NM-100) and barium sulphate, $BaSO_4$ (NM-220) since they already have a broad range of applications in industry and consumer products.

A standardized protocol for NMs dispersion was followed and the quality of the dispersion in the culture medium was evaluated by the dynamic light scattering technique. Different concentrations (0, 1, 3, 10, 30, 75 and 100 µg/cm^2) of each nanomaterial were used to expose A549 cells (human lung carcinoma cells) for cytotoxic evaluation through the MTT and clonogenic assays and genotoxicity assessment through the comet and the cytokinesis-blocked micronucleus (CBMN) assays.

The results showed a decrease in cell proliferation after exposure to cerium dioxide nanomaterials for 8 days, at the highest concentrations tested and a slight increase in the level of DNA breaks. Concerning the TiO_2 NMs, a statistically significant increase in the level of DNA breaks was found for both NMs; however the CBMN assay did not show any increase in the frequency of chromosomal breaks. $BaSO_4$ was the NM that showed the lowest toxicity in cyto- and genotoxicity assays.

Even though the present results contribute to assess the hazard of the tested NMs, the real effects of nanomaterials' exposure to human health are still unclear and an unequivocal conclusion is difficult to present, given the inconsistent and often conflicting results found in the literature. Thus, the application of some nanomaterials in consumer products should be carefully evaluated until definite conclusions about their safety are available.

Keywords: nanomaterials, cytotoxicity, genotoxicity, NMs dispersion, A549 cells

RESUMO

Diferentes nanomateriais têm sido aplicados em diferentes áreas, devido às suas propriedades físico-químicas únicas. Como o uso e as aplicações têm aumentado em algumas indústrias, os possíveis impactos no ambiente e na saúde humana têm sido questionadas e tem-se revelado um desafio as autoridades reguladoras.

Este trabalho tem como objectivo avaliar a toxicidade de três classes de NMs, nomeadamente, dióxido de cério, CeO_2 (NM-212), dióxido de titânio, TiO_2 (NM-101 e NM-100) e sulfato de bário, $BaSO_4$ (NM-220), visto que estes já possuem uma vasta aplicação na indústria e em produtos de consumo.

Foi seguido um protocolo padronizado para a dispersão dos nanomateriais e qualidade da dispersão no meio de cultura foi avaliada através da técnica de *dynamic light scattering*. Foram utilizadas diferentes concentrações (0, 1, 3, 10, 30, 75 e 100 µg/ cm^2) de cada nanomaterial, para expor a cultura de células A549 (células de carcinoma de pulmão humano) para avaliação da citotoxicidade através dos ensaios do MTT e clonogénico e dos ensaios do cometa e dos micronúcleos para o estudo da genotoxicidade.

Os resultados mostraram uma diminuição na proliferação de células após exposição aos nanomateriais de dióxido de cério, durante 8 dias, nas concentrações mais elevadas e um aumento ligeiro nas quebras do DNA. No que diz respeito ao TiO_2 verificou-se um aumento estatisticamente significativo no nível de quebras de DNA para ambos os NMs, no entanto o ensaio dos micronúcleos não apresentou nenhum aumento na frequência de quebras cromossómicas. O $BaSO_4$ foi o nanomaterial que apresentou menor toxicidade tanto nos ensaios de citotoxicicdade como genotoxicidade.

Apesar dos presentes resultados contribuírem para a avaliação do perigo dos NMs testados, os verdadeiros efeitos da sua exposição para a saúde humana ainda não são claros e é difícil apresentar uma conclusão inequívoca, dada a inconsistência dos resultados apresentados na literatura. Assim, a aplicação de alguns nanomateriais em produtos de consumo deve ser avaliada cuidadosamente até que estejam estabelecidas conclusões relativamente à sua segurança.

Palavras-chave: nanomateriais, citotoxicidade, genotoxicidade, dispersão de nanomateriais, células A549.

LIST OF CONTENTS

LIST OF FIGURES

LIST OF TABLES

ABBREVIATIONS

A549	Human epithelial lung adenocarcinoma cell line
ATCC	American Type culture Collection
$BaSO_4$	Barium Sulphate
BAuA	Federal Institute for Occupational Safety and Health
BET	Brunauer-Emmett-Teller
BSA	Bovine Serum Albumin
CBPI	Cytokinesis-Blocked Proliferation Index
CeO_2	Cerium Dioxide
DLS	Dynamic Light Scattering
DMEM	Dulbecco's Modified Eagle Medium
DMSO	Dimethyl Sulfoxide
DNA	Desoxyribonucleic Acid
EDTA	Ethylenediamine Tetraacetic Acid
EMS	Ethyl Methanesulfonate
FBS	Fetal Bovine Serum
FDA	Food and Drug Administration
FPG	Formamidopyrimidine DNA Glycosylase
HEPES	4-(2-hydroxyethyl)-1-piperazineethanesulfonic Acid
LDH	Lactate Dehydrogenase
MMC	Mitomycin C
MNBNC	Micronucleated Binucleated Cell
MTT	3-(4,5-dimethylthiazol-2-yl)-2,5-diphenyltetrazolium bromide
NM(s)	Nanomaterial(s)
NIOSH	National Institute for Occupational Safety and Health
OECD	Organization for Economic Co-operation and Development
PBS	Phosphate Buffered Saline
PdI	Polydispersity Index
ROS	Reactive oxygen species

RI	Replication Index
SD	Standard Deviation
SDS	Sodium Dodecyl Sulfate
TEM	Transmission electron microscopy
TiO_2	Titanium dioxide

1. INTRODUCTION

Nanotechnology involves the manipulation and application of engineered particles or systems that have at least one dimension under 100 nanometers (nm) in length (Stone et al. 2009; Arora et al. 2012; Ferreira et al. 2013).

Nano-object is defined as a material with one, two, or three external dimensions in the size range from approximately 1–100 nm. There are subcategories of nano-object such as nanoparticle (NP), defined as a nano-object with all three external dimensions at the nanoscale. Nano-objects are commonly incorporated in a larger matrix or substrate referred to as a nanomaterial (NM). The term manufactured nanomaterial describes nanoparticles (NPs) intentionally produced and designed with very specific properties or compositions (e.g., shape, size, surface properties, and chemistry) (NIOSH 2009). In 2011, the European Commission adopted the definition of nanomaterial (NM) as “a natural, incidental or manufactured material containing particles, in an unbound state or as an aggregate or as an agglomerate and where, for 50 % or more of the particles in the number size distribution, one or more external dimensions is in the size range 1 - 100 nm”. (http://ec.europa.eu/environment/chemicals/nanotech/faq/definition_en.htm; Consulted on 22/7/2015)

Some authors do not distinguish the term nanoparticle (NP) and nanomaterial (NM) in their works, using it indistinguishably and assuming the same definition. Hence, in this work these two terms will be assumed as being the same to facilitate the comprehension.

According to several authors, unique and unusual physical, chemical, and biological properties can be seen at the nanosize level. While the properties of bulk materials at the molecular level are largely understood there are new properties of materials being discovered in the zone between molecule and bulk. When bulk materials are made into smaller and smaller pieces of matter their surface chemistry changes and chemical reactivity increases or, in other words, there are a higher number of molecules available to react with the environment. Also, at the nanoscale, quantum physics can direct the behaviour of a particle; the influence of quantum effects can change important material properties, such as optical, magnetic, and electrical properties (Ferreira et al. 2013; Arora et al. 2012; Elsaesser & Howard 2012; Azqueta & Dusinska 2015).

These materials are increasingly being used in industry and consumer products such as fillers, opacifiers, catalysts, water filtration, semiconductors, microelectronics, cosmetics, or even in biomedical applications, leading to direct and indirect exposure of humans (Arora, Rajwade, and Paknikar 2012). Hence, the very same properties that lead to the technical advantages of using nanomaterials also may lead to unique biological effects. High reactivity potentially could be related to toxicity due to harmful interactions of nanomaterials with biological systems and the environment (Arora, Rajwade, and Paknikar 2012). Nanoparticles toxicity is extremely complex and multifactorial and depends on a multiplicity of physicochemical properties such as size, shape, surface properties, chemical composition, charge, surface structure and area, solubility and aggregation. Ultrafine or nanosize range (<100 nm) particles seem to be more toxic compared to larger particles of identical chemical composition (Ferreira,

Cemlyn-Jones, and Robalo Cordeiro 2013). Thus, concerns have been raised about their safety profiles. One particular area of concern is that of airborne nanomaterials and the potential harms that may result in the respiratory tract (Ferreira et al. 2013; Frieke Kuper et al. 2015).

1.1 Nanotoxicology

Nanotoxicology was proposed as a new branch of toxicology to address the gaps in knowledge about nanomaterials' toxic effects to human health and the environment towards the development of a sustainable and safe nanotechnology (Arora et al. 2012; Ferreira et al. 2013). In this sense, nanotoxicology encompasses the physicochemical properties, routes of exposure, biodistribution, molecular determinants, genotoxicity, and addresses also regulatory aspects. In addition, nanotoxicology is involved in proposing reliable, robust, and data-assured test protocols for nanomaterials in human and environmental risk assessment (Ferreira, Cemlyn-Jones, and Robalo Cordeiro 2013).

Toxicological assessment of manmade NMs requires information about the route of exposure (inhalation, oral or dermal). The most common scenarios for human exposure to NMs are occupational, environmental and the consumer ones and one of the most important routes of human exposure to airborne NPs is inhalation, both at the workplace and from the environment (Ferreira, Cemlyn-Jones, and Robalo Cordeiro 2013). When inhaled, particles reach the alveolar epithelial surface where they can interact with alveolar macrophages and epithelial cells (Herzog et al. 2007). The deposition mainly takes place in the alveolar region (Arora, Rajwade, and Paknikar 2012). After translocation across the lung epithelium, NMs can enter the blood and lymph circulation to reach cells in the bone marrow, lymph nodes, spleen and heart, among other organs (Arora, Rajwade, and Paknikar 2012).

Warheit (2008) has put a question "how meaningful are the results of nanotoxicity studies in the absence of adequate material characterization?" This suggests that it is extremely important to characterize the nanomaterials during the study in the culture medium where the cells are seeded. Recent research has demonstrated that NMs polydispersity and agglomeration stability can have profound impacts on NMs' toxicity in *in vitro* tests. Harmonized methods for *in vitro* nanotoxicity assessments must therefore include NMs dispersion preparation and characterization protocols that ensure fairly monodispersed and stabilized NM suspensions suitable for *in vitro* cellular studies (Cohen et al. 2013). In chapter 1.4.1- Nanomaterials' dynamic behavior and dispersion in aqueous medium- this subject will be discussed in more detail.

1.1.1. Cytotoxic effects of nanomaterials

Most of the NPs are expected to be biopersistent in biological settings, such as the respiratory system (Ferreira et al. 2013; Herzog et al. 2007). Besides, size, shape, presence of transition metals,

aggregation and the capacity to generate reactive oxygen species (ROS) also explain the potential for lung damage (Ferreira, Cemlyn-Jones, and Robalo Cordeiro 2013).

NMs can interact with cellular and mitochondrial membranes or alter mitochondrial function, provoking the production of reactive oxygen species and inducing DNA oxidation. ROS include free radicals such as the superoxide anion (O2•−), hydroxyl radicals (.OH) and the non-radical hydrogen peroxide (H_2O_2), which are also constantly generated in cells under normal conditions, as a consequence of aerobic metabolism (Arora, Rajwade, and Paknikar 2012). ROS, due to their high chemical reactivity, can react with DNA, proteins, carbohydrates and lipids causing cell death either by apoptosis or necrosis or even inflammatory responses.

1.1.2. Genotoxic effects of nanomaterials

The genotoxicity associated to nanomaterials may be classified as primary or secondary genotoxicity. The former may result from a direct pathway when NPs reach the nucleus (via nuclear pores or during mitosis) and directly interact with DNA organized in chromatin or chromosomes (depending on the phase of cell cycle). During interphase NPs can interact or bind to the DNA molecule and can influence its replication or transcription into RNA. During mitosis NPs can interact with chromosomes, causing clastogenic or aneugenic effects. NPs might induce breaks in chromosomes or disturb the process of mitosis, either mechanically or by chemical binding to DNA bases. Indirect genotoxicity may happen through interaction with nuclear proteins (involved in replication, transcription, repair), or with the mitotic spindle or its components, leading to aneuploidy (aneugenic effect); other indirect effects include the disturbance of cell cycle checkpoint functions, induction of ROS arising from NP surface or inhibition of the cellular antioxidant defense (Stone et al. 2009; Magdolenova et al. 2014). On the other hand, secondary genotoxicity implies a pathway of genetic damage resulting from oxidative DNA attack by ROS that are generated from phagocytes (neutrophils, macrophages) activation during particle-elicited inflammation. NMs can also induce genotoxic effects by depleting the antioxidant defenses or altering the DNA repair systems. All these events may result in pre-mutagenic lesions that can lead to mutations and, possibly, to cancer and other diseases on the long-term (Azqueta & Dusinska 2015; Magdolenova et al. 2014).

Many methods have been developed to assess the genotoxicity caused by nanomaterials that will be discussed in the next chapter 1.4.4.

1.2 The NANoREG Project

The NANoREG project is the first FP7 (7th Framework Programme for Research and Technological Development) project to deliver the answers needed by regulators and legislators on Environmental Health Science (EHS) by linking them to a scientific evaluation of data and test methods.

The aims of NANoREG project are: (i) provide answers and solutions from existing data, complemented with new knowledge, (ii) provide a tool box of relevant instruments for risk assessment,

characterization, toxicity testing and exposure measurements of manufactured nanomaterials, (iii) develop, for the long term, new testing strategies adapted to innovation requirements, (iv) establish a close collaboration among authorities, industry and science leading to efficient and practically applicable risk management approaches for manufactured NMs and products containing manufactured NMs. (http://www.nanoreg.eu/; consulted on 6th August 2016)

The NANoREG project has about 70 partner institutes (Fadeel et al. 2015) and in Portugal, the NANoREG project is represented by Institute of Welding and Quality (ISQ), which is coordinating a platform called PToNANO, formed by four entities whose competencies are complementary in the field of nanotechnology. The other 3 entities are the National Institute of Health Doutor Ricardo Jorge, I.P. (INSA), the Portuguese Institute for Quality, I.P. (IPQ) and the Directorate-General of Health (DGS)(http://www.nanoreg.eu/; consulted on 6th August 2016)

The NANoREG project uses benchmark nanomaterials from the Joint Research Center (JRC) repository (Fadeel et al. 2015).

1.3 Metallic Nanomaterials

1.3.1 Cerium Dioxide (CeO_2)

Cerium (Ce) is the most abundant rare-earth metals found in the earth's crust which has been recently introduced for specialty applications (Kumari et al. 2014; Dahle et al. 2015) and is found in nature along with other lanthanide elements in the minerals alanite, bastanite, monazite, cerite and samarskite. However, CeO_2 has fluorite as the most stable crystalline phase (Prospect Global Nanomaterials Safety 2010).

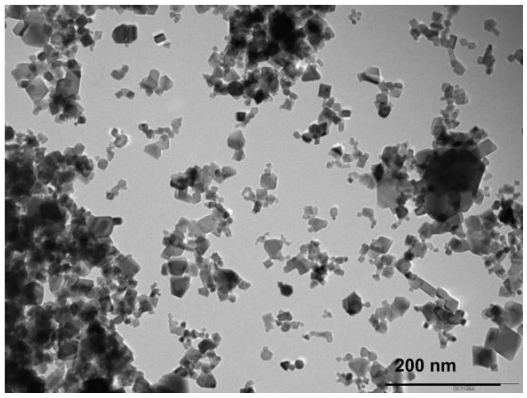

Figure 1.1- TEM image of NM-212, showing irregular and non-homogeneous primary particle size variation (C. Singh et al. 2014).

Larger particles of this material (bulk material) may induce optical lens grinding, itching, sensitivity to heat, skin lesions, pulmonary fibrosis (Rim, Koo, and Park 2013) and pneumoconiosis (Prospect Global Nanomaterials Safety 2010).

Owing to their large surface area to volume ratio, CeO_2 NPs (nanoceria, Figure 1.1) have unique electronic structure and the reduction in the particle size results in the formation of surface oxygen vacancies, which endows it with the ability to exist in either Ce^{3+} or Ce^{4+} state on the particle surface (Kumari et al. 2014).

Nanoceria play several catalytic roles such as catalysts in the petroleum refining industry, as additives to promote combustion of diesel fuels, in catalytic converters in cars enabling them to run at high temperatures, as sub-catalysts for automotive exhaust cleaning and as electrolytes in solid oxide fuel cells (Kumari et al. 2014; Dahle et al. 2015; Rim et al. 2013; Leung et al. 2015; Landsiedel et al. 2014; Keller et al. 2014). The CeO_2 NPs can also be employed as polishing agents, UV-scattering agents in non-irritating lipsticks, outdoor paint, wood care products, gas sensors, and in metallurgic and glass and ceramic applications (Kumari et al. 2014; Manier et al. 2013; Frieke Kuper et al. 2015; Van Koetsem et al. 2015). Recently, CeO_2 has been the subject of many studies regarding its use as potential material for ultraviolet (UV) filtration. In the UV radiation range reaching the Earth's atmosphere, the ultraviolet type B sub-range (UVB, 290–320 nm) is already well filtered by nanostructured TiO_2 in sunscreen cosmetic products (Truffault et al. 2010; Boutard et al. 2013).

Nanoceria, considered one of the most interesting nanomaterials for their catalytic properties, also are promising for therapeutic applications. Due to the presence of oxygen vacancy on its surface and the autoregenerative cycle of its two oxidation states, Ce^{3+} and Ce^{4+}, nanoceria can be used as an antioxidant agent. Because many human disorders are associated with oxidative stress, CeO_2 NPs might be used in future for the treatment of those pathologies (Rim et al. 2013; Leung et al. 2015). It was even proposed that nanoceria protect against hepatic oxidative damage and the progress of cardiomyopathy, which was attributed to their antioxidant properties (Leung et al. 2015). Consequently, they are considered to be of interest for biomedical applications for their antioxidant activity.

Some studies have been conducted with the aim to investigate these assumptions and try to explain why and when are these effects observed. The best explained and currently accepted mechanism to justify these results is the intrinsic material properties, including the mixed valence state of CeO_2 (Ce^{3+} and Ce^{4+}), allowing this material to act as a free radical scavenger (Xia et al. 2009; Schubert et al. 2006). Moreover, the electron defects in nano-ceria are relatively resistant to the radical damage, thereby allowing an autoregenerative reaction cycle ($Ce^{3+} \rightarrow Ce^{4+} \rightarrow Ce^{3+}$) that perpetuates the scavenging activity (Xia et al. 2009; Das et al. 2007). Hence, it was proposed that Ce^{3+} produced by the reduction of Ce^{4+} interacts with oxygen molecules (O_2), and generates superoxide anions. The two superoxide anion molecules interact and are converted to hydrogen peroxide, and then the hydrogen peroxide converts to hydroxyl radicals. The presence of the mixed valence states of Ce^{3+} and Ce^{4+} on the surface of the nanoceria acts as an anti-oxidant that allows the nanoparticles to scavenge free radicals from the culture system. Ce^{3+} reacts with hydroxyl radicals (Park et al. 2008). A review reported that nano ceria could also have superoxide dismutase, catalase and peroxidase mimetic activity besides the hydroxyl radical scavenging properties, already referred (Xu and Qu 2014).

There are other publications that report this radical scavenging of CeO_2 nanoparticles as the mechanism of neuro-protection in the spinal cord neurons of adult rats (Das et al. 2007) and the cerium NPs are neuro-protective in cultured HT22 cells, which are derived from the rodent nervous system (Schubert et al. 2006). Park et al. (2008) tried to justify their results in Beas-2B cells reporting that the particle which they prepared do not have the same arrangement and do not have the same Ce^{3+} ionic state enough to scavenge the oxygen radicals, when they addressed the antioxidant mechanism of cerium oxide nanoparticles. This may be the difference between the neuroprotection in adult rat spinal cord (referred study) and the cytotoxicity in Beas-2B cells obtained by the authors (Park et al. 2008). In fact there are already available some studies that report the effect of the size in the relative amount of cerium ions Ce^{3+} and Ce^{4+} saying that, in general, the fraction of Ce^{3+} ions in the particles increases with decreasing particle size (Xu & Qu 2014; Schubert et al. 2006). Besides the *in vitro* studies presented above, it was also related that nanoceria remains deposited in tissues and may decrease ROS in mice, thereby suggesting again that cerium oxide nanoparticles may be a useful anti-oxidant treatment for oxidative stress (Hirst et al. 2009).

However, biomedical and toxicity studies of nanoceria, which focused predominantly on their redox properties, have resulted in contradictory conclusions about their effects. While some authors documented that nanoceria may act as antioxidants and protect cells against oxidative damage and ionizing radiation, and improve cardiac function, others reports found them to be cytotoxic and to induce oxidative stress (Lee et al. 2012; Rim et al. 2013).

Because of the rapidly growing demand of cerium in nanotechnology, the release of this NM is expected to increase in the environment. The majority of Ce NPs residues are likely to be discharged in wastewater treatment plants and/or be partially accumulated in the sludge that is later used for soil amendments. Thus, industrial wastewaters serve as a significant environmental source of CeO_2 NPs (Dahle, Livi, and Arai 2015). For such reason, the Organization for Economic Co-operation and Development (OECD) in the Environment Directorate added CeO_2 NPs in the list of 14 NMs for testing and identified it as commercially relevant to the global economic impact of nanotechnology. It has been suggested that the most common route of CeO_2 exposure is likely to be through inhalation and/or ingestion (Kumari et al. 2014; Manier et al. 2013; Verstraelen et al. 2014; Franchi et al. 2015; Bour et al. 2015; Keller et al. 2014).

There is ongoing exposure of a large population set to new diesel emissions generated from fuel additives containing CeO_2 nanoparticles that may be inhaled by humans. Besides alveolar macrophages, bronchial and alveolar epithelial cells are among the principal cells that get into contact with airborne NPs that penetrate into the lung. As a consequence of this interaction, these cells are capable of producing pro-inflammatory mediators that have the ability to elicit both a local and systemic inflammatory response (Rim et al. 2013; Verstraelen et al. 2014; Kumari et al. 2014).

Concerning toxicity assessment, it was proposed that CeO_2 nanoparticles may cause oxidative stress and/or production of reactive oxygen species (ROS), cell membrane damage, or a rise in the intracellular ROS caused by the direct contact between the cells and the nanoparticles (Leung et al. 2015). The ROS production has been proposed as the cause of toxicity for different nano metal oxides,

such as TiO_2, ZnO, and CeO_2. It has been proposed that the nano metal oxide induced ROS can cause lipid peroxidation, cell membrane damage (Leung et al. 2015) and, possibly genotoxicity.

As to cell uptake of this NM, a study demonstrated the internalization of 8-20 nm CeO_2 NPs in A549 cell line (Mittal and Pandey 2014). A study in endothelial cells have reported that nanoceria can be uptaken into cells and widely distributed in multiple compartments of the cells. The results indicated that nanoceria can be also uptaken into cells through mediated endocytosis. Nanoceria were distributed throughout the cytoplasma but not into nucleus (S. Chen et al. 2013). Also in monocytes TEM revealed that CeO_2 NPs were internalized and found either in vesicles or free in the cytoplasm (Hussain et al. 2012). Moreover, an *in vivo* study in CD1 mice also showed the internalization, accumulation and translocation of CeO_2 NMs behind the pulmonary organs (Aalapati et al. 2014). The presence and retention of cerium oxide nanoparticles in lung tissue, and alveolar macrophages was also revealed (Ma et al. 2012).

1.3.2 Titanium Dioxide (TiO_2)

Titanium dioxide (TiO_2) is considered as an inert and safe material and has been used in many applications for decades. Furthermore, TiO_2 is accepted as a food and pharmaceutical additive. In the United States it is included in the Food and Drug Administration (FDA) Inactive Ingredients Guide for dental paste, oral capsules, suspensions, tablets, dermal preparations and in non-parenteral medicines. However, with the nanotechnologies' development, TiO_2 NPs (Figures 1.2, 1.3 and 1.4), displaying novel and useful properties are being increasingly manufactured and used. Therefore, increased human and environmental exposure can be expected, which has put TiO_2 NPs under toxicological scrutiny (Skocaj et al. 2011).

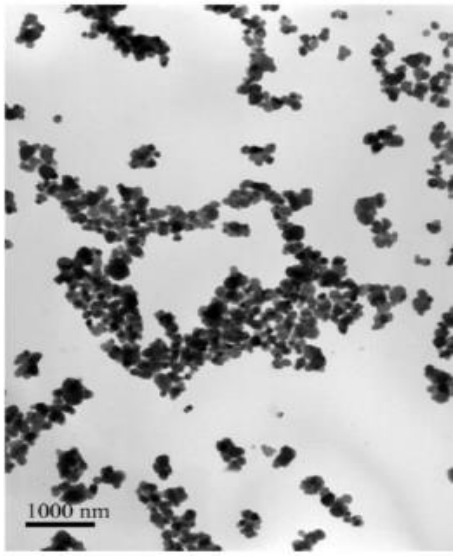

Figure 1. 2- TEM-micrograph of NM-100 showing the range in agglomerate and aggregate sizes in the material (Rasmussen et al. 2014).

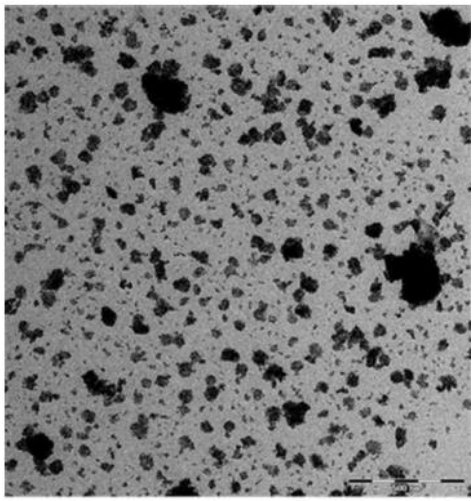

Figure 1. 3- Representative TEM micrograph of well-dispersed sample of NM-101 taken for quantitative TEM-analysis; scale bar is 500nm (Rasmussen et al. 2014).

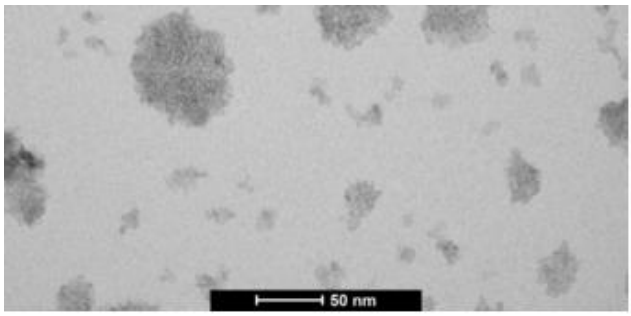

Figure 1. 4- Micrograph of NM-101, illustrating that the aggregates/agglomerates have a very irregular surface (Rasmussen et al. 2014).

Among NMs, TiO_2 is one of the most manufactured NM worldwide. TiO_2 NPs are widely used in industry for plastics, papers, inks, medicines, food products, cosmetics, toothpastes and skin care products, among others. It also has photocatalytic properties that have resulted in the use of TiO_2 NPs as an environment and wastewater disinfectant. Furthermore, TiO_2 NPs have been used as a photosensitizer for the photodynamic therapy of human colon carcinoma cells (Singh et al. 2009; Medina-Reyes et al. 2015; Jugan et al. 2012; Huerta-García et al. 2014; Chen et al. 2014). In fact, at present, titanium dioxide are the most common ingredient in mineral sunscreens. Because of their high photostability and low photoallergic potential, they are often preferred over organic filters (Boutard et al. 2013).

These particles are in the breathable size range and several toxic effects have been described after their inhalation. Tissue deposition of NPs and their toxicity are closely related to the route of exposure and, in this sense, keratinocytes have been studied as the primary target of dermal exposure, lung tissue as the target for inhalation, and intestines, kidney, and liver for oral exposure. The lung is

the best characterized organ regarding the toxic effects induced by TiO_2 NPs (Huerta-García et al. 2014).

Although these NPs are considered safe for use in sunscreens by the US FDA, there is a considerable concern with this ruling as sunlight because illuminated TiO_2 may induce DNA damage both *in vitro* and *in vivo*. When exposed to UV light, TiO_2 catalyses the generation of reactive oxygen species, such as superoxide anions, hydrogen peroxide, free hydroxyl radicals, and singlet oxygen in aqueous media (N. Singh et al. 2009).

In vivo studies have provided evidence that TiO_2 NPs can cause inflammation, fibrosis, pulmonary damage and even DNA damage. Toxicity assessment has been performed in rats tissues and revealed that this NM caused lungs injury and inflammation due the increasing number of red blood cells. The results of lung tissue lipid oxidation accessed by malondialdehyde (MDA) content confirmed that the damage of lung tissue was indeed related with the generation and accumulation of ROS (Tang et al. 2013). These authors explained that the toxicity and ROS formation begun in mitochondria that carried out aerobic respiration. Most of oxygen was combined with electrons which came from electronic transmission chain at inner mitochondrial plasmalemma and formed H_2O after a series of oxidation–reduction reactions. However, a small amount of oxygen formed superoxide which was the major source of ROS in cells. The cumulative ROS attacked the mitochondria and restrained the functional activity of mitochondria and, as a result, the cell was approaching to apoptosis (Tang et al. 2013; Huerta-García et al. 2014). A simple schematic representation of this mechanism is represented in figure 1.5.

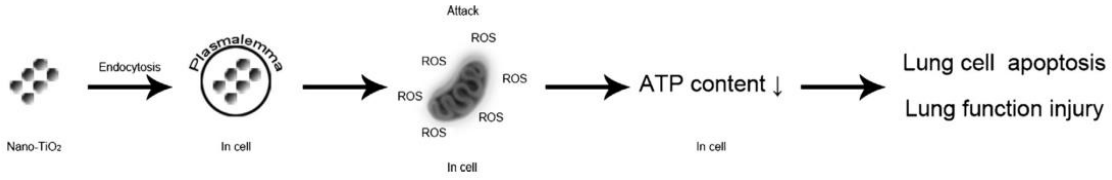

Figure 1. 5- Schematic representaion of the proposed mechanism for ROS formation and effects in the cell (from Tang et al. 2013)

However, these animal studies are limited and *in vitro* studies are required for more mechanistic insights.

Given that oxidative stress and inflammation are associated with indirect and secondary genotoxicity via the damaging activity of ROS, it seems likely that exposure to TiO_2 NPs may indirectly result in DNA lesions and several studies have demonstrated this effect (Singh et al. 2009; Jugan et al. 2012).

Based on the data available, the International Agency for Research of Cancer (IARC) has classified the TiO_2 NPs as a possible carcinogen to humans, and the National Institute for Occupational Safety and Health (NIOSH) has determined that TiO_2 is a potential occupational carcinogen by inhalation (Medina-Reyes et al. 2015).

In an exposure scenario, after absorption, TiO_2 NPs can be translocated to all regions of the respiratory tract (Huerta-García et al. 2014). In V79 (Chinese hamster lung cells) the viability was

significantly decreased at 24 and 48 hours, when exposed to 5 to 100 µg/mL of TiO_2 NPs (Chen et al. 2014).

Their small size facilitates uptake into cells and transcytosis across epithelial and endothelial cells into the blood and lymph circulation to reach potentially sensitive target sites, such as bone marrow, lymph nodes, spleen, and heart. There is increasing evidence that NPs can cross the blood–brain barrier independent of the route of exposure (Huerta-García et al. 2014). Because TiO_2 NPs can translocate to different organs and into the CNS (Huerta-García et al. 2014), diverse studies have been made in cell lines other than those representative of the respiratoty tract. A study evaluated their possible toxic effect on glial cells (U373 cells) and reported that TiO_2 NPs induce a strong oxidative stress in U373 cells, mediating changes in the cellular redox state, which was correlated with increase in antioxidant enzyme expression and lipoperoxidation (Huerta-García et al. 2014). In human fetal lung fibroblasts (HFL1) the results from MTT indicated that TiO_2 NMs (21 nm 80% A, 20% R) induced a decrease in cell viability at low doses (0.25 to 1.50 mg/mL) (Z. Qiang et al. 2013). A study in normal untransformed human fibroblasts (GM07492) with TiO_2 NPs in a range concentrations from 0 to 100 µg/mL also showed significant decrease in cell viability at 100 µg/mL (Franchi et al. 2015). The MTT assay in human amnion epithelial (WISH cells) cells revealed a concentration-dependent decline in the cell survival after exposure to TiO_2 NPs (30,6 nm) for 24 hours at 0.625 to 10 µg/mL (Saquib et al. 2012). Significant cytotoxicity, intracellular ROS generation, and to some extent G2/M cell cycle arrest were induced at the above specified treatment doses, and attributed to TiO2 NPs mediated oxidative stress in the WISH cells (Saquib et al. 2012).

As to the internalization studies of TiO_2 NPs, different techniques have been employed. The flow cytometry analyses revealed that these NPs were not only internalized but also adhered to the surface of A549 cells (Moschini et al. 2013). Another study also verified the accumulation of the smallest NPs in the cytoplasm and in the nucleus of A549 cells, once again proving the capacity of A549 cells to internalize NMs (Jugan et al. 2012). Other techniques as Raman imaging (Ahlinder et al. 2013) TEM (Aueviriyavit & Phummiratch 2012; Franchi et al. 2015) Static light scattering, in-vitro Raman microspectroscopy (Andersson et al. 2011) have shown the uptake to the nucleus (Ahlinder et al. 2013) and in the cytoplasm relating that the agglomerates can be taken up by the cells and largely accumulated in the endosomes, probably via endocytosis (Aueviriyavit & Phummiratch 2012; Franchi et al. 2015; Tang et al. 2013). All these studies were conducted in A549 cells. The internalization of TiO_2 NPs (30-70 nm) was also verified in the human liver cells (HepG2) through electron microscopy and flow cytometry (Vallabani et al. 2014).

Because NPs can be internalized by cells and some of these NPs also can cross the nuclear membrane, the direct interactions between NPs and the nucleus may be the main cause of genotoxicity, leading to DNA or chromosome breaks. When NPs do not reach the nucleus, the genetic material is exposed to the NMs during cellular division (Elsaesser and Howard 2012). In contrast to these data suggesting a significant genotoxic potential of TiO2 NPs, other authors show that acute exposure to TiO_2 NPs do not cause DNA damage (Xie et al. 2010; Bhattacharya et al. 2009; Landsiedel et al. 2010).

This discrepancy may be explained by differences in physicochemical properties of TiO_2 NPs and their suspensions, e.g., different NP diameter, crystalline phase, and/or specific surface area, or

different agglomeration status. It may also be explained by the use of different cell lines that may differ in terms of susceptibility to TiO_2 toxic potential (Jugan et al. 2012; Chen et al. 2014).

1.3.3 Barium Sulphate ($BaSO_4$)

Chronic exposure to high levels of micron-scale $BaSO_4$ may induce pneumoconiosis (baritosis) in miners (Konduru et al. 2014). Baritosis is one of the benign pneumoconioses in which inhaled particulate matter lies in the lungs for years without producing symptoms, abnormal physical signs, incapacity for work, interference with lung function, or liability to develop pulmonary or bronchial infections or other thoracic disease (Doig 1976).

Barium sulfate nanomaterials already have some applications in different industries and are considered a member of the poorly soluble particles (PSP) or poorly soluble low toxicity (PSLT) particle groups, as are cerium dioxide (CeO_2) and titanium dioxide (TiO_2); this nanomaterial is used as fillers in coatings (e.g. in motor vehicles) due to their mechanical, optical and chemical properties (Konduru et al. 2014) and it is also introduced into bone cements to increase radio-opacity so that they may be visualized through X-ray imaging, (Gillani et al. 2010). It is being used as a filling material in polymer compositions to increase scratch resistance while conserving transparency (Keller 2015), is a common agent added to catheters or endotracheal tubes which make such medical tubing radiopaque. In addition, $BaSO_4$ polymeric formulations have been shown to exhibit some antimicrobial activity (Aninwene et al. 2013).

Relatively to toxicity studies, there are only a few publications related to *in vivo* experiments. A study revealed that pulmonary exposure to instilled $BaSO_4$ NPs caused dose-dependent lung injury and inflammation. Four-week and 13-week inhalation exposures to a high concentration (50 mg/m^3) of $BaSO_4$ NPs elicited minimal pulmonary response and no systemic effects. Instilled and inhaled $BaSO_4$ NPs were cleared quickly yet resulted in higher tissue retention, exhibited lower toxicity and biopersistence in the lungs compared to other poorly soluble NPs such as CeO_2 and TiO_2 (Konduru et al. 2014).

To our knowledge, there are no available studies for *in vitro* assessment of $BaSO_4$ nanomaterials through inhalation exposure. Thus, one of the objectives of this work is to assess the cytotoxicity and genotoxicity of this nanomaterial.

1.4 Strategies and challenges in the *in vitro* characterization of nanomaterials' toxicity

1.4.1 Nanomaterials' dynamic behavior and dispersion in aqueous medium

NPs have the tendency to both aggregate and agglomerate. An agglomerate is a “collection of loosely bound particles or aggregates or mixtures of the two where the resulting external surface area is similar to the sum of the surface areas of the individual components,” while an aggregate is defined as a “particle comprising strongly bonded or fused particles where the resulting external surface area may be significantly smaller than the sum of the calculated surface areas of the individual components” (Sauer et al. 2015).

Many attempts have been made to generate stable suspensions or dispersions in case of insoluble NMs. However, it is often the case that the particles settle due to agglomeration and gravity over time in culture. It is probably therefore more appropriate to also express dose in terms of mass per unit surface area of the culture dish (μg/cm^2) (Stone, Johnston, and Schins 2009). The effective dosage is influenced by the sedimentation and diffusion properties that different NMs exhibit under the given cell culture conditions, which largely depend upon the effective densities and diameters of the suspended NM agglomerates (Sauer et al. 2015).

In culture medium or other biological fluids, NMs interact with proteins or phospholipids thereby forming a characteristic ‘corona’ on their surface. NMs’ tendency to agglomerate is governed by its surface properties that can change spontaneously due to protein adsorption. Consequently, corona formation directly affects the type and extent of NM agglomeration, and the type of NM dispersing agent used influences in vitro particle kinetics (Sauer et al. 2015; Cohen et al. 2013). *In vitro* test systems should be relevant for the *in vivo* situation they mimic. The biological proteins and lipids surrounding a NP determine its biological fate, since it is this corona that cells encounter and interact with. When nanoparticle-protein complexes pass from one biological fluid to another, the corona is assumed to change due to competitive adsorption of different biomolecules. Only the small fraction of NPs that can pass the air-blood-barrier would experience a corona shift towards the higher affinity of serum components, followed by a comparatively less pronounced, but still considerable agglomeration (Sauer et al. 2015).

Different NM dispersants have been investigated, including natural lung surfactants, phospholipids, organic solvents, and serum or albumin additives (Sauer et al. 2015). A number of studies have now demonstrated that small concentrations of protein (usually albumin below 1% final concentration) improve particle dispersion and the stability of that dispersion over time, especially if incorporated in the medium prior to particle addition, and if combined with a short sonication (e.g. 10 min) (Stone, Johnston, and Schins 2009). Of course, adding protein or other dispersants to the nanoparticles could influence their surface properties and therefore their interaction with cells and other biological molecules. This suggests that either the improved dispersion aids uptake of the smaller agglomerates and/or individual NPs or, alternatively, that the proteins adsorbed to the particle surface interact with cell surface receptors that facilitate uptake into the cells (Sauer et al. 2015).

To verify the stability of the NPs suspension there are some techniques already available that can be easily applied. Nanoparticle Tracking Analysis (NTA) and Dynamic Light Scattering (DLS) are some of those techniques. In this work DLS technique was performed. The principle of the DLS stands on the measurement of fluctuations in laser light scattered by vibrating particles suspended in a liquid as function of time. The vibration is due to Brownian motion caused by collision with solvent molecules.

The Brownian motion varies as a function of particle size and causes variation in the intensity of scattered light as function of time (Keld Alstrup Jensen 2014).

1.4.2 Experimental cell models

There are a number of obvious advantages to *in vitro* toxicity testing of any chemical or particle, including the ethical desire to reduce animal testing, the speed of results, and the relatively lower cost compared to *in vivo* studies (Stone, Johnston, and Schins 2009). *In vitro* model systems provide a rapid and effective means to assess NPs for a number of toxicological endpoints. They also allow development of mechanistic evaluations and provide refined information on how NPs interact with human cells in many ways. Such studies can be used to establish concentration–effect relationships and the effect-specific thresholds in cells. The revelation of primary effects on target cells in the absence of secondary effects caused by inflammation and the identification of primary mechanisms of toxicity in the absence of the physiological factors are some of the interactions allowed by *in vitro* tests (Arora, Rajwade, and Paknikar 2012). These assays are suited for high-throughput screening of an ever increasing number of new NMs obviating the need for *in vivo* testing of individual materials (Stone, Johnston, and Schins 2009). Other advantages are reduction in variability between experiments, reduced requirement of test materials thereby leading to generation of limited amounts of toxic wastes. (Arora, Rajwade, and Paknikar 2012). A limitation is that an *in vitro* system is not able to fully replicate the complex interactions that occur between multiple cell types *in vivo,* both within an organ and also between organs (Stone, Johnston, and Schins 2009),

There are a large number of different tumor and transformed cell-derived cell lines available. It is also possible to increase the complexity of these *in vitro* systems to include multiple cell types, e.g., the co-culture of epithelial cells and macrophages, with the aim to more closely mimic the *in vivo* situation (Stone, Johnston, and Schins 2009). The selection of a cell line for *in vitro* toxicity assessment is frequently driven by the toxicokinetics and toxicodynamics of the NM, namely, the main via of absorption and the primary site of contact or the target organ.

Franchi et al. (2015) discussed the main differences between transformed or cancer cells and untransformed cell lines. They agree that the use of cancer cell lines can provide vital information, however they referred that their use in nanotoxicological research, especially with the aim of predictive toxicology for human exposure scenarios, remains questionable as multiple molecular pathways are potentially deregulated (including DNA repair pathways). Transformed or cancer cell lines, due to several mutations in cell death-related pathways, may differ quite strongly in their response to NP-induced damage. Depending on the nature of the cancer cells and NPs, these differences may result in either higher sensitivity of the cancer cells or higher resistance, which may harden NP toxicity studies.

During the evaluation of nanomaterials' toxicity it is important to show experimentally or based on the literature reports whether the NPs are internalized into the cells to try to allow a better understanding of the mechanisms behind the nanomaterials toxicity. This knowledge allows also, in the case of negative results, to discard the hypothesis of inadequacy of the cell model used due a lack of

the interaction of the nanomaterial with the cellular components. In the present work, internalization was not accessed but the knowledge relies on the results from other laboratories that participated also in the NANoREG project.

1.4.3 Cytotoxicity Assessment

The development and validation of methods to evaluate the toxicity of NMs is regarded as one of the main future challenges relevant to the safety of nanotechnology (Herzog et al. 2007). In past years, a number of methods have been developed to study cell viability and the proliferation ability of cells in culture. The most convenient, modern assays have been optimized for the use of microtiterplates (96-well format). This miniaturization allows many samples to be analyzed rapidly and simultaneously. Colorimetric and luminescence based assays allow samples to be measured directly in the plate by using a microtiterplate reader or ELISA plate reader. Cytototoxicity assays have been developed which use different parameters associated with cell death and proliferation (Weyermann, Lochmann, and Zimmer 2005).

1.4.3.1. The MTT Assay

There are a wide variety of assays to assess cytotoxicity that are frequently based on cell viability measurement. One of the most common is the MTT (3-(4,5-dimethylthiazol-2-yl)-2,5-diphenyltetrazolium bromide) assay, or variations of this assay (MTS, XTT or WST-1). These assays principally determine cell viability through determination of mitochondrial function by measuring the activity of mitochondrial enzymes. The assay generates a colored product (a purple formazan), which can be quantified by spectrophotometric readings at a specific wavelength. The absorbance value generated is representative of both the cell number and the functional viability of those cells (Stepanenko & Dmitrenko 2015; Stone et al. 2009; Weyermann et al. 2005). Such assays can therefore detect proliferation as well as cytotoxicity.

When testing NPs' cytotoxicity, these assays end up with a suspension containing cell debris, the dissolved formazan, and particles themselves. It could be advantageous to centrifuge the sample at this stage, to transfer the supernatant to a fresh 96-well plate, and therefore to read the absorbance of the supernatant devoid of particles and cell debris. This reduces possible background interference due to the presence of particles. In fact, there are a number of additional control experiments that should be conducted before embarking upon a full MTT assay. First, a number of particles may generate an absorbance at the same wavelength as that used to quantify the colored product, leading to an overestimation of the cell viability (Stone et al. 2009; Stepanenko & Dmitrenko 2015).

It would also be useful to include a positive control that is linked to the hypothesis being tested and a negative control particle to benchmark against the particles under investigation. A positive control could include alpha quartz, or a relatively toxic nanoparticle such as copper oxide. A negative control

could include a larger version of the test particle under investigation, or perhaps a polystyrene nanoparticle (negatively charged) (Stepanenko and Dmitrenko 2015).

In the final stages of the MTT assay, solubilization of the formazan product is required using a solvent such as dimethylsulfoxide (DMSO) or isopropanol (Stone et al. 2009; Stepanenko & Dmitrenko 2015).

In order to increase the reliability of cytotoxicity assessment the combination of at least two different cytotoxicity assays should be employed, taking into consideration that they should measure different endpoints and therefore generate complementary results (Stone, Johnston, and Schins 2009).

1.4.3.2. The clonogenic assay

The clonogenic assay is used as an alternative method which avoids the use of any colorimetric or fluorescent indicator dye, thus eliminating the risk of interactions and allowing the assessment of true cytotoxicity. The clonogenic assay, also called colony formation efficiency (CFE) assay, is an *in vitro* cell survival based assay measuring the ability of a single cell to form a colony (Herzog et al. 2007). This is usually done by simple dilution after generating a single cell suspension and counting the colonies that arise from single cells. For effective and correct counting, a lower threshold, such as five or six doublings (32 or 64 cells/colony), is quantitated, taking into account the doubling time. For instance, the effect of a concentration of a drug on cell survival may be measured with this assay (Longo-Sorbello et al. 2006). Therefore, plating density must not be too high or colonies will coalesce and counting of single colonies will become impossible (Buch et al. 2012).

1.4.4 Genotoxicity Assessment

1.4.4.1. The cytokinesis-blocked micronucleus (CBMN) assay

Based on the micronucleus (MN) test data on nanomaterials, it was proposed that the in vitro MN test is quite appropriate to screen NPs for potential genotoxicity (Arora, Rajwade, and Paknikar 2012).

In the cytokinesis-block micronucleus (CBMN) assay, cells that have completed one nuclear division are blocked from performing cytokinesis using cytochalasin-B (Cyt-B) and are consequently readily identified by their binucleated appearance. Cyt-B is an inhibitor of actin polymerisation required for the formation of the microfilament ring that constricts the cytoplasm between the daughter nuclei during cytokinesis. The appropriate concentration of Cyt-B is usually between 3 and 6 µg/mL (Fenech 2000; OECD 2009). It is important to take into account that Cyt-B may take up to 6 h before it starts to exert its cytokinesis-blocking action (Michael Fenech 2000) and that it also inhibits endocytosis, an important mechanism of uptake of NMs into the cell (Azqueta and Dusinska 2015).

When using established or primary cell lines from dividing cell populations it is usual to add Cyt-B shortly after exposure to genotoxin to capture all cells undergoing their first nuclear division as binucleated cells — this usually requires an incubation period of about 24 to 48h (1.5 to 2 cycles), depending on the cell cycle duration, before harvesting the cells (Michael Fenech 2000). Micronuclei should only be scored in binucleated cells, i.e., cells that divided in the presence or immediately after exposure to the agent under study (Fenech 2000; OECD 2009).

MN are expressed in dividing cells and contain either chromosome breaks lacking centromeres (acentric fragments) or whole chromosomes that are unable to travel to the spindle poles during mitosis (Figure 1.6). At telophase, a nuclear envelope forms around the lagging chromosomes and fragments, which then uncoil and gradually assume the morphology of an interphase nucleus with the exception that they are smaller than the main nuclei in the cell, hence the term “micronucleus” (Fenech 2000; Fenech et al. 2011; Kotova et al. 2015; Bonassi et al. 2011; Terradas et al. 2010).

As micronuclei may arise from lagging chromosomes, there is the potential to detect aneuploidy-inducing agents that are difficult to study in conventional chromosomal aberration tests. However, the CBMN assay does not allow for the differentiation of chemicals inducing polyploidy from those inducing clastogenicity without special techniques such as fluorescence *in situ* hybridization (FISH) (OECD 2010). With probes targeted to the centromere region, it is possible to determine if a specific micronucleus contains an acentric chromosome fragment (i.e. resulting from a clastogenic event), or if it holds an entire chromosome (i.e. aneugenic effect) (Stone et al. 2009; Fenech et al. 2011; Terradas et al. 2010).

Micronuclei (MN), nucleoplasmic bridges (NPB) and nuclear buds (NBUD) are nuclear anomalies commonly seen in cancer and they represent a common phenotype of chromosomally unstable cells. Chromosomal instability leads to altered gene dosage and the potential for a cell to rapidly evolve and mutate, due to its genetic plasticity, into diverse abnormal genotypes that can escape the homeostatic control mechanisms and thus become immortalized and evade the immune system (Fenech et al. 2011; Bonassi et al. 2011).

Occasionally nucleoplasmic bridges are visible between nuclei; they are observed in binucleated cells following exposure to clastogens. These are probably dicentric chromosomes in which the two centromeres were pulled to opposite poles of the cell during anaphase and the DNA in the resulting bridge is covered by nuclear membrane. The width of a nucleoplasmic bridge may vary considerably but usually does not exceed 1/4th of the diameter of the nuclei within the cell. The nucleoplasmic bridge should have the same staining characteristics of the main nuclei. Thus, nucleoplasmic bridges in binucleated cells provide an additional and complementary measure of chromosome rearrangement, which can be scored together with the micronucleus count (Fenech 2000; Fenech et al. 2011).

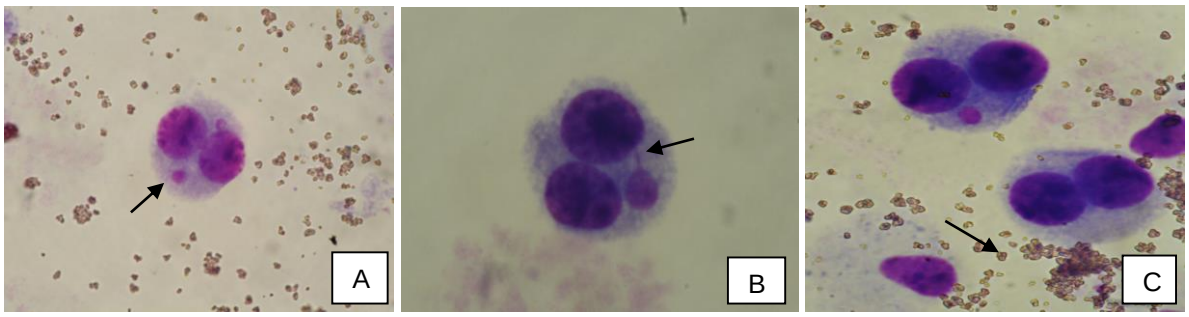

Figure 1. 6- A549 cells exposed to TiO_2 NMs. A- Binucleated cell with one micronucleus; B- Binucleated cell with one micronucleus and nucleoplasmatic bridge; C- Binucleated cells (one cell with micronucleus) surrounded by TiO_2 NMs. Images from the group lab.

When anaphase bridges break unevenly, which they almost always do, one of the daughter cells receives a chromosome with additional copies of genes and the other daughter cell loses some genes (M. Fenech et al. 2011). NPB are usually broken during cytokinesis but they can be accumulated in cytokinesis-blocked cells using the cytokinesis inhibitor cytochalasin-B (M. Fenech et al. 2011).

The NBUD are characterized by having the same morphology as a MN with the exception that they are connected to the nucleus by a narrow or wide stalk of nucleoplasmic material depending on the stage of the budding (M. Fenech et al. 2011).

1.4.4.2 Comet Assay

The comet assay or Single Cell Gel Electrophoresis (SCGE) (Tice et al. 2000; Azqueta & Collins 2013), has become the most popular method for measuring DNA damage of various sorts (Figure 1.7). It is used in genotoxicity testing, to screen novel chemicals and pharmaceuticals, cosmetics, or other chemicals for potential carcinogenic properties; tests can be carried out in vivo (with analysis of various tissues from the experimental animal) or in vitro using suitable cultured cell lines (Azqueta & Collins 2013; Collins 2014; Arora et al. 2012).

Comet assay has demonstrate high sensitivity for detecting low levels of DNA damage, requires small numbers of cells per sample, is flexible, is low costs, is ease to employ, and the study could be completed in a short time (Tice et al. 2000).

Tice et al. 2000 reported that the optimal version of the Comet assay for identifying agents with genotoxic activity was the alkaline- pH 13- version of the assay developed by Singh et al. 1988. The alkaline version is capable of detecting DNA single-strand breaks (SSB), alkali-labile sites (ALS), DNA-DNA/ DNA-protein cross-linking, and SSB associated with incomplete excision repair sites (Tice et al. 2000). At this pH, increased DNA migration is associated with increased levels of SSB, SSB associated with incomplete excision repair sites, and ALS. The induction of increased levels of SSB and ALS results in an increased ability of the DNA to migrate but, in contrast, the presence of DNA cross-linking reduces the ability of the DNA to migrate (Tice et al. 2000) (Azqueta and Collins 2013). Generally, DNA is denatured and unwound at pH values above 12 because of the disruption of hydrogen bonds between

double-stranded DNA. At pH conditions of 12,6 or higher, ALS (e.g., apurinic sites) are quickly transformed to strand breaks. A pH 13 would be expected to maximize the expression of ALS as SSB (Tice et al. 2000).

Because almost all genotoxic agents induce orders of magnitude more SSB and/or ALS than DSB, this version of the assay offered greatly increased sensitivity for identifying genotoxic agents (Tice et al. 2000).

The enzyme-modified comet assay has been widely used, particularly in human biomonitoring, to determine background levels of oxidised bases, which is a more specific indicator of oxidative attack is the presence of oxidised purines or pyrimidines. The basic comet assay was modified to detect these, by introducing an incubation of the nucleoids (just after lysis- described below) with bacterial repair enzymes. The enzymes combine a specific glycosylase activity, removing the damaged base and creating an apurinic/apyrimidinic (AP) site, and an AP lyase which converts the AP site to a break. Formamidopyrimidine DNA glycosylase (FPG) acts on 8-oxo-7,8 dihydroguanine (8-oxoGua) (Collins 2014; Azqueta & Collins 2013; Collins et al. 2014). An increase in % tail DNA after incubation with the enzyme, compared with an incubation with buffer alone, indicates the presence of oxidised bases (Collins 2014; Azqueta & Collins 2013). These methods can be used to provide mechanistic information on the types of DNA damage induced by a test substance or, in some situations, to eliminate the possibility that the observed increase in DNA migration is due to cytotoxicity (Tice et al. 2000). The relationship between break frequency and % tail DNA is virtually linear, but at around 80% tail DNA, saturation is approached and the relationship departs from linearity. When estimating oxidised bases with the comet assay, it is usual to subtract the value of % tail DNA with buffer incubation, from the % tail DNA with enzyme incubation to obtain 'net enzyme-sensitive sites' (Collins 2014).

Using independently coded slides and a blind slides scoring, at least 50 cells should be scored (Tice et al. 2000) in each mini gel. Each individual comet is scored to give a measure of DNA damage; it is often necessary to pool the results of 100 comets to obtain the overall damage level of a population of cells (Azqueta and Collins 2013). According to Tice et al. (2000) and (Azqueta and Collins 2013) the comets near the edges of the gel should not be scored. Also the particles or aggregates can localize at or near comet appearances, and affect their quantification due to their fluorescence or ability to quench DNA-staining agents such as ethidium bromide (Stone, Johnston, and Schins 2009).

Concurrent positive and negative controls must be included in each experiment. Examples of positive control substances to use in experiments include methyl methanesulphonate and ethyl methanesulphonate. Negative controls, consisting of solvent alone in the treatment medium, and treated in the same way as the treatment cultures, should be included (Tice et al. 2000).

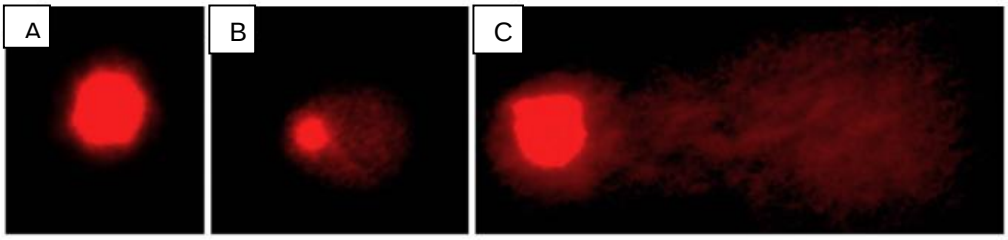

Figure 1. 7- Different levels of DNA damage. A- Nucleoid without DNA breaks; B- Nucleoid with medium level of DNA breaks; C- Nucleoid with high level of DNA breaks (Araldi et al. 2015).

2. OBJECTIVES

The main objective of this work was to contribute for the hazard assessment of different metallic nanomaterials, through the use of benchmark nanomaterials, standard procedures for NM preparation and toxicity assays, in order to reduce experimental variability.

Specifically, this projects aimed to:

i) characterize the dynamic behavior of the different nanomaterials in the culture medium and detect interferences with the bioassays output;

ii) characterize the potential of CeO_2, TiO_2 and $BaSO_4$ to induce cytotoxic or genotoxic effects in a human lung epithelial cell line (A549 cell line) in order to infer their possible hazard to the human respiratoty tract.

3. MATERIALS AND METHODS

3.1 Cell Culture/ Cell line

A549 cell line from American Type Culture Collection (ATCC® CCL-185™) delivered from Bundesanstalt für Arbeitsschutz und Arbeitsmedizin (BAuA, in English, Federal Institute for Occupational Safety and Health; Berlin) was the selected cellular model since this cells are from human lung carcinoma epithelia and this way it is possible to mimic environment in the lung when nanoparticles are inhaled. This line derives from an explant culture of lung carcinomatous tissue from a 58-year-old Caucasian male and is classified as level 1 in biosafety. The doubling time of this cell line is approximately 22 hours (Source: www.lgcstandards-atcc.org/Products/All/CCL-185.aspx?slp=1; consulted in 17th May 2016).

The growth medium used for this cells was DMEM (Gibco by Life Technologies, Carlsbad California, USA), supplemented with 10% heat-inactivated Hyclone Fetal Bovine Serum (Thermo Scientific Waltham, Massachusetts, USA), 1% Pen/Strep, 1% Fungizone (Invitrogen, Carlsbad, California, USA) and 2.5% HEPES (Invitrogen, Carlsbad, California, USA). When cells reached about 80% confluence, a subculture was performed: the culture medium was removed, the cells were washed and then incubated with 2 mL trypsin-EDTA (0.05%) for 4 minutes in at 37ºC (Invitrogen, Carlsbad, California, USA) (0.05%). When the cells were detached from the flask, the cells were subcultured in appropriate densities to perform the assays.

3.2 Nanomaterial preparation and characterization of nanomaterial dispersion in the culture medium

NMs produced, characterized and provided by the Joint Research Centre Repository (Institute for Health and Consumer Protection, European Commission, Ispra, Italy) were used for this study, namely cerium dioxide (NM-212), titanium dioxide (NM-101 and NM-100) and barium sulfate nanomaterials (NM-220). The detailed physicochemical characteristics of each nanomaterial was previously reported by Rasmussen et al. (2014) and Singh et al. (2014) and are presented in Table 3.1.

The dispersion of nanomaterial powder in aqueous medium was performed according to *the NANOGENOTOX dispersion protocol* (K.A. Jensen et al. 2011). Briefly, 15.36 mg of each nanomaterial was weighted in a vial to obtain a batch with a final and fixed concentration of 2.56 mg/mL. The nanomaterial was prewetted with ethanol (EtOH) (0,5 %; ≥ 96% purity) to handle hydrophobic materials followed by dispersion in 6 mL of sterile-filtered BSA-water consisting of water with BSA-(0.05%, w/v), using probe sonication. To carry on the sonication process, the vial containing the nanomaterial in EtOH and BSA water was placed in a box partially submerged into ice and sonicated at 400 W with 10% of amplitude for 16 minutes using a Branson Sonifier S-450D with 13 mm disruptor horn (Branson Ultrasonics Corporation, Danbury, USA). To proceed with the in vitro tests an working solution with a

concentration of 0,640 mg/mL was prepared for the lowest concentrations (3.2, 9.6 and 32 µg/mL); the concentrations of 96, 240 and 320 µg/mL were prepared directly from batch dispersion.

Table 3. 1- Characteristics of NMs studied (Rasmussen et al. 2014; Singh et al. 2014; and according to manufacturer information (Fraunhofer IME, Germany)).

	Core material	Morphology	Crystalline phase	Size (TEM)	Surface area (BET)	Content of core material [wt%]	Coating (organic/ inorganic)	Aggregation (TEM/SEM)
NM-212	CeO_2	Polyhedral	Cubic cerionite	<10 to 100 nm	27.2 m^2/g	81.62	-------	Yes
NM-101	TiO_2	Rounded or slightly elongated	Anatase	5 nm	316 m^2/g	98.1	Silanes, hexa- and oxydecanoic acids	Yes
NM-100	TiO_2	Rounded or slightly elongated	Anatase	20 to >100 nm	9 m^2/g	97.7	no	Yes
NM-220	$BaSO_4$	------	-------	pending	38 m^2/g	-------	no	-----

To verify the quality of the dispersion of the nanomaterial in the culture medium the hydrodynamic size-distribution was determined using Dynamic Light Scattering (DLS; Malvern Nano ZS, Malvern Inc., UK) according to *SOP for measurement of hydrodynamic Size- Distribution and Dispersion Stability by Dynamic Light Scattering (DLS)* (Keld Alstrup Jensen 2014). Samples were placed into 700 µL -polystyrene cuvettes and the most relevant parameters achieved in DLS: the Polydispersity Index (PdI) that indicates if a sample has a broad range of sizes or not; and the Z-Average size (Zav), which is an indicator of the average size of the particle, in nanometers of each suspension were assessed. The analysis was performed in the batch dispersion, soon after the sonication procedure, and in selected concentrations of the NMs diluted in cell culture medium: 3.2, 32 and 240 µg/mL, corresponding to 1, 3 and 10 µg/cm2. Each sample was analyzed at 0, 3, 24, 48 hours following preparation and incubation at 37ºC as well as and after 7 days-incubation. During this time, NM samples were incubated at 37ºC, 5% CO_2 to mimic best possible the *in vitro* test exposure conditions. Each analysis consisted in ten repeated measurements of hydrodynamic size were performed without pause. Results were compared to values that were obtained within the NANoREG Project and used as benchmark values.

3.3 Cytotoxicity Assays

3.3.1 MTT assay

For this assay, A549 cell line was seeded at a density of $0,5x10^4$ cells per well in 96-well plates and incubated for 24 hours at 37^oC with 5% CO_2. After this incubation time, the cells were exposed to the nanomaterials NM-212, NM-101, NM-100 and NM- 220 in a range of concentrations from 0 to 100 µg/cm^2 and incubated again in the same conditions for another 24 hours. The positive control used was a detergent, namely SDS at 0.01%. After this exposure period the treatment was removed and the cells were washed twice with PBS. A volume of 100 µL of MTT (Life Technologies, Carlsbad, California) solution was added in each well at final concentration of 0,5 mg/mL, previously prepared in PBS (5 mg/mL) and finally in culture medium to reach the desired concentration. The cell culture was incubated for a period from 2 to 4 hours in order to enable the viable cells to convert the MTT in the colored compound. After this time, the MTT solution was and DMSO solution was added in order to solubilize the purple precipitate produced by the cells and incubate for approximately for 20 minutes while agitating. The final procedure consisted in measuring the absorbances of each well in a Multiskan Ascent Spectrophotometer (Thermo LabSystems, Waltham, MA) at 570 nm (reference filter: 690 nm). To allow the separation the nanomaterial from the colored supernatant the plate was centrifuged 96 well plate centrifuge in a Sigma 4-16 S and the supernatant was transferred to a new plate; the absorbances were measured again at same conditions.

3.3.2 Clonogenic assay

A549 cell line was plated in a density of 100 cells per well, in a 6-well plate and allowed to attach for 18 hours before exposure. This incubation time was shorter than the doubling time of this cells (22 hours), in order to guarantee that the cells were attached but not divided ate the time of the treatment with nanomaterials. The cell culture were then exposed to the different concentrations (ranging from 0-100 µg/cm^2) of the nanomaterials and incubated for 7 days, at 37^oC, with 5% CO2. MMC was used as positive control at a final concentration of 0.00425 µg/mL. After 7 days of exposure to the nanomaterials, the cells were washed twice with PBS and fixed with absolute cold methanol (Merck; Darmstadt, Germany) for 10 minutes. Then, the plates were allowed to dry and the colonies was stained for 10 minutes with 10% Giemsa (Merck; Darmstadt, Germany), prepared in Gurr's buffer, washed twice with Gurr's phosphate buffer and allowed to dry. The colonies formed were counted and the platting effiency (PE) calculated by comparing the number of cells plated initially with the number of colonies formed after the treatment period as well as the surviving fraction (SF) through the comparison between the number of the treated cells and the cells in the control. Equations 1 and 2 show the way that SF and PE were calculated (Munshi, Hobbs, and Meyn 2007).

$$Plating\ efficiency\ (PE) = \frac{\text{number of colonies in the negative control}}{\text{number of cells plated in each well}} \text{ x } 100 \qquad \textit{(equation 1)}$$

$$Surviving\ fraction\ (SF) = \frac{\text{PE of treated cells}}{\text{PE of control}} \text{ x } 100 \qquad \textit{(equation 2)}$$

3.4 Genotoxicity Assays

3.4.1 Cytokinesis-blocked micronucleus assay (CBMN)

Micronucleus assay was performed mainly as described in OECD- Organisation for Economic Co-operation and Development TG487 (OECD 2010). A549 cells were seeded in 6-well plates at a density of $2x10^5$ cells per well, and incubated for 24 hours at 37ºC with 5% CO2. The cells were exposed to nanomaterial NM-212, NM-100 and NM- 220 in concentrations ranging from 0 to 100 µg/cm^2 and incubated for six hours at 37ºC with 5% CO2. After this time Cytochalasin-B was add to each well (final concentration of 6 µg/mL), and cells were incubated again until 48h of exposure. The selection of this timepoint for adding Cytochalasin-B intended to avoid interference of this chemical with the NMs uptake, as proposed by (Magdolenova et al. 2013). The positive control was Mitomycin C (MMC) (Sigma-Aldrich St. Louis, Missouri, EUA) which was prepared in PBS and in culture medium in a final concentration 0.1 µg/mL. When 48 hours were reached the cells were washed with PBS twice and trypsin EDTA was added to detached the cultures from the wells. The suspension was then centrifuged for 5 minutes at 1200 rpm, the supernatant was discarded and the cell pellet was ressuspended in culture medium. The next step was to submit the cells to a hypotonic shock with a solution of 73.5% sterile injectable bidistilled water, 24.5% of culture medium and 2% of inactivated FBS, added drop by drop while vortexing. The cells were centrifuged for 5 minutes at 1200 rpm again, the supernatant was discarded and the cells were ressuspended in the remained drop. Two drops of cell suspension were placed on microscope slides. For each treatment, two/three slides were prepared. The slides were dried at room temperature from 4 to 24 hours and then the cells were fixed in cold fixing solution- 3:1 methanol:acetic acid for 20. After a few hours or more the slides were ready to be stained with Giemsa. First of all the slides were immersed in Gurr's phosphate buffer (Gibco by Life Technologies, Germany) for 10 minutes, then in a solution with 4% Giemsa (Merck, Darmstadt, Germany), diluted in a Gurr's phosphate buffer for 15 minutes and finally washed twice in the same buffer for 5 minutes. Finally the slides were allowed to dry and mounted with Entellan (Merck Darmstadt, Germany) and cover slips (24x60). The slides were coded to be analyzed in an optical microscope (Axioskop 2 Plus, Zeiss) and micronuclei were scored in, at least, 2000 binucleated cells from two independent cultures.

The criteria for scoring was that the diameter of micronucleus may vary between 1/16th and 1/3rd of the diameter of the main nucleus (Michael Fenech 2000).

Also,the proportion of mono- (MC), bi- (BC) or multinucleate cells (MTC) was determined in a total of 1000 cells and the replication indexes- Cytokinesis-blocked proliferation index (CBPI) and replication index (RI) were calculated through the following equations (Tavares et al. 2014):

$$\mathrm{CBPI} = \frac{\text{nº mononucleated cells} + 2 \times \text{nº binucleated cells} + 3 \times \text{nº multinucleated cells}}{\text{Total nº of viable cells}} \qquad \textit{(equation 3)}$$

$$\mathrm{RI} = \frac{\left(\frac{\text{nº binucleated cells} + 2 \times \text{nº multinicleated cells}}{\text{Total number of cells}}\right)\text{treated cultures}}{\left(\frac{\text{nº binucleated cells} + 2 \times \text{nº multinucleated cells}}{\text{Total number of cells}}\right)\text{control culture}} \qquad \textit{(equation 4)}$$

3.4.2 Comet Assay

A549 cell line was plated at the density of 0.5×10^5 cells per well in a 24 well plate and incubated for 24 hours at 37ºC with 5% CO2. The culture were exposed for 24 hours to 0-100 µg/cm^2 of NM-212, NM-101, NM-100, NM-220. Ethyl methansulfonate (EMS) (Sigma-Aldrich St. Louis, Missouri, EUA), the positive control was diluted in PBS (Gibco by Life Technologies, Carlsbad, California,USA) in a final concentration of 5mM and applied 1 hour before harvesting the cells.

At the end of exposure, the cells were washed twice with PBS and detached from the well with trypsin-EDTA. Cells were centrifuged at 1000 rpm, 4ºC and 80 µL of 0,8% low melting agarose (Sigma-Aldrich), pre-warmed to 38°C, was added to the cell pellet. Cells were then spread on microscope slides, previously coated with 1% normal melting point agarose (GE Healthcare, Little Chalfont, UK), covered with a cover slip (20x20), and chilled on a cold surface to solidify and form a thin gel (Collins 2014). Four mini-gels were prepared in each slide, two slides per treatment condition.

The slides were immersed into lysis buffer, a solution consisting of high salts' concentration and detergents ($Na_2EDTA.H_2O$ 100 mM, NaCl 2.5 M,Tris-HCl 10 mM, 10% DMSO and 1% Triton-X100, pH 10.

The lysis solution allows the removal of the cellular membranes, allowing soluble cell and nuclear components to diffuse away, and detach histones from the DNA. The residual structures, containing highly condensed DNA, still resemble nuclei but are now known as nucleoids (Collins 2014). Slides were incubated in lysis buffer 1-24h at 4°C and then were washed twice for 10 min in F buffer (HEPES 40 mM, BSA 0.2 mg/mL, KCl 100 mM, acid EDTA 0.5 mM, pH 8).

Then, FPG enzyme (kindly provided by Dr. A. R. Collins, University of Oslo, Norway) diluted in F buffer, or F buffer alone, was added to each mini-gel and covered with a cover slip (24x60), and the slides were placed in a humidified atmosphere, to prevent dissecation, in an incubator (37°C) for 30 min.

Cover slips were removed and the slides were immersed in electrophoresis buffer (NaOH 0.3 M, $Na_2EDTA.H_2O$ 1 mM; pH=13), for 30 minutes, to allow unwinding and to produce single stranded DNA and to express ALS as SSB (Tice et al. 2000; Collins 2014).

Electrophoresis was performed for 25 minutes at 28 V and 300 mA at temperature around 5°C, since the use of a lower temperature is thought to provide increased reproducibility. During electrophoresis, DNA, being negatively charged, is attracted to the anode, but it only moves appreciably if it contains breaks (Tice et al. 2000).

The DNA is supercoiled because it was wound around the histone cores of nucleosomes. Although the histones are no longer present, the supercoiling remains because the DNA loops are constrained by their matrix attachment. A strand break relaxes supercoiling, and so broken loops are able to extend towards the anode, and it is these loops that form the comet tail. The relative size of the tail (most conveniently measured as the % of total fluorescence in the tail) reflects the number of DNA loops and therefore the frequency of DNA breaks (Collins 2014).

After the electrophoresis, the slides were washed for 10 min, first in cold PBS (Gibco by Life Technologies, Carlsbad, California,USA) and then, in a cold dH_2O to pH neutralization.

The slides were kept in a box, protected from the light, to dry at room temperature and were stained with 0,125 mg/mL ethidium bromide (Sigma-Aldrich St. Louis, Missouri, EUA).

The analysis of the slides was done in a fluorescence microscope (Axioplan2 Imaging, Zeiss), with the assistance of specific image-analysis software (Comet Imager 2.2, from Metasystems, GmbH). In each slide 50 nucleoids were randomly analyzed per mini-gel, which results in 100 nucleoids per treatment condition, in replicate cultures. Two independent assays were performed for this genotoxicity test.

3.5 Statistical analysis

All data obtained were analyzed with IBM SPSS Statistics 20.

In the cytotoxic assays, namely Clonogenic Assay and MTT the results were analyzed through One-Way ANOVA and Post- Hoc tests, provided the data followed a normal distribution. Otherwise, non-parametric tests were applied, such as Kruskal-Wallis and Mann-Whitney to compare differences between the tested concentrations and the negative control.

In the comet assay, it was assumed that the data follow a normal distribution and then One-Way ANOVA and Post-Hoc tests were applied. The differences between the results with and without FPG were analyzed using Student's t-test.

Two-sided Fisher's exact test was applied to analyze the results of Micronucleus Assay so it was possible to assess the frequency of micronucleated binucleated cells between nanomaterial exposed cultures and control cultures. For RI and CBPI analysis non-parametric Kruskal-Wallis test was required.

In addition, the existence of a dose-response relationship for the DNA in tail (%) was explored by regression analysis.

4. RESULTS

4.1 Cerium dioxide nanomaterials

4.1.1 Characterization of the nanomaterial dispersion in the culture medium

As mentioned before, the protocol used for the dispersion was a standard procedure that was developed in the NANOGENOTOX project, with the aim of ensuring the stable dispersion of the nanomaterials and reducing agglomeration/aggregation.

To verify the size of the NPs and the dispersion stability over time, the DLS technique was employed and the results are presented in Figures 4.1. to 4.4. The measurements were performed at 0 hours (right after the sonication), 24 hours, 48 hours and in a range time between 5 and 7 days, in the culture medium, for concentrations of 1, 10 and 75 µg/cm^2 (3.2, 32, 240 µg/mL), respectively. Each time was selected to match the times of exposure performed in each assay. The characterization of nanomaterials dispersion 3 hours after sonication was also performed in the first place, but results are not presented since they were not different from the initial dispersion and the 24 hours timepoint was more useful for the study.

Note that in this work the concentrations are expressed in µg/cm^2, but in some studies the concentrations are presented in µg/mL; that way the concentrations used here were 1, 3, 10, 30 and 100 µg/cm^2 corresponding to 3.2, 9.6, 32, 96, 240 and 320 µg/mL, respectively. It makes easier the comparison of the results.

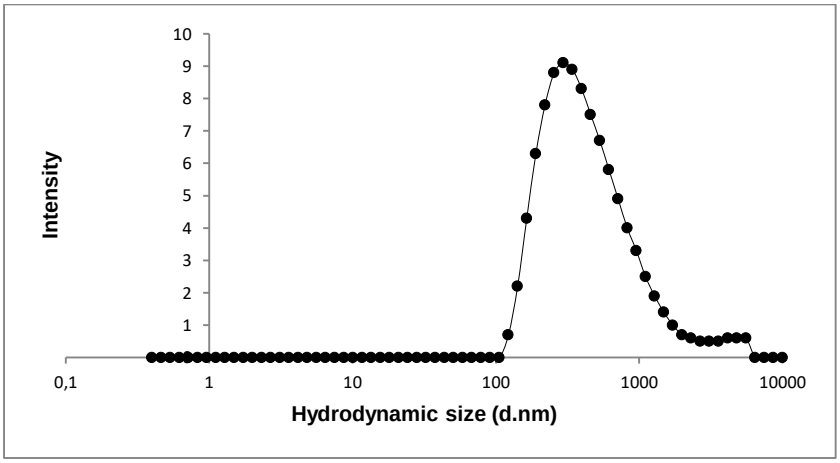

Figure 4. 1- Size distribution of the batch dispersion of NM- 212 (2.56 mg/mL) soon after sonication in 0.05%.BSA- water

The quality of the batch dispersion is an important feature to decide whether the assay should be carried out or not. Only size distributions in the nanomateric scale should be accepted to pursue

assays. Figure 4.1 shows the distribution of sizes for nanomaterial NM-212 immediately after the sonication in BSA-water. In this case PdI was 0.19 ± 0.11 and Zav was around 311.4 ± 66.61 nm, where is localized the main peak. These results agree with Nanoreg benchmark data where Zav was 321.1 nm and PdI 0.31.

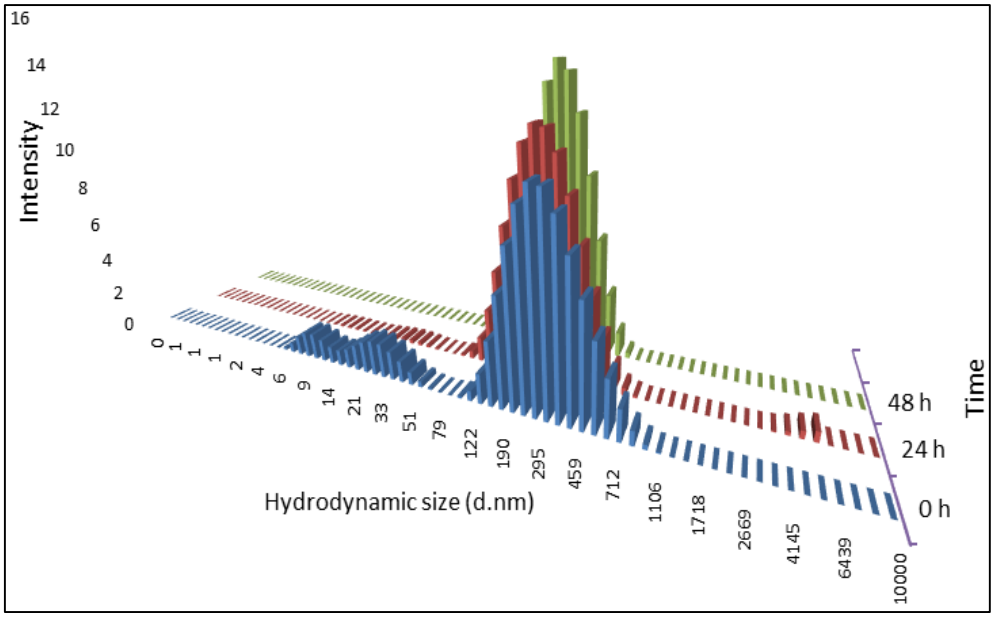

Figure 4. 2- Size distribution of NM- 212 for concentration 3.2 µg/mL in cell culture medium at 0, 24 and 48 hours after dispersion and incubation at 37ºC.

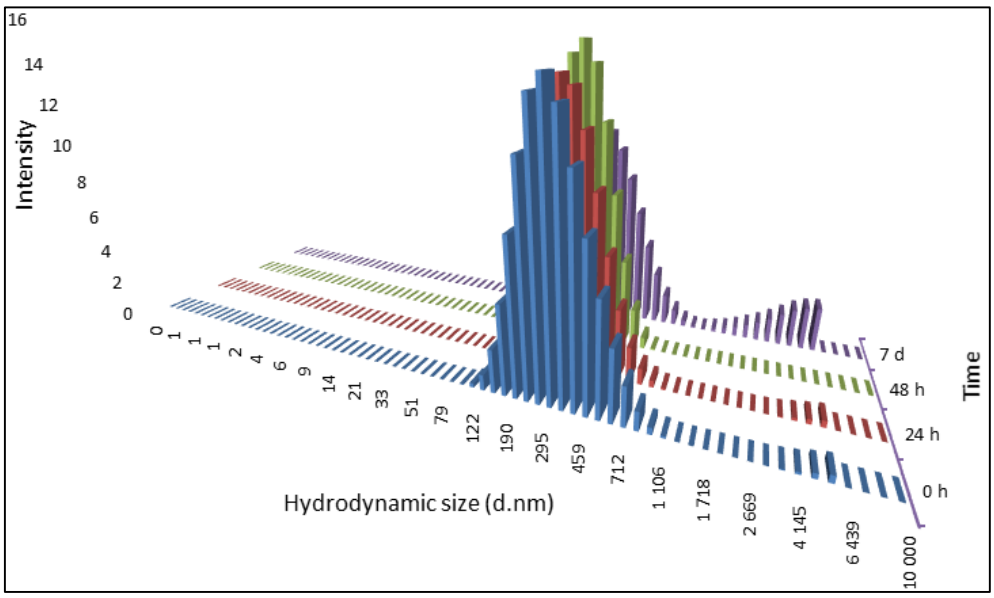

Figure 4. 3- Size distribution of NM- 212 for concentration 32 µg/mL in cell culture medium at 0, 24, 48 hours and 7 days after dispersion and incubation at 37ºC.

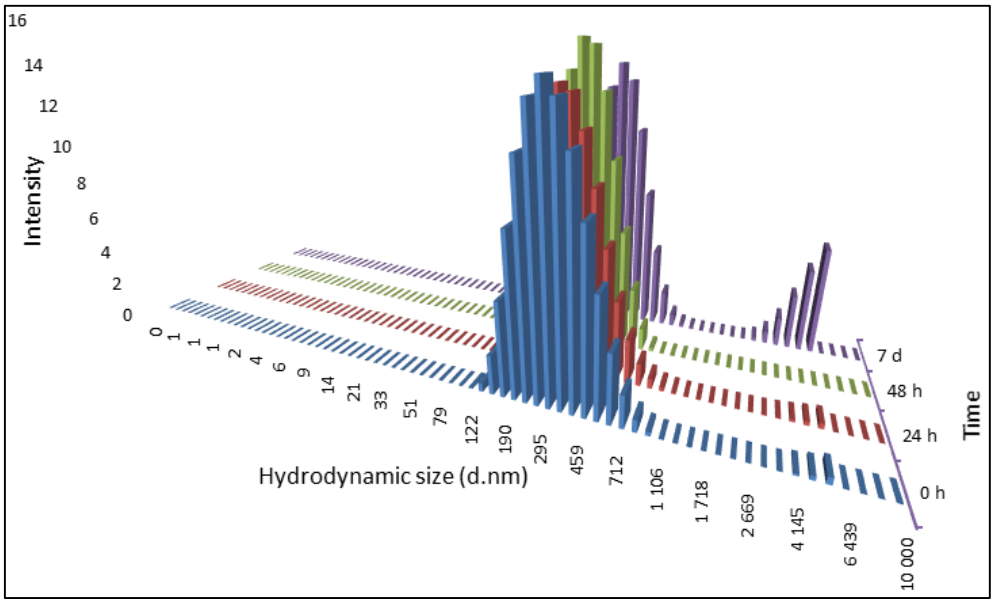

Figure 4. 4- Size distribution of NM- 212 for concentration 240 µg/mL in cell culture medium at 0, 24, 48 hours and 7 days after dispersion and incubation at 37ºC.

The figures 4.2., 4.3 and 4.4 present the size-distributions of each tested concentration (3.2, 32 and 240 µg/mL at different time points: right after the sonication, after 24 and 48 hours and 7 days. The PdI and Zav values are presented in table I.1 (see annexes). It is possible to see that the dispersion was stable in culture medium all over the time, since the peaks showed up well defined, with a fine dispersion. However, for concentrations 32 µg/mL after 7 days, a secondary peak appears and it was intensified in concentration 240 µg/mL also after 7 days. These secondary peaks may correspond to aggregated or agglomerated nanoparticles, since the Zav value also increases indicating an increment in particles size.

4.1.2 Cytotoxicity Assessment

To assess the possible cytotoxicity of each nanomaterial two assays were performed, with different times of exposure, namely the MTT (24h) and the clonogenic assay (7 days). Moreover, the CBPI and the RI obtained from the micronucleus assay give also a measure of the cells capacity to divide and proliferate and thereby the results of these indexes are also herein presented.

The results for MTT assay, following cells exposure to NM-212 during 24 hours are presented in figure 4.5. Although absorbance readings were made before and after microplates centrifugation (to reduce NPs interference in the colorimetric readings), the results before the centrifugation are the only ones here presented because any differences were detected between the two colorimetric readings.

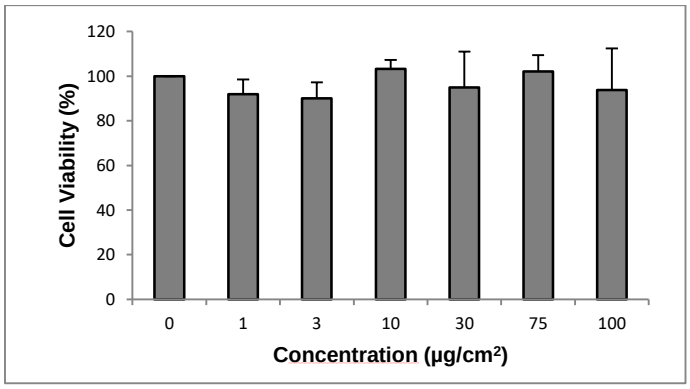

Figure 4. 5- Results for cell viabiliy after 24 hours of cells exposure to NM-212.

As can be observed, NM-212 did not have significant effects on cell viability (p=0.35) and no dose response could be detected. Positive control (SDS) led to a marked decrease in cell viability up to 34.72±2.59.

The clonogenic assay has a longer time of exposure and evaluates the capacity of a single cell to form a colony when it is exposed to NMs. The results obtained are presented in the figure 4.6.

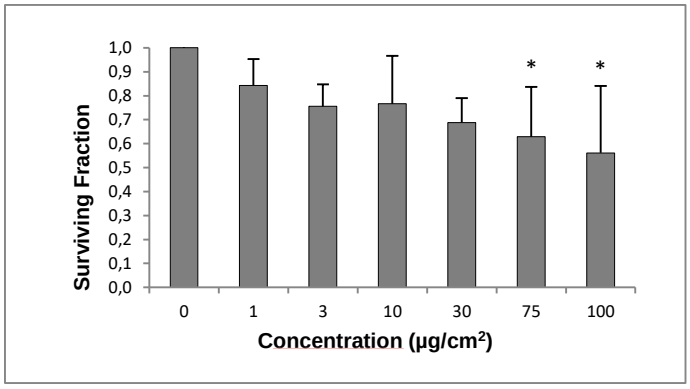

Figure 4. 6- Results of the clonogenic assay after 7 days cells exposure to NM-212. * Significantly different from the negative control (Tukey Post-Hoc test).

Significant differences were observed in the cells viability (or the surviving fraction) when the concentrations of CeO_2 nanomaterials increased (p=0,003). The SF of cells after exposure to the concentrations of 75 and 100 µg/cm^2 were significantly different from those of the negative controls (p=0.01 and p=0.002, respectively). However, no dose-response curve could be attributed to this NM. MMC induced significant decreases in SF when compared with negative control (p=0.001).

The results of the CBPI and RI are displayed in Figures 4.7- A and B, respectively.

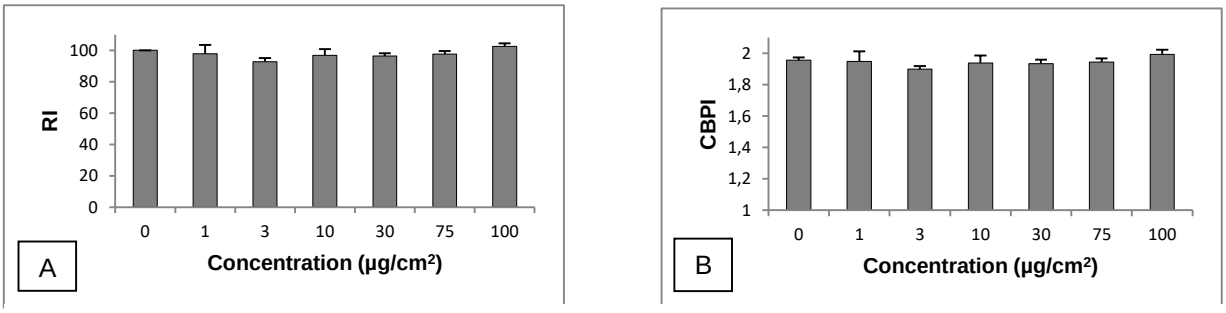

Figure 4. 7- A- Results of RI after 48 hours of exposure to NM-212; B- Results of CBPI after 48 hours of exposure to NM-212.

As can be seen, CeO_2 NMs did not any variation in these indexes, irrespectively of the concentration tested

A significant difference was seen in the CBPI and RI values when comparing the positive control (MMC) with the negative control (p<0.001 and p=0.01 respectively).

4.1.3 Genotoxicity Assessment

To quantify the breaks in DNA and oxidative stress arising from cells exposure to nanomaterials, the modified comet assay with FPG was employed with two different time points: 3 and 24 hours. The results are shown in Figures 4.8-A (3 hours) and 4.8-B (24 hours).

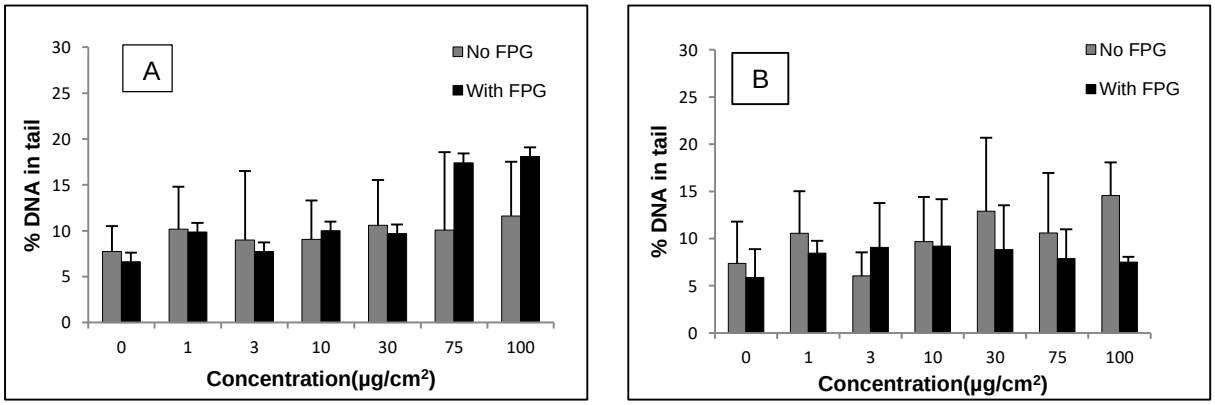

Figure 4. 8- A- % of DNA in tail after 3 hours of cells exposure to NM-212. B- % of DNA in tail after 24 hours of cells exposure to NM-212.

In the Figure 4.8-A it is possible to see that there is a two-fold increase in % of DNA in tail for the FPG results at the highest concentrations tested, although not reaching statistical significance.

The exposure to the positive control (EMS) yield significant differences in DNA damage, with FPG (p=0.001 and p=0.002, for the experience with 24 and 3 hours exposure, respectively), or without FPG (p=0.015 and p=0.577, for the experience with 24 and 3 hours exposure, respectively). The values for % DNA in tail corresponding to EMS results are presented in table III-2 and III-4 (annex III).

This cytokinesis-blocked micronucleus assay is more accurate to identify permanent damages in DNA cells (comparing with Comet assay), that results from DNA breakage or loss and remains in daughter cells after division. The results for this assay are presented in Figure 4.9.

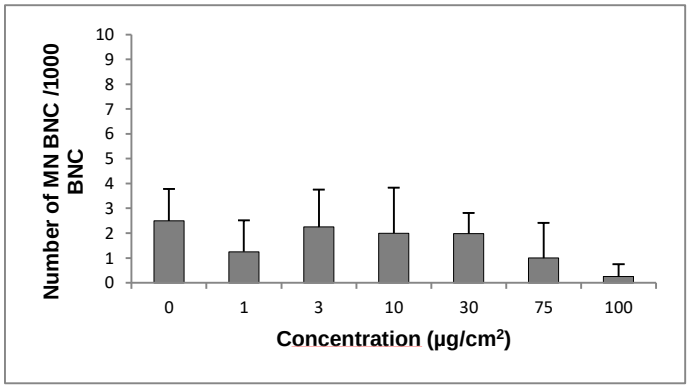

Figure 4. 9- Micronucleated binuclated cells after 48 hours of exposure to NM-212. In CBMN assay the micronucleus frequency was not increased when the cells were exposed to CeO_2 nanomaterials. The statistical analysis did not show significant differences between any of the NM concentrations tested and the negative control. MMC, used as a positive control, significantly increased the MN frequency over the negative control leading to a value of MNBNC of 21.96±8.43 (p<0.001).

4.2 Titanium dioxide nanomaterials

4.2.1. Characterization of nanomaterial dispersion in the culture medium

As shown in Figure 4.10 the dispersion of NM-100 was achieved and the range of size distribution is relatively low (PdI= 0.18±0.02) and Zav value of 239.5±5.95 nm. These values are similar to the NANoREG benchmark values of batch dispersions – 235.9 nm for Zav and 0.16 for PdI.

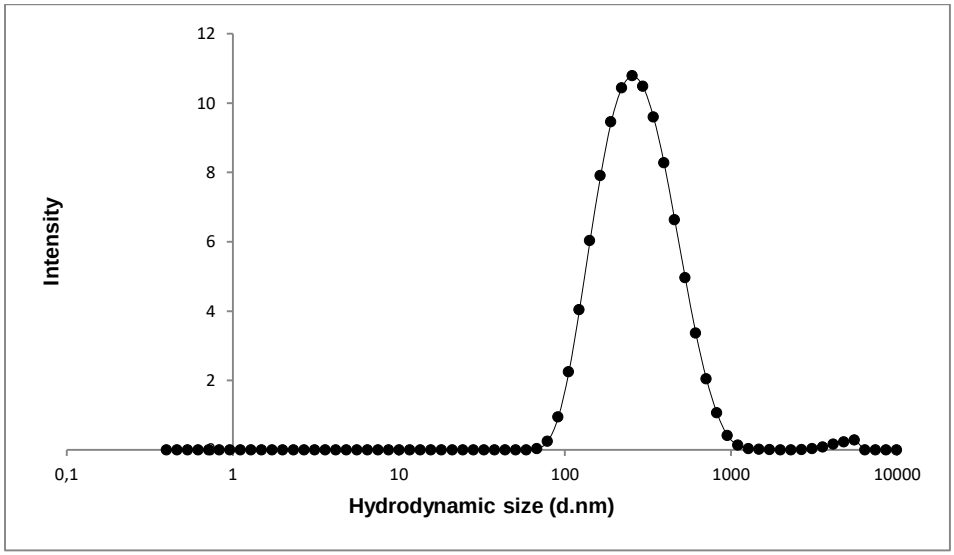

Figure 4. 10- Size distribution of the batch dispersion of NM-100 (2.56 mg/mL) soon after the sonication in BSA water 0.05%.

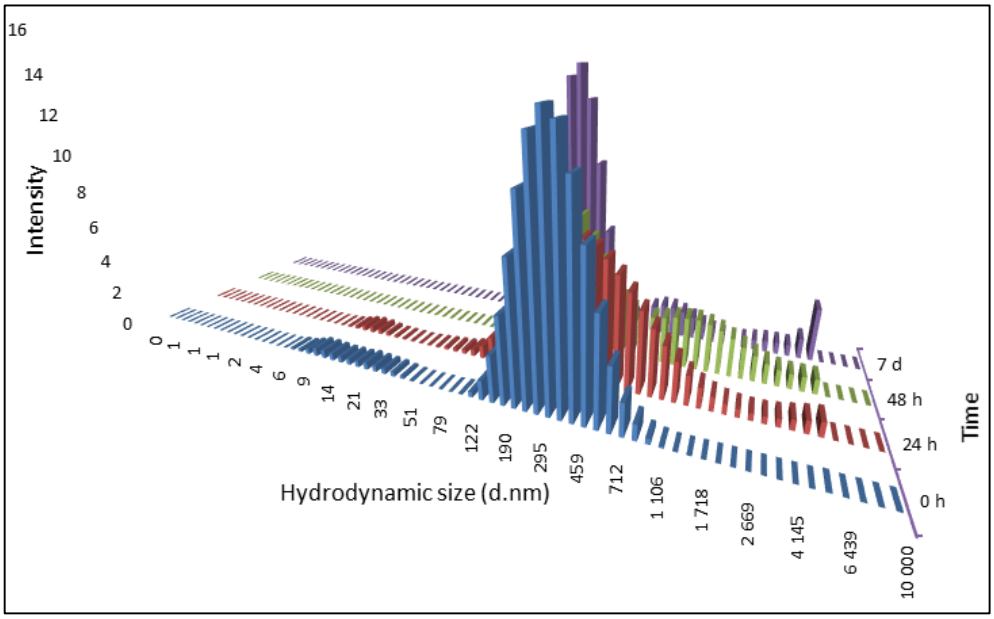

Figure 4. 11- Size distribution of NM-100 for concentration 3.2 µg/mL in cell culture medium at 0, 24, 48 hours and 7 days after dispersion and incubation at 37ºC.

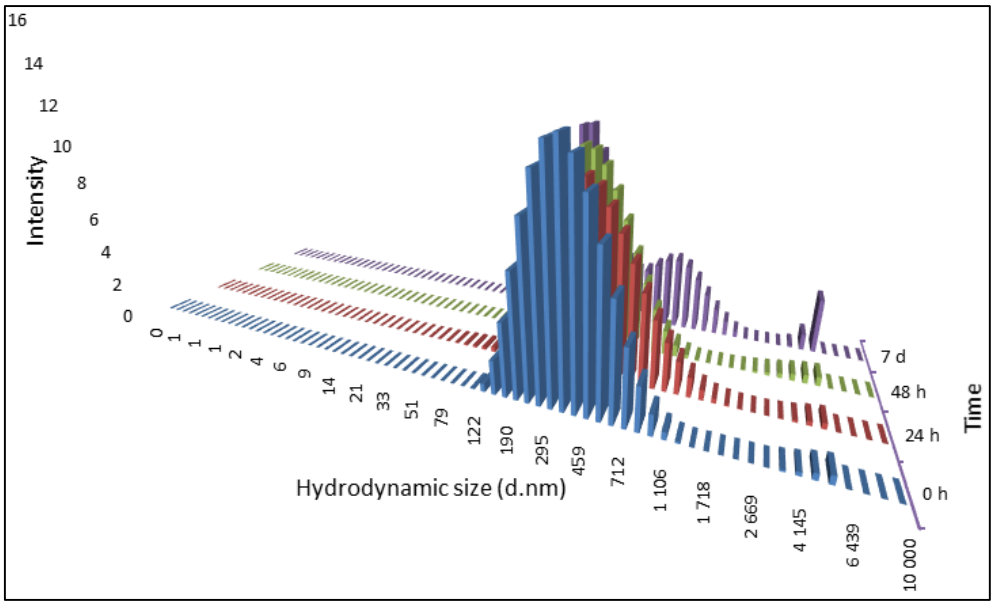

Figure 4. 12- Size distribution of NM- 100 for concentration 32 µg/mL in cell culture medium at 0, 24, 48 hours and 7 days after dispersion and incubation at 37ºC.

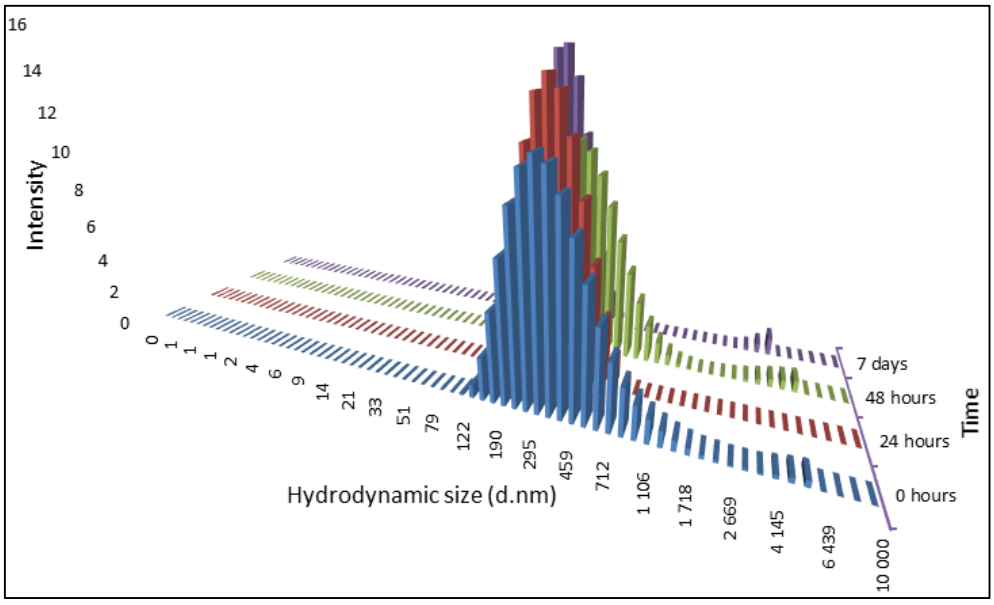

Figure 4. 13- Size distribution of NM- 100 for concentration 240 µg/mL in cell culture medium at 0, 24, 48 hours and 7 days after dispersion and incubation at 37ºC.

This nanomaterial remained relatively stable over time for the three tested concentrations. Nevertheless, there are some particularities that should be noted as the light increase of PdI and Zav for concentrations of 3.2 and 32 µg/mL after 7 days in the culture medium, which possibly means an increase in size distribution and particle size (probably derived from particle agglomeration/aggregation). This observation can also be noticed from the graphs when a secondary peak is present after the main peak.

For NM-101, the Zav is higher than for NM-100, with a value of 487.1±13.5 nm and a PdI of 0.35±0.03. These data present an unimodal size distribution, since PdI value is relatively small. Values are consistent with NANoREG benchmark values (0.28 and 426.2 nm for PdI and Zav values, respectively).

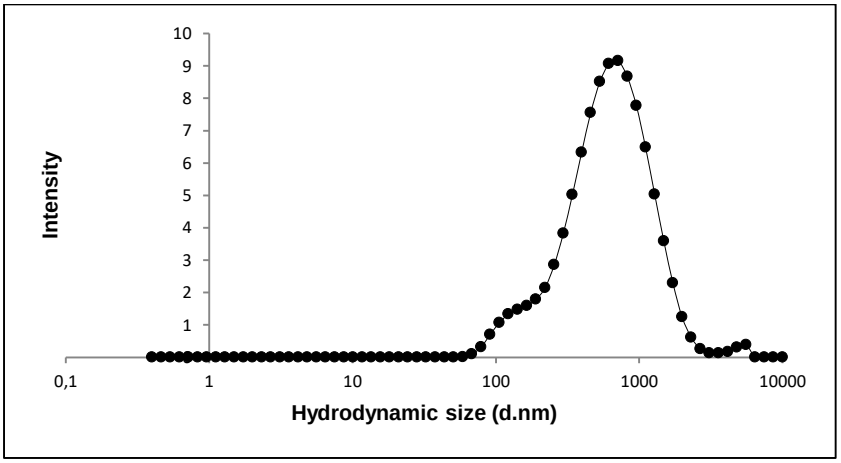

Figure 4. 14- Size distribution of the batch dispersion of NM- 101 (2.56 mg/mL) soon after sonication protocol in BSA water 0.05%.

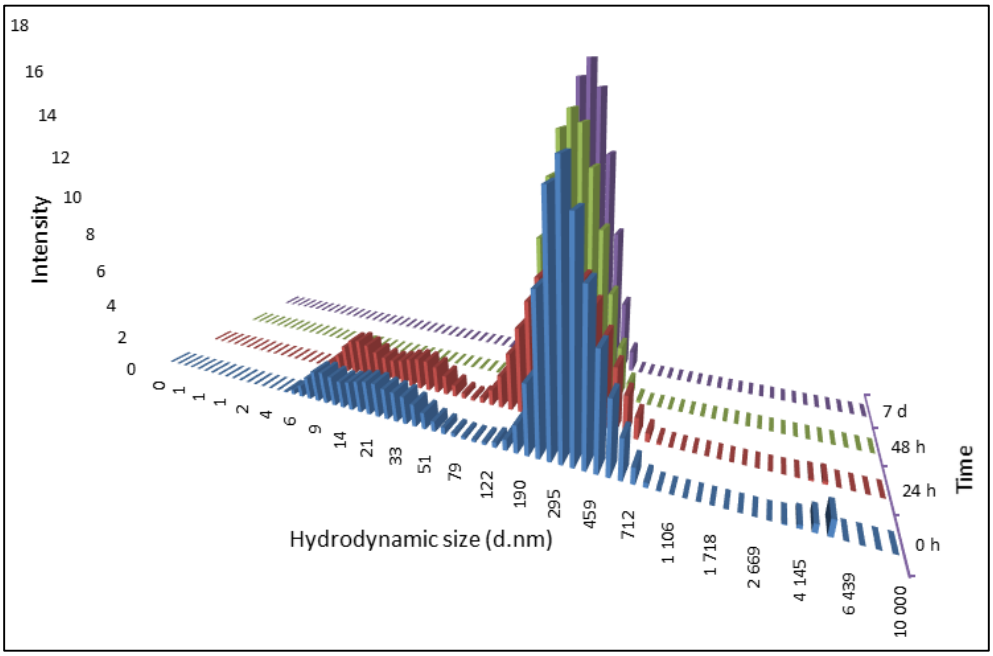

Figure 4. 15- Size distribution of NM- 101 for concentration 3.2 µg/mL in cell culture medium at 0, 24, 48 hours and 7 days after dispersion and incubation at 37ºC.

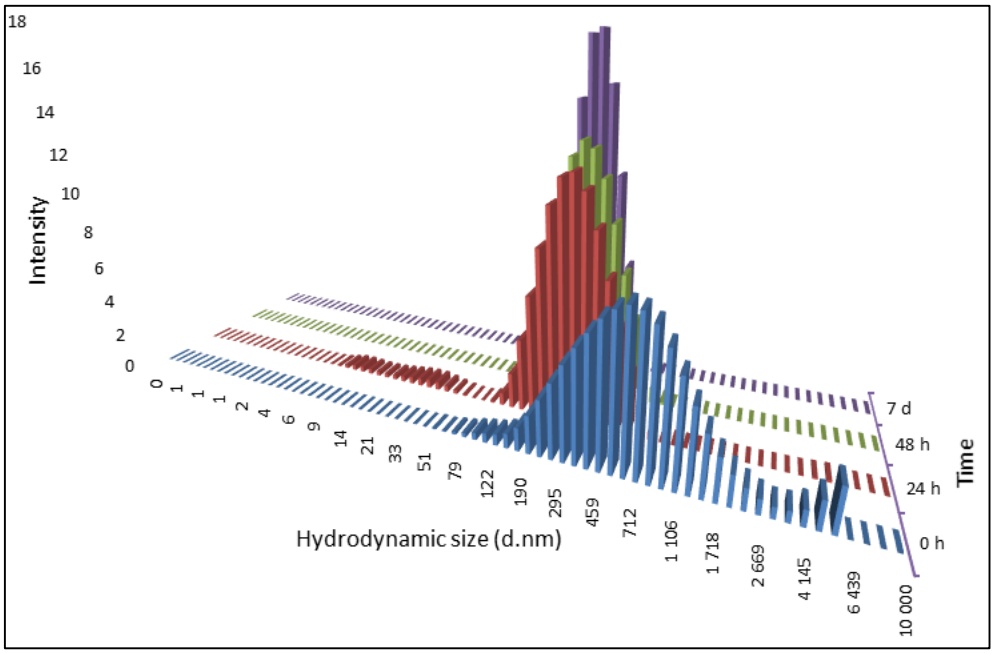

Figure 4. 16- Size distribution of NM- 101 for concentration 32 µg/mL in cell culture medium at 0, 24, 48 hours and 7 days after dispersion and incubation at 37ºC.

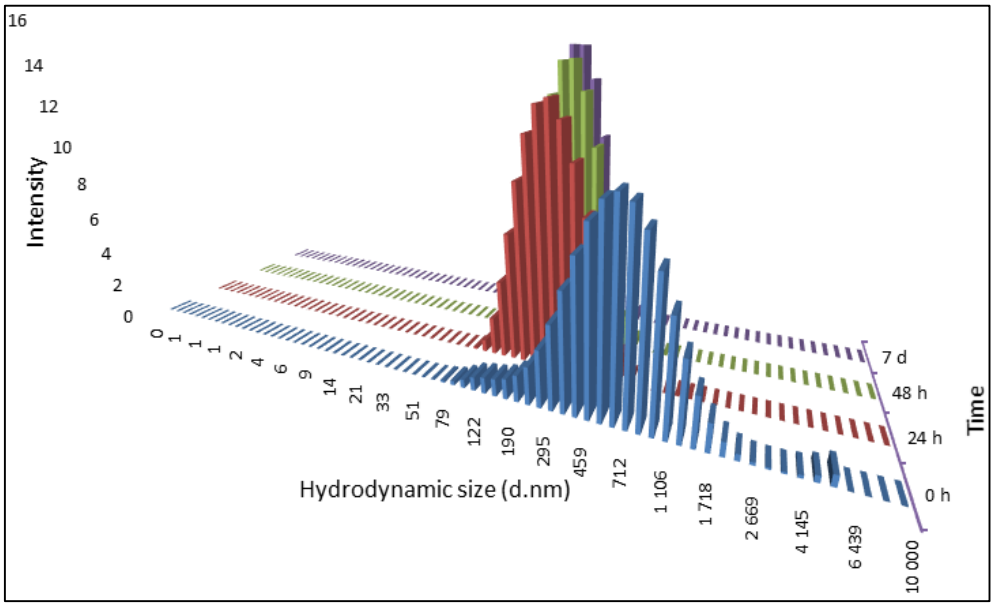

Figure 4. 17- Size distribution of NM- 101 for concentration 240 µg/mL in cell culture medium at 0, 24, 48 hours and 7 days after dispersion and incubation at 37ºC.

When the batch dispersion of NM-101 was diluted in culture medium, it was observed, through DLS results, that the Zav decreased and the PdI increased, showing that the dilution in such medium affected the size distribution. After 24 hours the concentration 3.2 µg/mL is the most critical one because

the correspondent PdI is 0.94, compatible with a multimodal distribution. Also, measurements referent to concentrations of 32 and 240 µg/mL indicate higher particle size immediately after sonication but in the other tested time points the particle size and PdI decreased (peak shifted to the left), suggesting the deposition of the larger particles with the incubation period and a stable dispersion of the smallest NPs.

4.2.2 Cytotoxicity Assessment

The results of the MTT assay in A549 cells after the exposure to titanium dioxide nanomaterials during 24 hours are presented in Figure 4.18.

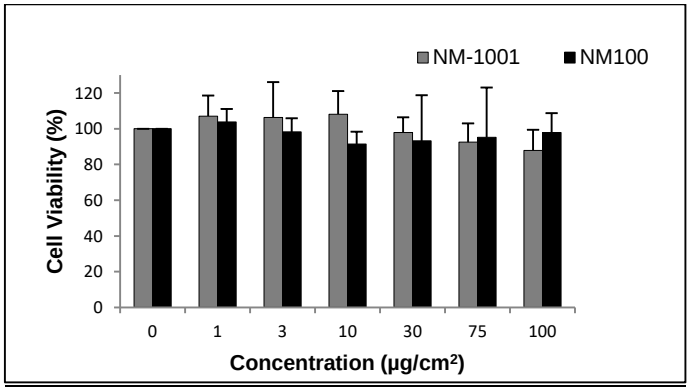

Figure 4. 18- Results for cell viabiliy after 24 hours of exposure to NM-101 and NM- 100.

Neither NM-100 nor NM-101 caused significant decreases in cell viability, while the positive control decreased significantly the viability as compared to negative controls (p<0.001 and p=0.001 for NM-100 and NM-101, respectively). Likewise, the CBPI and RI results (figures 3.21 and 3.22 respectively) did not show any alteration or any relevant cytotoxicity for NM-100. However it was possible to see a sharp decrease of these indexes for MMC (table II-3 in annex II).

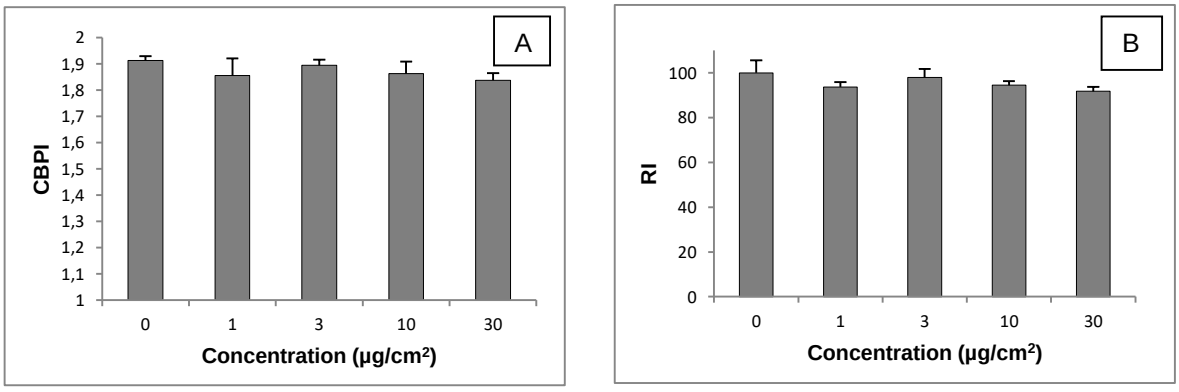

Figure 4. 19- A- Results of CBPI after 48 hours of exposure to NM-100; B- Results of RI after 48 hours of exposure to NM-100.

4.2.3 Genotoxicity Assessment

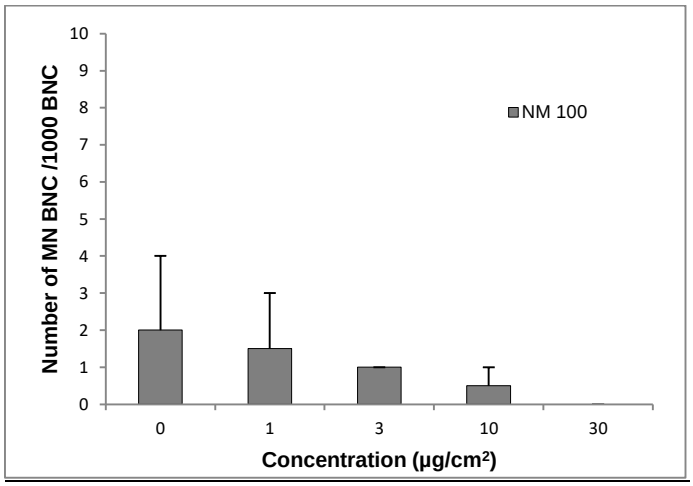

Figure 4. 20- Micronucleated binuclated cells after 48 hours of exposure to NM-100. The concentration 30 µg/cm^2 does not present any bar because the number of micronuclei scored was 0.

The frequency of micronuclei in binucleated cells was not significantly increased when A549 cells were exposed to NM-100 and comparing the results of the tested concentrations with those of the negative control. Concerning the frequency of micronuclei following exposure to MMC, the frequency was 12.50±12.02 micronuclei per 1000 BNC (p<0.001). However, not all slides were analyzed beacuse in higher concentrations (75 and 100 µg/cm^2) the large amount of nanomaterials accumulated over the cells and did not allow micronucleus scoring. In the Figure 4.21 it is possible to observe some of these situations.

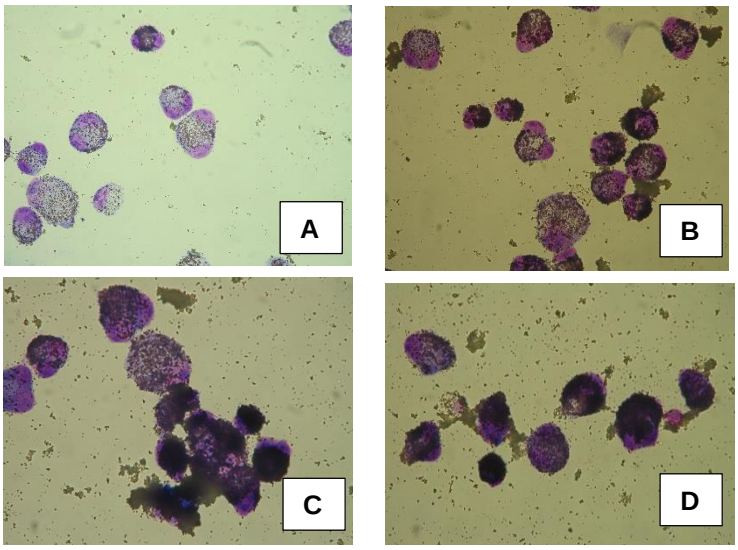

Figure 4. 21- Microscopical photos of A549 cells after 48 hours exposure to NM-100 (10x40). A- 30 µg/cm^2 ; B- 75 µg/cm^2; C and D- 100 µg/cm^2. It is visible the increase of NM when the concentrations increase.

The results of the comet assay following 3 and 24 hours cells exposure to NM-100 are graphically presented in Figures 4.22-A and 4.22-B .

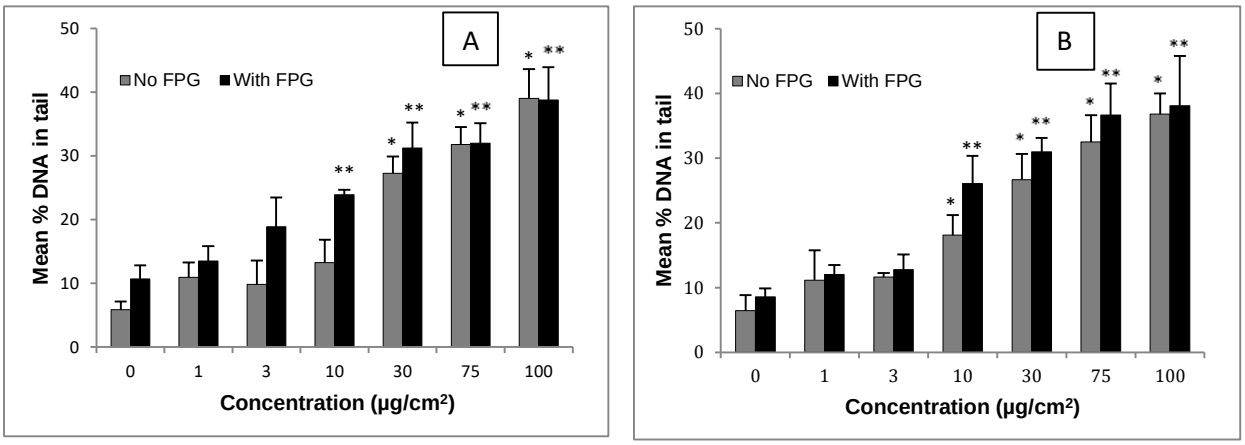

Figure 4. 22- A- % of DNA in tail after 3 hours of exposure to NM-100. *- significantly different from the control without FPG; **-significantly different from the control with FPG; B- % of DNA in tail after 24 hours of exposure to NM-100. *- significantly different from the control without FPG; **-significantly different from the control with FPG.

At 3 hours of exposure a significant overall increase in the level of DNA breaks was observed over the negative control both, with or without FPG treatment (p<0.0001). Pairwised comparisons showed that the level of DNA damage (without FPG treatment) induced by NM-100 concentrations of 30, 75 and 100 µg/cm^2 was significantly increased over the control level (p<0.001). The DNA damage measured after FPG treatment was significantly increased in concentrations higher than 10 µg/cm^2 (p<0.001).

The best fit-model found was a linear function, but it was only possible to adjust the results obtained without FPG. The dose-response relationship, for 3 hours of exposure, can be described through the linear equation $y = 0.303x + 10.237$ with R^2= 0.86 (p<0.001, ANOVA test; p<0.001, t-Student test, for the coefficients).

The results for 24 hours exposure (Figure 4.22-B) similarly showed a significant increase in the level of DNA damage over the control for the treatment with and without FPG (p<0.001, One-way ANOVA test). Pairwised comparisons showed significant increases in the level of DNA damage for concentrations of 10, 30, 75, 100 µg/cm^2 (p≤0.001) over the control, irrespectively of the FPG treatment. The results for 24 hours exposure without FPG can be described through the following equation: $y = 0.272x + 11.958$ with R^2= 0.82 (p<0.001, ANOVA test; p<0.001, t-Student test for the coefficients). The dose-response relationship for the results of 24 hours with FPG can be represented through a quadratic equation: $y = -0.005x^2 + 0.776x + 11.991$, with a correlation R^2=0.84 and significant parameters (p<0.001, ANOVA test; p<0.001, t-Student test).

Comparing the results obtained with or without FPG, significant differences were observed after 3h exposure for the concentrations of 3 and 10 µg/cm^2 (p= 0.023 and 0.008, respectively, Student's t-

test) whereas at 24h exposure the only significant difference was observed for the 10 µg/cm^2 (p= 0.024). These data are suggestive of the induction of oxidative DNA lesions under these conditions.

For both assays, 3 and 24 hours, with and without FPG, EMS concentration showed significant increases in the level of DNA damage p value < 0.001.

Figure 4.23 represent a microphotography of a comet formed in A549 cells after exposure to NM-100 (10x20). When the slides of comet assay were analyzed it was possible to observe brightest comets due the deposition on titanium dioxide nanomaterials (and it was for both nanomaterials, NM-100 and NM-101). In the image below it is observable that the head of the comet is brighter than the tail.

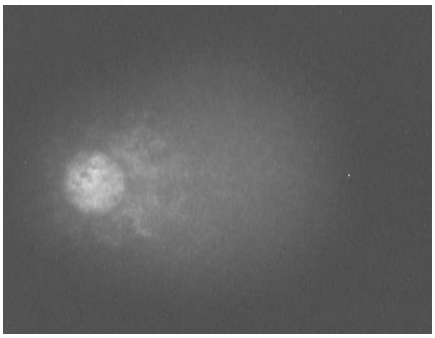

Figure 4. 23- Microphtography of a comet obtained after exposure to NM-100.

The results obtained from Comet assay in cells exposed to NM-101 during 3 and 24 hours are displayed in the Figures 4.24- A and 4.24- B.

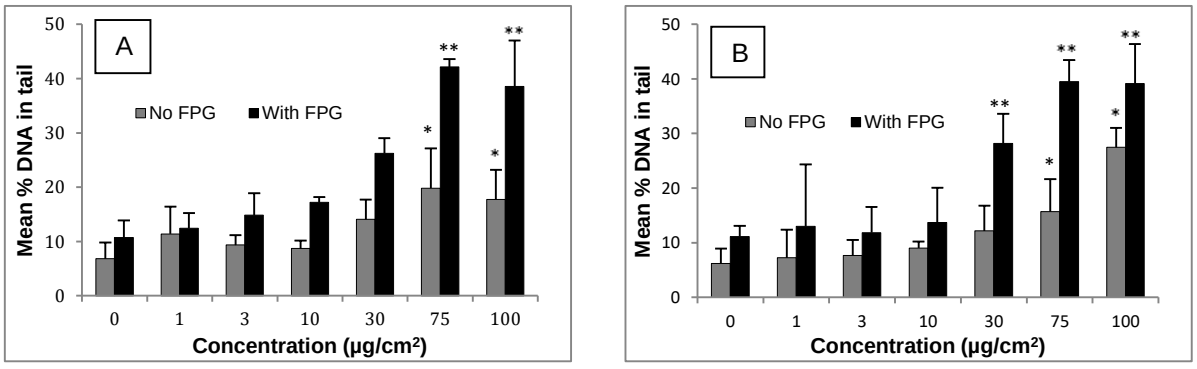

Figure 4. 24- A- % of DNA in tail after 3 hours of exposure to NM-101. *- significantly different from the control without FPG; **-significantly different from the control with FPG; B- % of DNA in tail after 24 hours of exposure to NM-101. *- significantly different from the control without FPG; **-significantly different from the control with FPG.

In Figure 4.24-A the results of the comet assay with 3 hours cells exposure to NM-101 are presented. Considering the overall results, significant increases were observed in DNA damage with or without FPG (p<0.001). Pairwised comparisons showed significant differences between the results

obtained for the 75 or 100 µg/cm^2 and the negative control (p= 0.003 and p=0.014, respectively), without FPG. Concentrations of 30, 75 or 100 µg/cm^2 with FPG yielded significant increases of DNA damage over the negative control (p<0.001) with FPG.

A dose-response relationship was detected for the results of FPG-comet assay after 3 hours of exposure with a linear function whose equation is $y = 0.303x + 13.694$, with R^2=0.87(p<0.001, ANOVA test; p<0.001, t-Student test of all the parameters). On the other hand, no dose-response was determined for the data without FPG.

Following the 24h-exposure, there were significant differences in the cells exposed to NM-101 with or without FPG (p≤0.001). For this timepoint, pairwised comparisons showed significant differences in DNA damage after the concentrations of 75 and 100 µg/cm^2 (p= 0.004 and p<0.001,), without the FPG enzyme, while the results with the enzyme for 30, 75 and 100 µg/cm^2 showed significant increases in DNA damage (p<0.013). Dose-response effects were observed that corresponded to quadratic functions: $y = -0.004\,x^2 + 0.667x + 10.469$, R^2= 0.82, without FPG (p<0.001, ANOVA test; p<0.01, Student's t-test for the parameters) and $y = -0.001\,x^2 + 0.035x + 7.547$, R^2= 0.82, with FPG (p<0.001, ANOVA; t-Student test of the coefficients are not significant).

At both timepoints, significant increases in DNA damage were observed when using FPG assay, as compared to the conventional comet, at the two highest concentrations (p≤0.001), showing the induction of oxidative DNA lesions by NM-101.

For both timepoints and for both conditions, with and without FPG, the positive control- EMS showed significant increases in DNA damage when compared with the negative control (p<0.003).

4.3 Barium sulphate nanomaterials

4.3.1 Characterization of nanomaterial dispersion in the culture medium for NM-220

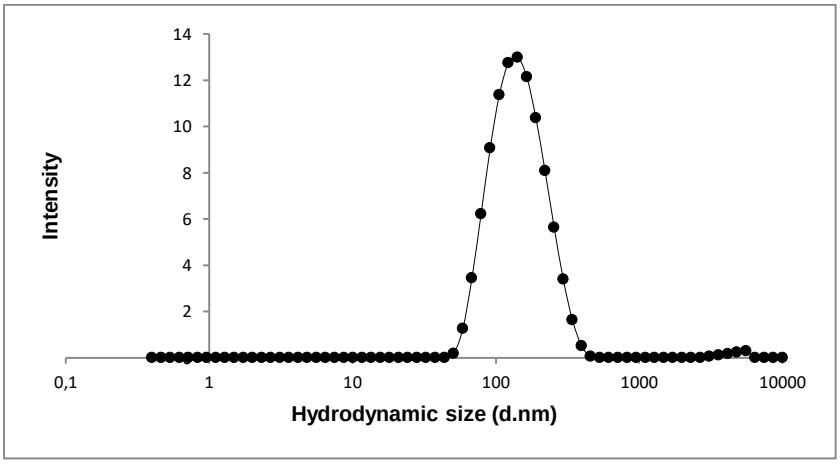

Figure 4. 25- Size distribution of the batch dispersion of NM- 220 (2.56 mg/mL) soon after the sonication in BSA water 0.05%.

For NM-220 a homogenous batch dispersion in BSA water 0.05% was achieved The Zav obtained was 133.95±1.25 nm and the PdI=0.18±0.01, which is in accordance with the NANoREG benchmark - 118 nm for Zav and 0.12 for PdI.

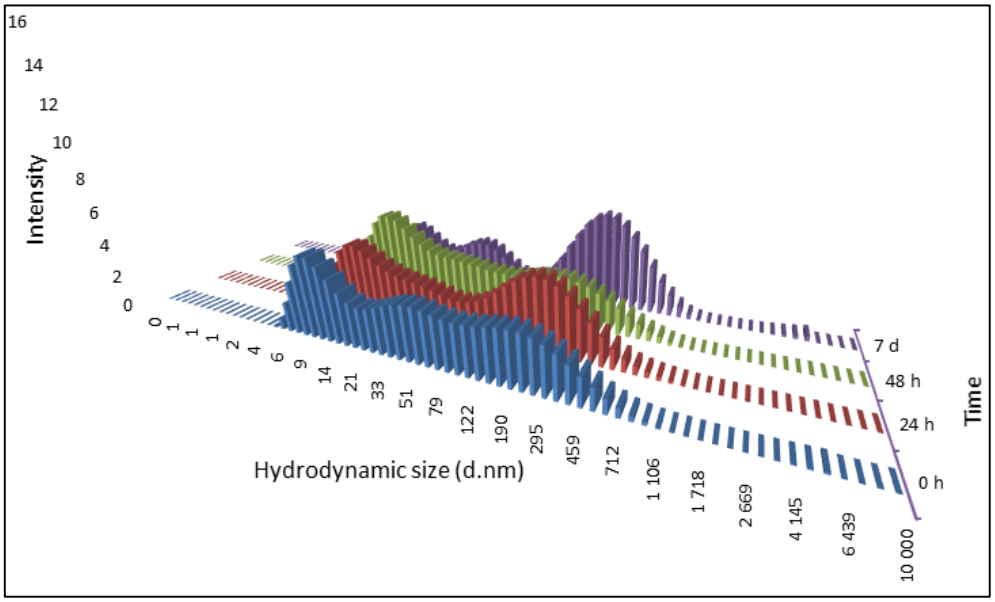

Figure 4. 26- Size distribution of NM- 220 for concentration 3.2 µg/mL in cell culture medium at 0, 24, 48 hours and 7 days after dispersion and incubation at 37ºC.

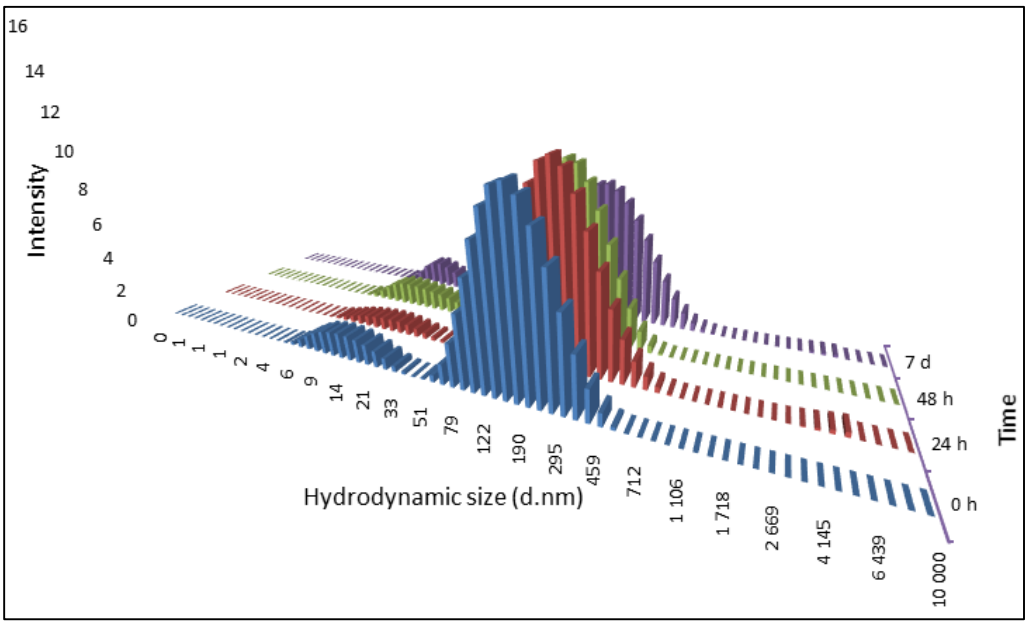

Figure 4. 27- Size distribution of NM- 220 for concentration 32 µg/mL in cell culture medium at 0, 24, 48 hours and 7 days after dispersion and incubation at 37ºC.

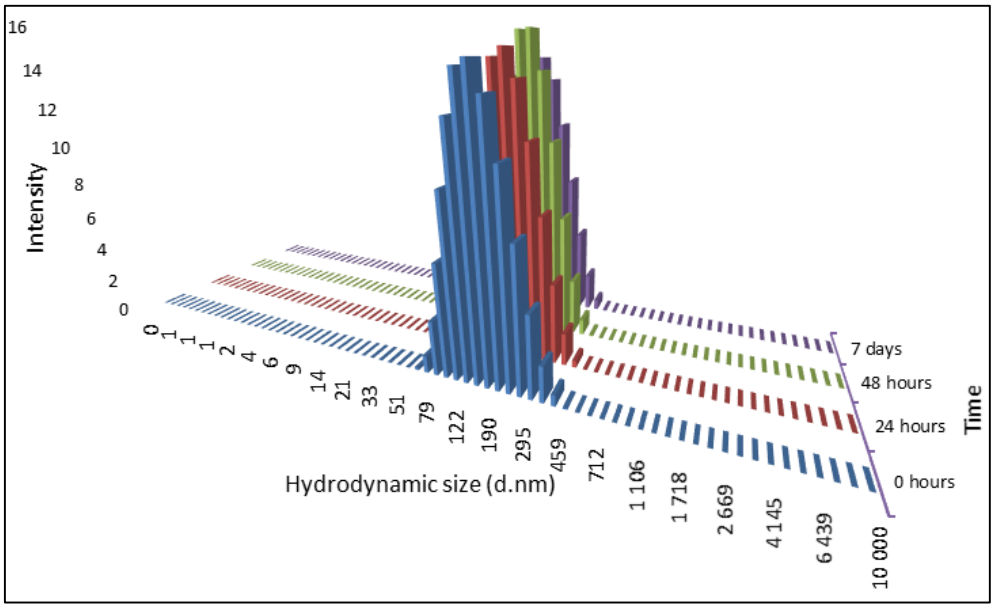

Figure 4. 28- Size distribution of NM- 220 for concentration 240 µg/mL in cell culture medium at 0, 24, 48 hours and 7 days after dispersion and incubation at 37ºC.

From the graphs above and the values presented in the correspondent table (annex I.4) it is possible to verify that the coarsest dispersion in the culture medium occurs for the concentration of 3.2 µg/mL. The PdI values indicate a broad range of size distribution and a small particle size. However the PdI is smaller for concentrations 32 and 240 µg/mL when this values decrease. It is also observable that the nanoparticle size greatly increases for the last two concentrations, probably due the formation of aggregates/agglomerates. It is also easily noted from all the graphs that when concentrations rise the dispersions change from coarse to finest, possibly because the larger agglomerates tend to become deposited and the single NPs remain stably dispersed.

4.3.2 Cytotoxicity Assessment

The data obtained for the assay with 24 hours exposure is presented in Figure 4.29.

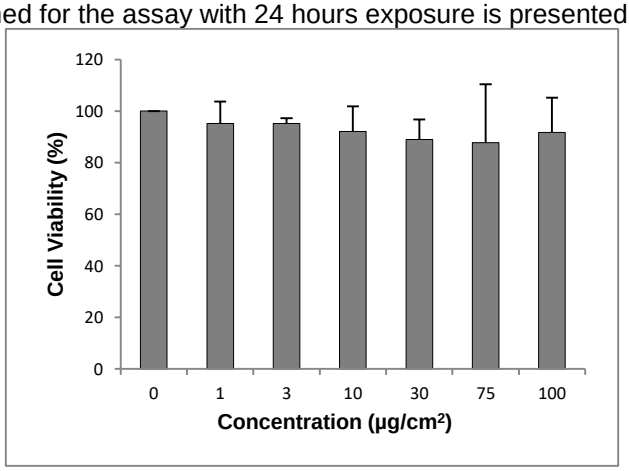

Figure 4. 29- Results for cell viabiliy after 24 hours of exposure NM- 220.

There were not significant differences between the negative control and the other NMs' concentrations (p=0.67). However, as expected, SDS 0.01% did show significance comparing to negative control (p<0.001).

Similarly, the CBPI and RI values (Figure 4.30) did not show any significant difference comparatively to the control value (p=0.08). The positive control decreased both indexes although not significantly (details in table II.3 in the annex).

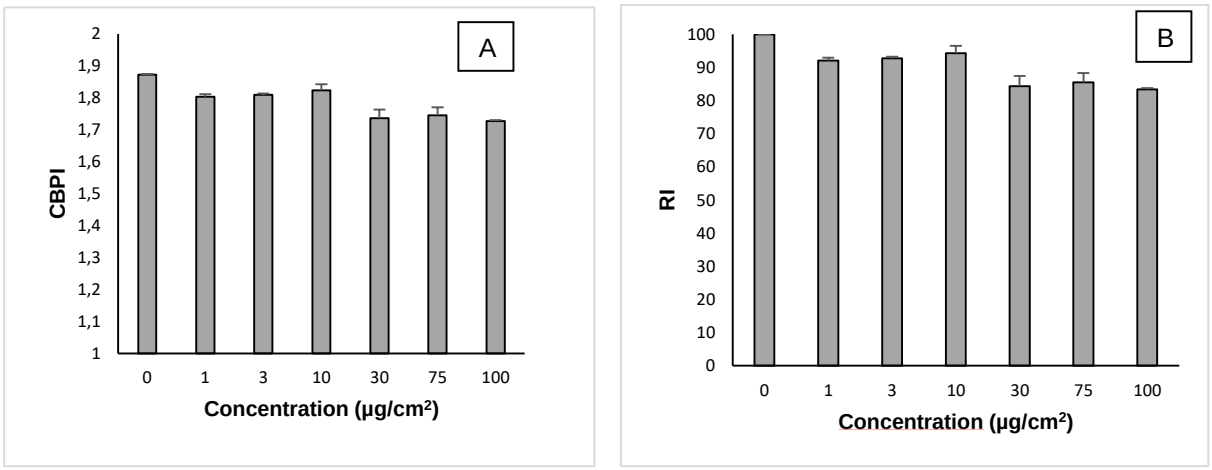

Figure 4. 30- A- Results of CBPI after 48 hours of exposure to NM-220; B- Results of RI after 48 hours of exposure to NM-220.

4.3.3 Genotoxicity Assessment

The results for the micronucleus assays are represented in Figure 4.31.

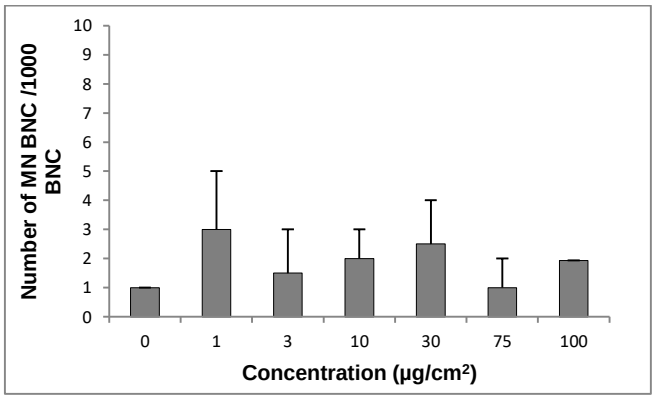

Figure 4. 31- Micronucleated binuclated cells after 48 hours of exposure to NM-220.

The frequency of micronuclei of A549 cells exposed to $BaSO_4$ NMs was not significantly increased over the control. The results for MMC showed a significance of (p<0.001).

The results of DNA breaks correspondent to NM-220 are represented in the Figures 4.32-A and 4.32- B. Figure 4.32- A correspond to 3 hours of exposure and the Figure B corresponds to 24 hours of exposure.

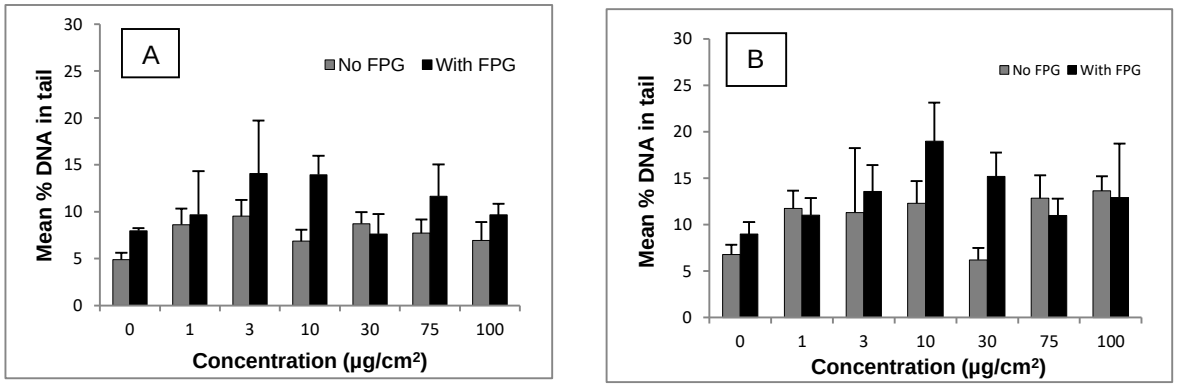

Figure 4. 32- A- % of DNA in tail after 3 hours of exposure to NM-220; B- % of DNA in tail after 24 hours of exposure to NM-220.

As can be seen, any marked increase in the level of DNA breaks was detected after 3 hours and 24 hours of cells exposure to barium sulphate nanomaterials. Nevertheless, a two-fold increase in the level of DNA damage was noted after treatment with 3 and 10 µg/cm^2 (3h) or with µg/cm^2 (24h) by the FPG-modified assay suggesting a slight induction of oxidative DNA damage. However, any statistically significant differences were detected both for the shorter and the longer exposure durations, with and without the FPG enzyme.

Only the positive control for 3 hours of exposure without FPG showed significance (p=0.001); however the remaining results in tables III.1 and III.2 in the annex III show an increase in DNA breaks after EMS exposure.

4.4. Overview of the cytotoxicity and genotoxicity assessment of the tested NMs

In Table 4.1. an overview of the assays performed as well as the results obtained is presented.

Table 4. 1- Overview of the results of cyto- and genotoxicity obtained for NM-212, NM-101, NM-100 and NM-220.

	NM-212	NM-101	NM-100	NM-220
MTT assay	-	-	-	-
Clonogenic assay	+	+*	-*	-*
CBMN assay	-	-*	-	-
Comet assay- 3h	-	+	+	-
Comet assay – 3h with FPG	-	+	+	-
Comet assay- 24h	-	+	+	-
Comet assay- 24h with FPG	-	+	+	-

- negative results; + positive results; * done by another team member

5. DISCUSSION

The synthesis and production of metal oxide NPs are consistently expanding due to their distinctive physico-chemical characteristics and increasing industrial and medical applications (Saquib et al. 2012). This has evoked serious concerns about their potential impact on the environment and human health and constitutes an additional challenge for the regulatory authorities (Saquib et al. 2012; Park et al. 2008).

Current knowledge is still unsystematic, not well understood and restricted to particular aspects of NPs' capability to induce toxic and pathological processes or to alter the structure and function of different cell types (Pagliari et al. 2012; Park et al. 2008). Recent data have suggested that nanoparticles exposure is often associated to increases in cellular ROS, that can originate at the particle surface as a result of the material semiconductor or electronic properties as well as the capability of some materials to perturb electronic transfer processes in cell such as in the mitochondrial inner membrane (Rim et al. 2012; Park et al. 2008).

To date, there are few studies directly investigating the toxicity of these nanoparticles and making a comparison of their subsequent toxic effects. It is known that cellular effects of nanoparticles are strongly dependent on chemical and structural characteristics, surface/mass ratio, solubility, and shape (Qiang et al. 2013). Nanomaterials are composed of primary and agglomerated particles that can vary in size (actually, the sizes of the particles in suspension are different from the original primary size) shape, charge, crystallinity, chemical composition and other characteristics, and this variety will increase even further in the future (Braakhuis et al. 2014; Qiang et al. 2013). Thus, an adequate risk assessment of nanomaterials requires information on both the exposure and hazard of their component particles (Braakhuis et al. 2014).

Inhalation is considered to be an important route of exposure to nanoparticles, especially in occupational and consumer settings (Braakhuis et al. 2014). The most reported effect is pulmonary inflammation, largely indicated by an influx of neutrophils that can be observed in the broncho-alveolar lavage fluid in rodents and the induction of inflammatory cytokines in *in vitro* lung models (Braakhuis et al. 2014). Comparison across studies is often difficult due to the use of different experimental protocols and choice of endpoints, which largely influences the results.

Another important point to underline is that after deposition, some agglomerates can disagglomerate into the primary particles, or primary particles can agglomerate after contact with the protein-rich cells culture medium or with the lung lining fluid *in vivo* (Braakhuis et al. 2014). A deagglomeration mechanism, enhanced by the acidic environment close to the lipid nuclear membrane, is proposed to explain those findings. Upon internalization in the nucleus, the nanoparticles reagglomerate and are observed as larger agglomerates under electronic microscopy. These findings are important for understanding the toxicity of nanoparticles, and provide evidence of the possibility of direct (or short-distance) interactions between nanoparticles and DNA as a cause of genotoxicity (Ahlinder et al. 2013).

5.1 The analysis of the NMs dispersion

To avoid aggregation and obtain stable suspensions, NMs are usually sonicated and well dispersed before the assays.

In this work a general increase in the primary size of the nanomaterials was observed when they entered into contact with aqueous medium. This observation has been reported in other works and it was found that metal oxides adsorb medium components such as Ca^{2+} and serum proteins, which then affects their agglomeration/aggregation state and size distribution (Panas et al. 2014). Hence, agglomeration commonly occurs when particles are introduced into the aqueous medium (Shukla et al. 2011). Although all nanomaterials initially adsorb similar amount of serum from the media, the total amounts of adsorbed protein decreased with time and the extent of protein desorption was material dependent (Panas et al. 2014; Konduru et al. 2014). The size of the aggregates seemed to be concentration-dependent, i.e., the higher the concentration, the larger the hydrodynamic diameter (Panas et al. 2014; Konduru et al. 2014). This suggests that only a fraction of the nanoparticles exposed to the cells exist as single particles, given that NPs tend to aggregate in the culture medium (Eom and Choi 2009).

Due to the adsorption of medium components at the NPs surface forming the so-called protein corona, the NPs acquire a secondary size and also secondary physicochemical properties (Bruinink, Wang, and Wick 2015). However, despite the formation of aggregates, the NPs still are able to exert toxicity. It was demonstrated that aggregates of TiO_2 NPs (1.44 μm) have been more toxic than similarly sized aggregates of their larger counterparts (Johnston et al. 2009). It was also demonstrated the ability of CeO_2 NPs to form aggregates/ agglomerates (Bruinink, Wang, and Wick 2015).

5.2 Cytotoxicity and genotoxicity of CeO_2 nanomaterials

In this work two different cytotoxicity assays were performed. The colorimetric assay, MTT, had a time of exposure of 24 hours and did not show any decrease in cellular viability following cells exposure to CeO_2, indicating that these NPs do not interfere with the mitochondria function. Likewise, replicative indexes- RI and CBPI- from the CBMN assay (48h exposure) also did not show cytotoxic effects. However, the results of the clonogenic assay, where the cells had a more prolonged exposure – 7 days - did show a decrease in the capacity of A549 cells to form colonies in a concentration-dependent manner. A possible explanation for the cytotoxic results obtained in the later assay is the that CeO_2 may produce ROS leading to oxidative stress and damaging the cellular membrane through lipid peroxidation, thus preventing cells proliferation (Kim et al. 2010; Mittal & Pandey 2014). Another hypothesis is that cell death induction could be due to dissolution and release of the metal ions in the culture medium, as has been described for other metallic NPs. However, CeO_2 NPs do not dissolve in medium and so their toxicity is due to NPs and not to cerium ions (Mittal & Pandey 2014).

On the other hand, the document from JRC, that describes the physico-chemical properties of the NM-212 under study, reports that this specific NM has 93.1% of Ce^{4+} and 6.9% of Ce^{3+} and the NPs are cubic. An *in vitro* study tested different forms of CeO_2 NPs: rod-like, octahedron-like and cube-like

nano-CeO_2. Rod-like and octahedron-like protected and inhibited DNA damage by scavenging ·OH, but cube-like nano-CeO_2 did not eliminate ·OH (L. Wang et al. 2015). This suggests that the form, superficial area and consequent different arrangement and ionic state also could be an important influence triggering or protecting against the cytotoxicity.

The present results agree with those of Kim et al. (2010) Kim et al. (2010) that showed no cytotoxic effects of a high concentration (1000 µg/mL) of CeO_2 NPs (15 and 30 nm) in A549 cells (WST-1 assay), while a long-term exposure to a concentration range from 0.5 to 500 µg/mL, dramatically reduced the colony number, as assessed by the clonogenic assay. The authors associated this reduction in the colony forming ability to the significant membrane damage observed by the LDH Leakage Assay in the same cell line However, this study also tested CeO_2 in L-132 cells (normal human lung epithelial cells) showing no release of LDH (Kim, Baek, and Choi 2010). On the other hand, oxidative stress was revealed by the increase of ROS and lipid peroxidation levels and by reduction of the GSH levels (Kim, Baek, and Choi 2010). Another study using CeO_2 NPs (8-20 nm) in concentrations from 1 µg/mL to 100 µg/mL in A549 cell line during 3, 6, 24, and 48 hours, concluded that CeO_2 NPs got internalized in cells and produced increased amount of ROS, which contributed to extensive DNA damage and perturbation of the cell cycle, in parallel with an increasing number of apoptotic cells (Mittal and Pandey 2014). Another study of CeO_2 NPs (20 nm) in the A549 cell line, showed a decrease of cells viability for concentrations of 3.5, 10.5 and 23.3 µg/mL, after 72 hours exposure (colorimetric SRB assay and the LDH leakage assay) (Lin et al. 2006). Furthermore, cytotoxicity assessment by the propidium iodide (PI) uptake assay, and the trypan blue assay showed a decrease in viability after 24 and 48 hours for concentrations of 25, 50 and 100 µg/mL (Mittal and Pandey 2014).

Other studies were performed with the aim of assessing the effects of different sizes of CeO_2 NMs in pulmonary cells. Overall, the effect of size is still unclear for CeO_2 NPs since there is not a consensus about the results obtained until the present. A study in Beas-2B (human bronchial epithelial cell), using CeO_2 NPs with different diameter sizes of 15, 30, 45 nm suggested that 1 mg/L of CeO_2 nanoparticles, during 24 hours, may exert their toxicity through oxidative stress, as they cause significant increases in the cellular ROS concentrations, although a quantification analysis did not indicate any size-dependent effect (Eom and Choi 2009). The MTT assay was performed in Beas-2B treated with 10, 20, and 40 µg/ml of CeO_2 NPs (30 nm) for 24, 48, 72, and 96 hours. The results of viability test showed that toxicity of 30 nm cerium dioxide nanoparticles appeared in the cells treated with 10 µg/mL and higher concentrations at 24 h exposure. Different sizes of cerium oxide nanoparticles were also compared through this toxicity test but no statistically differences were found among groups treated with 15, 25, 30, and 40 nm-particles. It was also reported the induction of ROS and decrease of intracellular GSH in cultured Beas-2B cells (Park et al. 2008). (Park et al. 2008)(Park et al. 2008)These authors tried to justify the results in Beas-2B cells reporting that the particle that they prepared do not have the same arrangement of the nanoparticles used in other studies showing anti-oxidant properties, and do not have the same Ce^{3+} ionic state enough to scavenge the oxygen radicals. In fact, there are some studies already available that report the effect of the size in the relative amount of cerium ions Ce^{3+} and Ce^{4+} saying that, in general, the fraction of Ce^{3+} ions in the particles increases with decreasing particle size (Xu & Qu 2014; Schubert et al. 2006). Concerning what was explained above about the low amount of

Ce^{3+} ions in the NPs herein studied, this could be another factor that justifies the cytotoxicity obtained in the clonogenic assay. Moreover, in cancer cells (e.g., A549 cells), the high metabolism puts high levels of stress on the endosomal system. This can result in higher uptake of NPs, or even in slight differences in endosomal pH levels. The pro- or anti-oxidant roles of CeO_2 NPs are linked to the surrounding pH. In acidic environments, CeO_2 NPs favor the scavenging of superoxide radical over hydroxyl peroxide resulting in accumulation of the latter whereas in neutral pH CeO_2 NPs scavenge both. The differences in the intracellular microenvironment of cancer cells and normal cells can thus lead to different cellular responses to CeO_2 NPs (Franchi et al. 2015).

The evaluation of the toxicity of this nanomaterial has been performed and assessed in other cell lines from different organs. An *in vitro* study in human neutrophils demonstrated the release of some indicators of inflammatory process with the degranulation of these cells, when exposed to CeO_2 NPs (Babin et al. 2013). Also, in human hepatocarcinoma cells (SMMC-7721 cell line) CeO_2 nanoparticles caused morphological damage, reduced cell viability and induced significant apoptosis and suggested that CeO_2 nanoparticles could induce oxidative stress (Cheng et al. 2013). MTT assay in ECs revealed that nanoceria were cytotoxic to ECs at all tested concentrations (5, 10, 20, and 40 μg/mL) and exposure times (24, 48, and 72 hours) (Chen et al. 2013). Negative results were also obtained by the MTT assay in NCTC2544 cells demonstrating that CeO2 are not toxic at the highest concentration tested (80 μg/mL) (Boutard et al. 2013).

In vivo studies have also been performed in order to try to correlate the results of the *in vitro* tests. An *in vivo* study in rats, through inhalation of 15-30 nm CeO_2, demonstrated a significant decrease in cell viability of bronchoalveolar lavage fluid (BALF) of the exposed rats up to 14 days post inhalation exposure period of 641 mg/m^3, suggesting that nanoparticles induced apoptosis and this was further supported by elevated levels of LDH activity in BALF. The increase in lipid peroxidation resulted in cells membrane damage as indicated by LDH release. These results suggest that acute exposure to CeO_2 NPs through inhalation route may induce cytotoxicity via oxidative stress and may lead to a chronic inflammatory response (Srinivas et al. 2011). A study with CD1 mice that consisted in inhalation exposure of 2 mg/m^3 of CeO_2 NPs, with 45 nm of diameter, for 28 days demonstrated that it can induce inflammatory response and oxidative stress. In this publication it is also reported that the particles once deposited are hard to be cleared and may provoke a range of long term toxicological effects (Aalapati et al. 2014). It was also demonstrated in an *in vivo* study with rats that CeO_2 NPs (6.4–14.8 nm) with final concentrations at 0.15, 0.5, 1.0, 3.5 or 7 mg/kg body weight through intratracheal instillation up to 28 days post-exposure that this nanoparticles induce a range of mediators involved in lung inflammation and pulmonary fibrosis (Ma et al. 2012).

Regarding the antioxidant/oxidant effect of ceria nanoparticles, it seemed that ceria nanoparticles have different modes of action according to the types of cells. It is possible that some cellular physiology related with antioxidant effects among the different types of cells, or some media environment may be one of the differences in exerting cytotoxicities (Park et al. 2008).

As to the genotoxic effects of CeO_2 in A549 cells, the FPG-Comet assay results showed a two-fold increase in the level of DNA damage following 3 hours exposure to the two highest CeO_2 NPs concentrations, compared to the control, although no statistically significant differences were found. This observation suggests a mild and transient induction of oxidative DNA damage. At 24 hours exposure the results were all negative. The results from the CBMN assay with 48 hours of exposure did not show any increase in the number of MN. Thus, from these data it can be concluded that the CeO_2 under study is not genotoxic. In contrast to the numerous studies on CeO_2 cytotoxicity there are only a few studies assessing its genotoxicity. A549 cells exposed to 25 µg/mL, 50 µg/mL, and 100 µg/mL concentration of CeO_2 NPs (8-20 nm) for 6 hours exhibited a significant induction in DNA damage compared to control cells as evidenced by the % tail DNA in standard alkaline comet assay. Moreover, the values for % tail DNA in the FPG-modified Comet assay were significantly higher than those of the standard alkaline comet assay (Mittal and Pandey 2014). On the contrary, a study performed in human lens epithelial (HLE-B3) cells with 5 µg/mL and 10 µg/mL of CeO_2 NPs (~6 nm) during 24 hours did not show DNA damage when the alkaline comet assay was performed (Pierscionek et al. 2010). The assumption that the different effects of CeO_2 are dependent of the NM physico-chemical properties, e.g., shape and the surface content of Ce^{3+} and Ce^{4+} ions and also of the cell type, is evidenced in these and other studies. Furthermore, the complex balance between the anti-oxidant properties of CeO_2 NMs and the oxidative stress induction reported in some studies makes it difficult to predict whether ROS generation might have been expected to induce DNA damage and subsequent chromosome breakage and micronucleus induction. In line with the present results, an *in vivo* study performed during 3 and 6 months did not show genotoxicity in rats (erythrocytes and leukocytes) through alkaline comet assay and micronucleus assay after exposure to NM-212 (Cordelli et al. 2016).

5.3 Cytotoxicity and genotoxicity of TiO_2 nanomaterials

In this work two different TiO_2 NMs were tested, presenting different sizes, surface areas and coatings. As presented in Table 3.1 (chapter Materials and Methods), NM-101 has a smallest size and consequent higher superficial area than NM-100 and both NMs have anatase crystalline phase.

Relatively to cytotoxicity assessment, both NMs did not show cytotoxicity by the MTT assay. RI and CBPI obtained from CBMN assay performed with NM-100 also did not reveal any significant alterations and the results reported by Santos (2015) also did not reveal any alteration in RI and CBPI for NM-101. Even though the uptake of the TiO_2 NPs was not investigated in the present study, several works have already demonstrated that A549 cells are able to internalize TiO_2 NPs of different sizes and crystalline phases (Moschini et al. 2013; Aueviriyavit & Phummiratch 2012; Franchi et al. 2015). Thus, an hypothetical lack of these NPs uptake can be discarded.

Some studies have already assessed the toxicity of diverse TiO_2 NPs in the A549 cell line and the results are often contradictory. In agreement with the present data, another study (using the WST-1 assay) performed in A549 and L-132 cells (from normal human lung epithelia) showed that TiO_2 NPs did not significantly inhibit cell proliferation of both cell types up to the highest concentration tested (1000

µg/ml), after 72 hours of exposure. However, TiO_2 reduced about 20% colony formation at the concentration range of 0.5 to 500 µg/ml in A549 cell line (Kim, Baek, and Choi 2010). These results are similar to those obtained in this work for MTT assay, where it was not observed any decrease in viability and for clonogenic assay when Santos (2015) exposed A549 cell line to NM-101 and verified an increase in cytotoxicity starting in 30 µg/cm^2 (figure IV.2, annex IV). The ability of NM-101 (5 nm, sylane coated) to impair cells proliferation was further confirmed by our team; NM-100 (20-100 nm, uncoated), in turn, did not reveal significant cytotoxic potential by the clonogenic assay (figure IV.1, annex IV). Other studies using different cytotoxic assays (MTT, neutral red, PI staining and LDH test) to screen cytotoxicity after exposure to TiO_2 NMs (~50 nm) in a range concentration from 1 to 100 µg/mL during 3 and 24 hours in A549 cells showed neither significant reduction in cell viability nor increase in intracellular ROS production (Moschini et al. 2013). Similar results were obtained even for the pro-inflammatory response (IL-8 release) and for the induction of cell oxidative damages (Moschini et al. 2013). The production of ROS is an important endpoint to evaluate since nanoparticles exposure is often associated with increases in cellular reactive oxygen species (ROS), as mentioned above. Although this study did not show oxidative damages there are studies in literature that reveal the increase of ROS or oxidative stress in a concentration- and time-dependent manner from TiO_2 NPs (Kim et al. 2010; Aueviriyavit & Phummiratch 2012; Jugan et al. 2012; Andersson et al. 2011; Shukla et al. 2013).

In another work, when the A549 cell line was exposed to a concentration range from 0 to 200 µg/mL of TiO_2 NPs (5 nm) for 24, 48, and 72 hours to assess cell viability through MTT assay, TiO_2 anatase NPs strongly inhibited A549 cell proliferation in a dose- and time-dependent manner (Wang et al. 2015). Also MTS assay showed a dose-dependent decrease in cell viability after 24 hours for the two highest concentrations tested (5 to 500 µg/mL) of the anatase form of TiO_2 NPs (20 nm) in A549 cells (Aueviriyavit & Phummiratch, 2012). Another assay in A549 cells showed a dose-dependent decrease in cell viability as well as in ATP levels, demonstrated by CCK-8 assay after exposure to TiO_2 NPs (20-50 nm) in a concentration range from 50 to 300 µg/mL, for 4 hours. In Beas- 2B, TiO2-NP did not induce cytotoxic effects up to a tested concentration of 50 µg/cm^2 (Bhattacharya et al. 2009). MTT and NRU assays exhibited cytotoxicity after 24 and 48 hours at the highest concentrations (40 and 80 µg/mL), while no significant cytotoxicity was detected after 6 hours exposure in human liver cells (HepG2) (Shukla et al. 2013).

In this work the cytotoxicity of TiO_2 could be related with some NPs characteristics like coating, since NM-100, without coating did not revealed cytotoxicity in the cell proliferation assay while the coated NM-101 induced a decrease of the colony formation ability in the same assay. The coating of NMs could be determinant in the effects of NMs in the cells because it will favor (or not) some biomolecules to bind to NMs, forming the corona protein and thus modifying their reactivity and ability to be uptaken by cells.

A smaller NP have a higher surface area, which means that this nanomaterial is more reactive. NM-101 has a higher superficial area than NM-100 and this characteristic could also explain the results obtained in the clonogenic assay.

Sometimes the discrepant results are also justified with the different sizes, crystalline phases, times of exposure, endpoints assessed or cell lines. There are already some studies where authors try to understand the influence of size and crystalline phase on cytotoxicity. A study in A549 cell line with different sizes (12-140 nm) and crystalline forms (rutile and anatase) of TiO_2- A12, - A25,- A140, -R68, -R20- (A means anatase, R means rutile and the following number is the diameter in nanometer), was performed. The assays were conducted in a range concentrations of 1–200 mg/mL of NP suspensions. In the MTT assay (4-48 hours of exposure) TiO_2-NPs, both rutile and anatase, with diameters lower than 100 nm exerted more pronounced toxic effects than TiO_2-NPs with diameters higher than 100 nm (Jugan et al. 2012). Hence, in this study the characteristic that most influenced the results was the size of NP. Other studies showed that the anatase phase is more toxic than the rutile and so the crystalline phase can be an important feature (Chen et al. 2014; Wang et al. 2015; Hamzeh & Sunahara 2013; Hsiao & Huang 2011; Sayes et al. 2006; Demir et al. 2015). A study performed in the A549 cell line, related cytotoxicity and inflammation from different crystalline phases and surface areas of TiO_2 NMs. The cellular responses exhibited dose- and time dependent behavior. The extent to which nanoscale titania affected cellular behavior was not dependent on sample surface area because smaller nanoparticles had effects comparable to larger nanoparticles. What correlated strongly to cytotoxicity, however, was the phase composition of the nano-scale titania. Anatase TiO2 was more toxic than an equivalent sample of rutile TiO_2. The most cytotoxic nanoparticle samples were also the most effective at generating reactive oxygen species (Sayes et al. 2006).

Besides the cytotoxicity tests that have been presented in this discussion there are other features or endpoints that could have been assessed to better understand the effects of NMs in the cells. The morphology of the cells was one of these characteristics. In A549 cells typical apoptotic morphological changes consisting of cell shrinkage in response to TiO_2 NP were observed by others authors in a concentration-dependent manner, which suggested that TiO_2 NPs induce apoptosis and increases the proportion of G2/M phase cells (Wang et al. 2015). This observations could also explain the reduction of cell proliferation in the clonogenic assay for NM-101. The cells remain in phase G2 (checkpoint of cellular cycle) instead of going to a cellular division (mitosis). In human fetal lung fibroblasts, at the lower dose (0.25 mg/mL), the morphology of the cells appeared to be altered and with increasing doses cell morphology was destroyed (Z. Qiang et al. 2013). Significant cytotoxicity, intracellular ROS generation, and to some extent G2/M cell cycle arrest were induced at the above specified treatment dose, and attributed to TiO_2 NPs mediated oxidative stress in the WISH cells (Saquib et al. 2012). Also, in untransformed human fibroblasts, TiO_2 NPs were found to induce apoptosis at later time points, as a delayed effect of cellular NP exposure (Franchi et al. 2015).

In addition, in vivo studies have also been performed and demonstrated that when rats were submitted to 10, 50, 200 mg/kg of TiO_2 NPs once a day for 30 consecutive days these NPs could induce DNA double strand breaks in bone marrow cells after oral administration, despite that no chromosomes and mitotic apparatus damage were found. The formation of gamma-H_2AX foci, the biomarker of DNA double strand breaks (DSB) formation, detected that TiO_2 NPs induced genotoxic effects, as also

verified by the comet assay when showed an increased in DNA breaks despite no induction in micronuclei was observed (Chen et al. 2014). On the other hand another in vivo study in rats indicated that a single intratracheal instillation of anatase TiO_2 nanoparticles (5 mg/kg) or repeated intratracheal instillation (1 mg/kg) once a week for 5 weeks did not induce DNA damage, in the lungs in rats but induced an inflammatory response with the presence of macrophages and neutrophils (Naya et al. 2012).

In the present study, the comet assay was performed to assess DNA breaks in A549 cells after exposure to NM-101 and NM-100. In addition, the CBMN assay was conducted to evaluate the induction of chromosome breaks after cells exposure to NM-100. Using the Comet assay a concentration-dependent increase in DNA breaks was observed for NM-100, which was accentuated following the treatment with the FPG enzyme. Cells treatment with NM-101 also resulted in a significant increase in the level of DNA damage for the two highest concentrations tested (plus FPG treatment). Santos (2015) has previously performed the Comet assay at the same conditions and also verified a significant increase in DNA damage 24 hours after exposure to NM-101 (without FPG). Another study in A549 cells with different concentrations of TiO_2 NPs (0 to 52 µg/cm^2) for 48 hours reported that the percentage of tail DNA was significantly increased with the increase in dose of TiO_2 NPs, which suggested the induction of DNA damage in a dose-dependent manner (Wang et al. 2015). In a study performed with different sizes and crystalline phases of TiO2 NPs, the authors related an increase in the level of DNA breaks after 4 hours of exposure and a further increased after 24 hours, but it was significant only after exposure to TiO_2-A12, -A25 and -R20, but not to TiO_2-R68 and -A140. However, after 48 hours the frequency of breaks drastically decreased in exposed cells (Jugan et al. 2012). Other study revealed that TiO_2 NPs exposure only increased the percentage of DNA in the tail at the concentration of 100 µg/mL and at 24 hours in V79 cells (Chen et al. 2014). Induction of DNA breaks was obtained with nano-TiO_2 anatase, but only at the highest dose tested (100 mg/mL) in HEK293 (human embryonic kidney) and NIH/3T3 (mouse embryo fibroblast cells) cell lines (Eşref Demir, Hakan Akça, Fatma Turna, Sezgin Aksakal and Bülent Kaya, Onur Tokgün, Gerard Vales 2015). The exposure for 6 hours has also induced a significant level of DNA damage at a concentration of 20 µg/mL in WISH cells (Saquib et al. 2012).

Our results in comet assay can be related with the crystalline phase, anatase, which was previously reported in this work, as the more toxic and so the most effective at generating reactive oxygen species which can be the cause of DNA breaks

For the CBMN assay, no significant differences in the mean frequency of MNBNC were observed in the present work. Similarly, no induction of MNBNC has been previously reported by Santos (2015) after NM-101 treatment but a reference to the difficulty in the slides scoring due to deposition of NMs on the cells was found. A study in A549 cells did not report differences for CBPI after exposure to TiO_2 NMs (7- 9 nm). The authors referred that the results from CBMN assay are not available because the MN were obscured by NM agglomerates over the cells and thus could not be scored (Corradi et al. 2012). In HepG2 a significant induction in micronucleus formation was observed at 20 µg/mL of TiO_2

NPs (30-70 nm). However, further treatment with higher concentrations (40 and 80 µg/mL) showed a decrease in the micronucleus formation. The authors associated these results in the micronucleus frequency also with the accumulation of TiO_2 NPs on prepared slides, which hinders the counting of micronucleus (Vallabani et al. 2014). In another study, TiO_2 NPs induced an increase in the number of micronucleated cells at 20 µg/mL. However, with further increasing concentrations (40 and 80 mg/ml), the micronucleus formation decreased (Shukla et al. 2013).

In other studies, when the MN assay was used to demonstrate the clastogenic/ aneugenic potential of nano-TiO_2, significant increases in the frequency of MNBNC were observed in the two cell lines (HEK293 and NIH/3T3), but only at the highest tested dose (1000 mg/mL) and anatase form (Demir et al. 2015). Also, Tavares et al. (2014) reported a significant increase in the micronucleus frequency in human lymphocytes after exposure to TiO_2 anatase (NM–102). It has been reported that the induction of micronucleus by nano-TiO_2 is affected by the characteristics of the culture medium, getting positive results only with medium that facilitates the lowest amount of agglomeration. Our observations also suggested a high agglomeration of TiO_2 when the slides were analyzed although the dispersion results seemed good. This would explain, in part, some of the negative results reported in the micronucleus assay by several authors.

No other mechanism out of the oxidative damage has been proposed to explain the ability of nano-TiO_2 to induce micronuclei and, as consequence, the observed increase of micronuclei would be the result of chromosome breaks (Eşref Demir, Hakan Akça, Fatma Turna, Sezgin Aksakal and Bülent Kaya, Onur Tokgün, Gerard Vales 2015).

The results of CBMN assay are inconclusive since the preparations from the cells subjected to the highest concentrations could not be analysed. On the other hand, it was clear the induction of DNA breaks, by the comet assay, for both nanomaterials.

5.4 Cytotoxicity and genotoxicity of $BaSO_4$ nanomaterials

In respect to the cytotoxicity assessment, the MTT assay and replication indexes (RI and CBPI) did not show decrease in cell viability. Also comet and CBMN assays did not reveal any genotoxicity.

As already said there are not many studies reporting the toxicity of barium sulphate NPs. To the best of our knowledge, no in vitro studies were published about the toxicity of this NM. There are only some reports about in vivo studies in rats or mices. These studies demonstrated that 3 or 6-month inhalation exposure to 50 mg/m^3 $BaSO_4$ NM-220 did not elicit genotoxicity in either the alkaline Comet assay or the micronucleus test, in rats (Cordelli et al. 2016). Another study examined the effects of short-term (4-week) and subchronic (13-week) inhalation exposure and a single IT instillation of $BaSO_4$ NPs in rats. Data showed that inhaled $BaSO_4$ NPs elicited minimal pulmonary response and no systemic effects. Four weeks of inhalation of 50 mg/m3 $BaSO_4$ resulted in no pulmonary toxicity by 35 days post-exposure. The study underscores the high Ba bioavailability and clearance of $BaSO_4$ NPs deposited in

the lungs. Unlike CeO_2 and TiO_2, $BaSO_4$ NPs are retained to a lesser extent in the lungs after inhalation. Even at lung burdens, similar to CeO_2 and TiO_2, $BaSO_4$ NPs cause lower pulmonary toxicity and biopersistence (Konduru et al. 2014).

Although these results are from in vivo experiments, they are in accordance with those obtained in this work for A549 cells, where it was not detected cytotoxicity, DNA or chromosomes breaks. Thus, for a non-toxic NM, a good *in vitro – in vivo* correlation was found, i.e., the *in vitro* results could have predicted the effects observed *in vivo*.

6. CONCLUSION

This study was aimed at characterizing the potential toxicity of different nanomaterials from the group of poorly soluble particles, CeO_2, TiO_2 and $BaSO_4$ NMs in an alveolar cell line.

As summarized in Table 4.1 CeO_2 NM was cytotoxic after a long-term A549 cells exposure but did not reveal toxicity for a short-term exposure, as assessed by the MTT assay. No genotoxicity was detected under the tested conditions.

Further ongoing assays, using other *in vitro* and *in vivo* systems to test the genotoxicity of this NM, will improve the knowledge base for the evaluation of genotoxic risks associated with this NM. Because nano- CeO_2 is being studied to be employed in medical applications, due to its antioxidant and protective effects, it is important to try to understand and distinguish what causes the adverse effects and the beneficial effects in order to drive the synthesis of safest nano-CeO_2 while preserving its antioxidant beneficial effects.

Both TiO_2 NMs showed genotoxicity through the comet assay and these results are supported by many publications that report the capacity of some TiO_2 NPs, mostly anatase TiO_2 NPs, to interfere with the cells' genetic material and consequently, having the potential to be mutagenic and carcinogenic.

Studying TiO_2 NMs with different physico-chemical properties highlighted the importance of some characteristics, e.g., coating and surface area in relation to the possible observed effects.

Although TiO_2 NPs are approved by FDA to be used in cosmetic products (and others), concerning the results here presented and other publications some applications and products where nano- TiO_2 is present should be revised.

$BaSO_4$ NMs have shown some amazing applications in the medical field, and although the lack of toxicity studies for this NPs, it seems to be one of the less toxic NMs, as proved in this work and in the publications where *in vivo* tests were carried out.

Further studies, focused in different properties of the same NM, in different cell lines, *in vitro* as well as *in vivo* approaches will contribute to understand the main characteristics that determine their toxicity, allowing a ‘‘safer-by-design’’ approach.

7. REFERENCES

Aalapati, Srinivas, Selvam Ganapathy, Saikumar Manapuram, Goparaju Anumolu, and Balakrishna Murthy Prakya. 2014. “Toxicity and Bio-Accumulation of Inhaled Cerium Oxide Nanoparticles in CD1 Mice.” *Nanotoxicology* 8 (7): 786–98. doi:10.3109/17435390.2013.829877.

Ahlinder, Linnea, Barbro Ekstrand-Hammarström, Paul Geladi, and Lars Österlund. 2013. “Large Uptake of Titania and Iron Oxide Nanoparticles in the Nucleus of Lung Epithelial Cells as Measured by Raman Imaging and Multivariate Classification.” *Biophysical Journal* 105 (2): 310–19. doi:10.1016/j.bpj.2013.06.017.

Andersson, Per Ola, Christian Lejon, Barbro Ekstrand-Hammarström, Christine Akfur, Linnéa Ahlinder, Anders Bucht, and Lars Österlund. 2011. “Polymorph- and Size-Dependent Uptake and Toxicity of TiO2 Nanoparticles in Living Lung Epithelial Cells.” *Small* 7 (4): 514–23. doi:10.1002/smll.201001832.

Aninwene, George E., David Stout, Zifan Yang, and Thomas J. Webster. 2013. “Nano-BaSO4: A Novel Antimicrobial Additive to Pellethane.” *International Journal of Nanomedicine* 8: 1197–1205. doi:10.2147/IJN.S40300.

Araldi, Rodrigo Pinheiro, Thatiana Corrêa de Melo, Thais Biude Mendes, Paulo Luiz de Sá Júnior, Bruno Heidi Nakano Nozima, Eliana Tiemi Ito, Rodrigo Franco de Carvalho, Edislane Barreiros de Souza, and Rita de Cassia Stocco. 2015. “Using the Comet and Micronucleus Assays for Genotoxicity Studies: A Review.” *Biomedicine & Pharmacotherapy* 72: 74–82. doi:10.1016/j.biopha.2015.04.004.

Arora, Sumit, Jyutika M. Rajwade, and Kishore M. Paknikar. 2012. “Nanotoxicology and in Vitro Studies: The Need of the Hour.” *Toxicology and Applied Pharmacology* 258 (2). Elsevier Inc.: 151–65. doi:10.1016/j.taap.2011.11.010.

Aueviriyavit, Sasitorn, and Duangkamol Phummiratch. 2012. “Titanium Dioxide Nanoparticles-Mediated In Vitro Cytotoxicity Does Not Induce Hsp70 and Grp78 Expression in Human Bronchial Epithelial A549 Cells,” 123–32. doi:10.1007/s12011-012-9403-z.

Azqueta, Amaya, and Andrew R. Collins. 2013. “The Essential Comet Assay: A Comprehensive Guide to Measuring DNA Damage and Repair.” *Archives of Toxicology* 87 (6): 949–68. doi:10.1007/s00204-013-1070-0.

Azqueta, Amaya, and Maria Dusinska. 2015. “The Use of the Comet Assay for the Evaluation of the Genotoxicity of Nanomaterials.” *Frontiers in Genetics* 6 (July): 1–4. doi:10.3389/fgene.2015.00239.

Babin, Kim, Francis Antoine, David Miguel Goncalves, and Denis Girard. 2013. “TiO2, CeO2 and ZnO Nanoparticles and Modulation of the Degranulation Process in Human Neutrophils.” *Toxicology Letters* 221: 57–63. doi:10.1016/j.toxlet.2013.05.010.

Bhattacharya, Kunal, Maria Davoren, Jens Boertz, Roel Pf Schins, Eik Hoffmann, and Elke Dopp. 2009. “Titanium Dioxide Nanoparticles Induce Oxidative Stress and DNA-Adduct Formation but Not DNA-Breakage in Human Lung Cells.” *Particle and Fibre Toxicology* 6: 17. doi:10.1186/1743-

8977-6-17.

Bonassi, Stefano, Randa El-Zein, Claudia Bolognesi, and Michael Fenech. 2011. “Micronuclei Frequency in Peripheral Blood Lymphocytes and Cancer Risk: Evidence from Human Studies.” *Mutagenesis* 26 (1): 93–100. doi:10.1093/mutage/geq075.

Bour, Agathe, Florence Mouchet, Laurent Verneuil, Lauris Evariste, JérÔme Silvestre, Eric Pinelli, and Laury Gauthier. 2015. “Toxicity of CeO2 Nanoparticles at Different Trophic Levels - Effects on Diatoms, Chironomids and Amphibians.” *Chemosphere* 120. Elsevier Ltd: 230–36. doi:10.1016/j.chemosphere.2014.07.012.

Boutard, Tifenn, Bénédicte Rousseau, Céline Couteau, Christophe Tomasoni, Cyriaque Simonnard, Catherine Jacquot, Laurence J M Coiffard, Konstantin Konstantinov, Thierry Devers, and Christos Roussakis. 2013. “Comparison of Photoprotection Efficiency and Antiproliferative Activity of ZnO Commercial Sunscreens and CeO2.” *Materials Letters* 108 (3): 13–16. doi:10.1016/j.matlet.2013.06.085.

Braakhuis, Hedwig M, Margriet V D Z Park, Ilse Gosens, Wim H De Jong, and Flemming R Cassee. 2014. “Physicochemical Characteristics of Nanomaterials That Affect Pulmonary Inflammation.”

Bruinink, Arie, Jing Wang, and Peter Wick. 2015. “Effect of Particle Agglomeration in Nanotoxicology,” 659–75. doi:10.1007/s00204-015-1460-6.

Buch, Karl, Tanja Peters, Thomas Nawroth, Markus Sänger, Heinz Schmidberger, and Peter Langguth. 2012. “Determination of Cell Survival after Irradiation via Clonogenic Assay versus Multiple MTT Assay--a Comparative Study.” *Radiation Oncology (London, England)* 7 (1). BioMed Central Ltd: 1. doi:10.1186/1748-717X-7-1.

Chen, Shizhu, Yingjian Hou, Gong Cheng, Cuimiao Zhang, Shuxiang Wang, and Jinchao Zhang. 2013. “Cerium Oxide Nanoparticles Protect Endothelial Cells from Apoptosis Induced by Oxidative Stress.” *Biological Trace Element Research* 154 (1): 156–66. doi:10.1007/s12011-013-9678-8.

Chen, Tao, Jian Yan, and Yan Li. 2014. “Genotoxicity of Titanium Dioxide Nanoparticles.” *Journal of Food and Drug Analysis* 22 (1). Elsevier Masson SAS: 95–104. doi:10.1016/j.jfda.2014.01.008.

Chen, Zhangjian, Yun Wang, Te Ba, Yang Li, Ji Pu, Tian Chen, Yanshuang Song, et al. 2014. “Genotoxic Evaluation of Titanium Dioxide Nanoparticles in Vivo and in Vitro” 226: 314–19. doi:10.1016/j.toxlet.2014.02.020.

Cheng, Guilin, Wei Guo, Lu Han, Erlei Chen, Lingfang Kong, Lili Wang, Wenchao Ai, Naining Song, Haishan Li, and Huiming Chen. 2013. “Cerium Oxide Nanoparticles Induce Cytotoxicity in Human Hepatoma SMMC-7721 Cells via Oxidative Stress and the Activation of MAPK Signaling Pathways.” *Toxicology in Vitro : An International Journal Published in Association with BIBRA* 27 (3): 1082–88. doi:10.1016/j.tiv.2013.02.005.

Cohen, Joel, Glen Deloid, Georgios Pyrgiotakis, and Philip Demokritou. 2013. “Interactions of Engineered Nanomaterials in Physiological Media and Implications for in Vitro Dosimetry.” *Nanotoxicology* 7 (4): 417–31. doi:10.3109/17435390.2012.666576.

Collins, Andrew R. 2014. “Measuring Oxidative Damage to DNA and Its Repair with the Comet Assay.” *BBA - General Subjects* 1840 (2). Elsevier B.V.: 794–800. doi:10.1016/j.bbagen.2013.04.022.

Collins, Andrew R., Naouale El Yamani, Yolanda Lorenzo, Sergey Shaposhnikov, Gunnar Brunborg,

and Amaya Azqueta. 2014. “Controlling Variation in the Comet Assay.” *Frontiers in Genetics* 5 (October): 1–6. doi:10.3389/fgene.2014.00359.

Cordelli, Eugenia, Jana Keller, Patrizia Eleuteri, Paola Villani, Lan Ma-Hock, Markus Schulz, Robert Landsiedel, and Francesca Pacchierotti. 2016. “No Genotoxicity in Rat Blood Cells upon 3- or 6-Month Inhalation Exposure to CeO 2 or BaSO 4 Nanomaterials.” *Mutagenesis*, no. 11: gew005. doi:10.1093/mutage/gew005.

Corradi, Sara, Laetitia Gonzalez, Leen C J Thomassen, Dagmar Bilaniˇ, Renie K Birkedal, Giulio Pojana, Antonio Marcomini, Keld A Jensen, Luc Leyns, and Micheline Kirsch-volders. 2012. “Influence of Serum on in Situ Proliferation and Genotoxicity in A549 Human Lung Cells Exposed to Nanomaterials” 745: 21–27. doi:10.1016/j.mrgentox.2011.10.007.

Dahle, Jessica T, Ken Livi, and Yuji Arai. 2015. “Effects of pH and Phosphate on CeO2 Nanoparticle Dissolution.” *Chemosphere* 119: 1365–71. doi:10.1016/j.chemosphere.2014.02.027.

Das, Mainak, Swanand Patil, Neelima Bhargava, Jung Fong Kang, Lisa M. Riedel, Sudipta Seal, and James J. Hickman. 2007. “Auto-Catalytic Ceria Nanoparticles Offer Neuroprotection to Adult Rat Spinal Cord Neurons.” *Biomaterials* 28 (10): 1918–25. doi:10.1016/j.biomaterials.2006.11.036.

Doig, A T. 1976. “Baritosis: A Benign Pneumoconiosis.” *Thorax* 31: 30–39.

Elsaesser, Andreas, and C. Vyvyan Howard. 2012. “Toxicology of Nanoparticles.” *Advanced Drug Delivery Reviews* 64 (2). Elsevier B.V.: 129–37. doi:10.1016/j.addr.2011.09.001.

Eom, Hyun-Jeong, and Jinhee Choi. 2009. “Oxidative Stress of CeO2 Nanoparticles via p38-Nrf-2 Signaling Pathway in Human Bronchial Epithelial Cell, Beas-2B.” *Toxicology in Vitro* 23 (7): 1326–32. doi:10.1016/j.tiv.2009.07.010.

Eşref Demir, Hakan Akça, Fatma Turna, Sezgin Aksakal, Durmuş Burgucu, and Amadeu Creus Ricard Marcos Bülent Kaya, Onur Tokgün, Gerard Vales. 2015. “Genotoxic and Cell-Transforming Effects of Titanium Dioxide Nanoparticles.” *Environmental Research* 136: 300–308. doi:10.1016/j.envres.2014.10.032.

Fadeel, Bengt, Andrea Fornara, Muhammet S. Toprak, and Kunal Bhattacharya. 2015. “Keeping It Real: The Importance of Material Characterization in Nanotoxicology.” *Biochemical and Biophysical Research Communications*. Elsevier Ltd, 1–6. doi:10.1016/j.bbrc.2015.06.178.

Fenech, M., M. Kirsch-Volders, A. T. Natarajan, J. Surralles, J. W. Crott, J. Parry, H. Norppa, D. A. Eastmond, J. D. Tucker, and P. Thomas. 2011. “Molecular Mechanisms of Micronucleus, Nucleoplasmic Bridge and Nuclear Bud Formation in Mammalian and Human Cells.” *Mutagenesis* 26 (1): 125–32. doi:10.1093/mutage/geq052.

Fenech, Michael. 2000. “The in Vitro Micronucleus Technique.” *Mutation Research/Fundamental and Molecular Mechanisms of Mutagenesis* 455 (1–2): 81–95. doi:10.1016/S0027-5107(00)00065-8.

Ferreira, a.J. J, J. Cemlyn-Jones, and C. Robalo Cordeiro. 2013. “Nanoparticles, Nanotechnology and Pulmonary Nanotoxicology.” *Revista Portuguesa de Pneumologia* 19 (1). Sociedade Portuguesa de Pneumologia: 28–37. doi:10.1016/j.rppnen.2013.01.004.

Franchi, Leonardo P, Bella B Manshian, Tiago A J de Souza, Stefaan J Soenen, Elaine Y Matsubara, J Mauricio Rosolen, and Catarina S Takahashi. 2015. “Cyto- and Genotoxic Effects of Metallic Nanoparticles in Untransformed Human Fibroblast.” *Toxicology in Vitro : An International Journal*

Published in Association with BIBRA 29 (7). Elsevier Ltd: 1319–31. doi:10.1016/j.tiv.2015.05.010.

Frieke Kuper, C., Mariska Gröllers-Mulderij, Thérèse Maarschalkerweerd, Nicole M.M. Meulendijks, Astrid Reus, Frédérique van Acker, Esther K. Zondervan-van den Beuken, Mariëlle E.L. Wouters, Sabina Bijlsma, and Ingeborg M. Kooter. 2015. "Toxicity Assessment of Aggregated/agglomerated Cerium Oxide Nanoparticles in an in Vitro 3D Airway Model: The Influence of Mucociliary Clearance." *Toxicology in Vitro* 29 (2). Elsevier Ltd: 389–97. doi:10.1016/j.tiv.2014.10.017.

Gillani, Riaz, Batur Ercan, Alex Qiao, and Thomas J. Webster. 2010. "Nanofunctionalized Zirconia and Barium Sulfate Particles as Bone Cement Additives." *International Journal of Nanomedicine* 5 (1): 1–11. doi:10.2147/IJN.S7603.

Hamzeh, Mahsa, and Geoffrey I Sunahara. 2013. "In Vitro Cytotoxicity and Genotoxicity Studies of Titanium Dioxide (TiO2) Nanoparticles in Chinese Hamster Lung Fibroblast Cells." *TOXICOLOGY IN VITRO* 27 (2): 864–73. doi:10.1016/j.tiv.2012.12.018.

Herzog, Eva, Alan Casey, Fiona M. Lyng, Gordon Chambers, Hugh J. Byrne, and Maria Davoren. 2007. "A New Approach to the Toxicity Testing of Carbon-Based Nanomaterials-The Clonogenic Assay." *Toxicology Letters* 174 (1–3): 49–60. doi:10.1016/j.toxlet.2007.08.009.

Hirst, Suzanne Marie, Ajay Karakoti, Sanjay Singh, William Self, Ron Tyler, Sudipta Seal, and Christopher M. Reilly. 2009. "Bio-Distribution and In Vivo Antioxidant Effects of Cerium Oxide Nanoparticles in Mice." *Environmental Toxicology* 24 (3): 296–303. doi:10.1002/tox.

Hsiao, I-Lun, and Yuh-Jeen Huang. 2011. "Effects of Various Physicochemical Characteristics on the Toxicities of ZnO and TiO 2 Nanoparticles toward Human Lung Epithelial Cells." *Science of the Total Environment, The* 409 (7). Elsevier B.V.: 1219–28. doi:10.1016/j.scitotenv.2010.12.033.

Huerta-García, Elizabeth, José Antonio Pérez-Arizti, Sandra Gissela Márquez-Ramírez, Norma Laura Delgado-Buenrostro, Yolanda Irasema Chirino, Gisela Gutiérrez Iglesias, and Rebeca López-Marure. 2014. "Titanium Dioxide Nanoparticles Induce Strong Oxidative Stress and Mitochondrial Damage in Glial Cells." *Free Radical Biology & Medicine* 73C. Elsevier: 84–94. doi:10.1016/j.freeradbiomed.2014.04.026.

Hussain, S, F Al-Nsour, a B Rice, J Marshburn, B Yingling, Z Ji, J I Zink, N J Walker, and S Garantziotis. 2012. "Cerium Dioxide Nanoparticles Induce Apoptosis and Autophagy in Human Peripheral Blood Monocytes." *ACS Nano* 6 (7): 5820–29. doi:10.1021/nn302235u.

Jensen, K.A., Y. Kembouche, E. Christiansen, N.R. Jacobsen, H. Wallin, C. Guiot, O. Spalla, and O. Witschger. 2011. "Towards a Method for Detecting the Potential Genotoxicity of Nanomaterials Final Protocol for Producing Suitable Manufactured Nanomaterial Exposure Media Web-Report The Generic NANOGENOTOX Dispersion Protocol Standard Operation Procedure (SOP) October ,."

Jensen, Keld Alstrup. 2014. "SOP for Measurement of Hydrodynamic Size- Distribution and Dispersion Stability by Dynamic Light Scattering (DLS)," no. 310584: 1–13.

Johnston, Helinor J, Gary R Hutchison, Frans M Christensen, Sheona Peters, Steve Hankin, and Vicki Stone. 2009. "Identification of the Mechanisms That Drive the Toxicity of TiO(2)Particulates: The Contribution of Physicochemical Characteristics." *Particle and Fibre Toxicology* 6: 33. doi:10.1186/1743-8977-6-33.

Jugan, Mary-Line, Sabrina Barillet, Angelique Simon-Deckers, Nathalie Herlin-Boime, Sylvie Sauvaigo, Thierry Douki, and Marie Carriere. 2012. “Titanium Dioxide Nanoparticles Exhibit Genotoxicity and Impair DNA Repair Activity in A549 Cells.” *Nanotoxicology* 6 (5): 501–13. doi:10.3109/17435390.2011.587903.

Keller, Jana. n.d. “Biokinetics and Inhalation Toxicity of Cerium Dioxide and Barium Sulfate Biokinetics and Inhalation Toxicity of Cerium Dioxide and Barium Sulfate Nanoparticles after 1 , 4 , 13 and 52 Weeks.” doi:10.1016/j.jcpa.2014.10.075.

Keller, Jana, Wendel Wohlleben, Lan Ma-Hock, Volker Strauss, Sibylle Gröters, Karin Küttler, Karin Wiench, et al. 2014. “Time Course of Lung Retention and Toxicity of Inhaled Particles: Short-Term Exposure to Nano-Ceria.” *Archives of Toxicology* 88 (11): 2033–59. doi:10.1007/s00204-014-1349-9.

Kim, In-Sun, Miri Baek, and Soo-Jin Choi. 2010. “Comparative Cytotoxicity of Al 2 O 3 , CeO 2 , TiO 2 and ZnO Nanoparticles to Human Lung Cells.” *Journal of Nanoscience and Nanotechnology* 10 (5): 3453–58. doi:10.1166/jnn.2010.2340.

Konduru, Nagarjun, Jana Keller, Lan Ma-Hock, Sibylle Gröters, Robert Landsiedel, Thomas C Donaghey, Joseph D Brain, Wendel Wohlleben, and Ramon M Molina. 2014. “Biokinetics and Effects of Barium Sulfate Nanoparticles.” *Particle and Fibre Toxicology* 11: 55. doi:10.1186/s12989-014-0055-3.

Kotova, N, N Hebert, E-L Härnwall, D Vare, C Mazurier, L Douay, D Jenssen, and J Grawé. 2015. “A Novel Micronucleus in Vitro Assay Utilizing Human Hematopoietic Stem Cells.” *Toxicology in Vitro : An International Journal Published in Association with BIBRA* 29 (7). Elsevier Ltd: 1897–1905. doi:10.1016/j.tiv.2015.07.018.

Kumari, Monika, Srinivas Indu Kumari, Sarika Srinivas Kalyan Kamal, and Paramjit Grover. 2014. “Genotoxicity Assessment of Cerium Oxide Nanoparticles in Female Wistar Rats after Acute Oral Exposure.” *Mutation Research. Genetic Toxicology and Environmental Mutagenesis* 775–776. Elsevier B.V.: 7–19. doi:10.1016/j.mrgentox.2014.09.009.

Landsiedel, Robert, Lan Ma-hock, Thomas Hofmann, Martin Wiemann, Volker Strauss, Silke Treumann, Wendel Wohlleben, Sibylle Gröters, Karin Wiench, and Bennard Van Ravenzwaay. 2014. “Application of Short-Term Inhalation Studies to Assess the Inhalation Toxicity of Nanomaterials.” doi:10.1186/1743-8977-11-16.

Landsiedel, Robert, Lan Ma-Hock, Ben Van Ravenzwaay, Markus Schulz, Karin Wiench, Samantha Champ, Stefan Schulte, Wendel Wohlleben, and Franz Oesch. 2010. “Gene Toxicity Studies on Titanium Dioxide and Zinc Oxide Nanomaterials Used for UV-Protection in Cosmetic Formulations.” *Nanotoxicology* 4 (December): 364–81. doi:10.3109/17435390.2010.506694.

Lee, Tin Lap, Joan M. Raitano, Owen M. Rennert, Siu Wai Chan, and Wai Yee Chan. 2012. “Accessing the Genomic Effects of Naked Nanoceria in Murine Neuronal Cells.” *Nanomedicine: Nanotechnology, Biology, and Medicine* 8 (5). Elsevier B.V.: 599–608. doi:10.1016/j.nano.2011.08.005.

Leung, Yu Hang, Mana M.N. Yung, Alan M.C. Ng, Angel P.Y. Ma, Stella W.Y. Wong, Charis M.N. Chan, Yip Hang Ng, et al. 2015. “Toxicity of CeO2 Nanoparticles – The Effect of Nanoparticle Properties.”

Journal of Photochemistry and Photobiology B: Biology 145: 48–59. doi:10.1016/j.jphotobiol.2015.01.017.

Lin, Weisheng, Yue-Wern Huang, Xiao-Dong Zhou, and Yinfa Ma. 2006. “Toxicity of Cerium Oxide Nanoparticles in Human Lung Cancer Cells.” *International Journal of Toxicology* 25 (6): 451–57. doi:10.1080/10915810600959543.

Longo-Sorbello, Giuseppe S A, Guray Saydam, Debabrata Banerjee, and Joseph R. Bertino. 2006. “Cytotoxicity and Cell Growth Assays.” *Cell Biology, Four-Volume Set* 1: 315–24. doi:10.1016/B978-012164730-8/50039-3.

Ma, Jane Y., Robert R. Mercer, Mark Barger, Diane Schwegler-Berry, James Scabilloni, Joseph K. Ma, and Vincent Castranova. 2012. “Induction of Pulmonary Fibrosis by Cerium Oxide Nanoparticles.” *Toxicology and Applied Pharmacology* 262 (3). Elsevier B.V.: 255–64. doi:10.1016/j.taap.2012.05.005.

Magdolenova, Zuzana, Andrew Collins, Ashutosh Kumar, Alok Dhawan, Vicki Stone, and Maria Dusinska. 2013. “Mechanisms of Genotoxicity. A Review of in Vitro and in Vivo Studies with Engineered Nanoparticles.” *Nanotoxicology* 8: 233–78. doi:10.3109/17435390.2013.773464.

Manier, Nicolas, Anne Bado-Nilles, Patrice Delalain, Olivier Aguerre-Chariol, and Pascal Pandard. 2013. “Ecotoxicity of Non-Aged and Aged CeO2 Nanomaterials towards Freshwater Microalgae.” *Environmental Pollution* 180. Elsevier Ltd: 63–70. doi:10.1016/j.envpol.2013.04.040.

Medina-Reyes, Estefany I., Alejandro Déciga-Alcaraz, Verónica Freyre-Fonseca, Norma L. Delgado-Buenrostro, José O. Flores-Flores, Gustavo F. Gutiérrez-López, Yesennia Sánchez-Pérez, Claudia M. García-Cuéllar, José Pedraza-Chaverri, and Yolanda I. Chirino. 2015. “Titanium Dioxide Nanoparticles Induce an Adaptive Inflammatory Response and Invasion and Proliferation of Lung Epithelial Cells in Chorioallantoic Membrane.” *Environmental Research* 136. Elsevier: 424–34. doi:10.1016/j.envres.2014.10.016.

Mittal, Sandeep, and Alok K. Pandey. 2014. “Cerium Oxide Nanoparticles Induced Toxicity in Human Lung Cells: Role of ROS Mediated DNA Damage and Apoptosis.” *BioMed Research International* 2014. Hindawi Publishing Corporation. doi:10.1155/2014/891934.

Moschini, Elisa, Maurizio Gualtieri, Miriam Colombo, Umberto Fascio, and Paride Mantecca. 2013. “The Modality of Cell – Particle Interactions Drives the Toxicity of Nanosized CuO and TiO 2 in Human Alveolar Epithelial Cells.” *Toxicology Letters* 222 (2). Elsevier Ireland Ltd: 102–16. doi:10.1016/j.toxlet.2013.07.019.

Munshi, Anupama, Marvette Hobbs, and Raymond E. Meyn. 2007. *IN VITRO MEASURES OF CHEMOSENSITIVITY*. *Strength And Conditioning*. Vol. 21.

Naya, Masato, Norihiro Kobayashi, Makoto Ema, Sawako Kasamoto, Masahito Fukumuro, Shigeaki Takami, Madoka Nakajima, Makoto Hayashi, and Junko Nakanishi. 2012. “In Vivo Genotoxicity Study of Titanium Dioxide Nanoparticles Using Comet Assay Following Intratracheal Instillation in Rats.” *REGULATORY TOXICOLOGY AND PHARMACOLOGY* 62 (1). Elsevier Inc.: 1–6. doi:10.1016/j.yrtph.2011.12.002.

NIOSH. 2009. “Approaches to Safe Nanotechnology,” 86. doi:10.1007/s11125-005-4273-1.

OECD. 2010. “OECD Guideline for the Testing of Chemicals - In Vitro Mammalian Cell Micronucleus

Test. TG487." Vol. 412.

Pagliari, Francesca, Corrado Mandoli, Giancarlo Forte, Eugenio Magnani, Stefania Pagliari, Giorgia Nardone, Silvia Licoccia, et al. 2012. "Cerium Oxide Nanoparticles Protect Cardiac Progenitor Cells from Oxidative Stress." *ACS Nano* 6 (5): 3767–75. doi:10.1021/nn2048069.

Panas, Alicja, Andreas Comouth, Harald Saathoff, Thomas Leisner, Marco Al-Rawi, Michael Simon, Gunnar Seemann, et al. 2014. "Nanomaterial Cytotoxicity Is Composition , Size , and Cell Type Dependent." *Beilstein Journal of Nanotechnology* 5 (1): 1590–1602.

Park, Eun Jung, Jinhee Choi, Young Kwon Park, and Kwangsik Park. 2008. "Oxidative Stress Induced by Cerium Oxide Nanoparticles in Cultured BEAS-2B Cells." *Toxicology* 245 (1–2): 90–100. doi:10.1016/j.tox.2007.12.022.

Pierscionek, Barbara K, Yuebin Li, Akeel a Yasseen, Liza M Colhoun, Ronald a Schachar, and Wei Chen. 2010. "Nanoceria Have No Genotoxic Effect on Human Lens Epithelial Cells." *Nanotechnology* 21 (3): 35102. doi:10.1088/0957-4484/21/3/035102.

Prospect Global Nanomaterials Safety. 2010. "Toxicological Review of Nano Cerium Oxide."

Rasmussen, Kirsten, Jan Mast, Pieter-jan De Temmerman, Eveline Verleysen, Nadia Waegeneers, Frederic Van Steen, Jean Christophe Pizzolon, et al. 2014. "Titanium Dioxide, NM-100, NM-101, NM-102, NM-103, NM-104, NM-105: Characterisation and Physico- Chemical Properties." doi:10.2788/79554.

Rim, Kyung Taek, Soo Jin Kim, Se Wook Song, and Jung Sun Park. 2012. "Effect of Cerium Oxide Nanoparticles to Inflammation and Oxidative DNA Damages in H9c2 Cells." *Molecular and Cellular Toxicology* 8 (3): 271–80. doi:10.1007/s13273-012-0033-5.

Rim, Kyung Taek, Kwon Ho Koo, and Jung Sun Park. 2013. "Toxicological Evaluations of Rare Earths and Their Health Impacts to Workers: A Literature Review." *Safety and Health at Work* 4 (1). Elsevier Masson SAS: 12–26. doi:10.5491/SHAW.2013.4.1.12.

Santos, Joana. 2015. "Nanotoxicology: Study of Nanomaterials' Genotoxic Effects in Cell Lines."

Saquib, Quaiser, Abdulaziz A. Al-Khedhairy, Maqsood A Siddiqui, Faisal M. Abou-Tarboush, Ameer Azam, and Javed Musarrat. 2012. "Titanium Dioxide Nanoparticles Induced Cytotoxicity, Oxidative Stress and DNA Damage in Human Amnion Epithelial (WISH) Cells." *Toxicology in Vitro* 26 (2). Elsevier Ltd: 351–61. doi:10.1016/j.tiv.2011.12.011.

Sauer, Ursula G., Alexandra Aumann, Lan Ma-Hock, Robert Landsiedel, and Wendel Wohlleben. 2015. "Influence of Dispersive Agent on Nanomaterial Agglomeration and Implications for Biological Effects in Vivo or in Vitro." *Toxicology in Vitro* 29 (1). Elsevier Ltd: 182–86. doi:10.1016/j.tiv.2014.10.011.

Sayes, Christie M., Rajeev Wahi, Preetha A. Kurian, Yunping Liu, Jennifer L. West, Kevin D. Ausman, David B. Warheit, and Vicki L. Colvin. 2006. "Correlating Nanoscale Titania Structure with Toxicity: A Cytotoxicity and Inflammatory Response Study with Human Dermal Fibroblasts and Human Lung Epithelial Cells." *Toxicological Sciences* 92 (1): 174–85. doi:10.1093/toxsci/kfj197.

Schubert, David, Richard Dargusch, Joan Raitano, and Siu W. Chan. 2006. "Cerium and Yttrium Oxide Nanoparticles Are Neuroprotective." *Biochemical and Biophysical Research Communications* 342 (1): 86–91. doi:10.1016/j.bbrc.2006.01.129.

Shukla, Ritesh K., Vyom Sharma, Alok K. Pandey, Shashi Singh, Sarwat Sultana, and Alok Dhawan. 2011. “ROS-Mediated Genotoxicity Induced by Titanium Dioxide Nanoparticles in Human Epidermal Cells.” *Toxicology in Vitro* 25 (1). Elsevier Ltd: 231–41. doi:10.1016/j.tiv.2010.11.008.

Shukla, Ritesh K, Ashutosh Kumar, Deepak Gurbani, Alok K Pandey, Shashi Singh, and Alok Dhawan. 2013. “TiO 2 Nanoparticles Induce Oxidative DNA Damage and Apoptosis in Human Liver Cells.” *Nanotoxicology* 7 (1): 48–60. doi:10.3109/17435390.2011.629747.

Singh, Charanjeet, Steffi Friedrichs, Neil Gibson, Keld Alstrup Jensen, Heidi Goenaga Infante, David Carlander, and Kirsten Rasmussen. 2014. “Cerium Dioxide: Characterisation and Test Item Preparation.” *JRC Repository: NM-Series of Representative Manufactured Nanomaterials*. doi:10.2788/80330.

Singh, Narendra P., Michael T. McCoy, Raymond R. Tice, and Edward L. Schneider. 1988. “A Simple Technique for Quantitation of Low Levels of DNA Damage in Individual Cells.” *Experimental Cell Research* 175 (1): 184–91. doi:10.1016/0014-4827(88)90265-0.

Singh, Neenu, Bella Manshian, Gareth J S Jenkins, Sioned M. Griffiths, Paul M. Williams, Thierry G G Maffeis, Chris J. Wright, and Shareen H. Doak. 2009. “NanoGenotoxicology: The DNA Damaging Potential of Engineered Nanomaterials.” *Biomaterials* 30 (23–24). Elsevier Ltd: 3891–3914. doi:10.1016/j.biomaterials.2009.04.009.

Skocaj, Matej, Metka Filipic, Jana Petkovic, and Sasa Novak. 2011. “Titanium Dioxide in Our Everyday Life; Is It Safe?” *Radiology and Oncology* 45 (4): 227–47. doi:10.2478/v10019-011-0037-0.

Srinivas, A., P. Jaganmohan Rao, G. Selvam, P. Balakrishna Murthy, and P. Neelakanta Reddy. 2011. “Acute Inhalation Toxicity of Cerium Oxide Nanoparticles in Rats.” *Toxicology Letters* 205 (2). Elsevier Ireland Ltd: 105–15. doi:10.1016/j.toxlet.2011.05.1027.

Stepanenko, A.A., and V.V. Dmitrenko. 2015. “Pitfalls of the MTT Assay: Direct and off-Target Effects of Inhibitors Can Result in Over/underestimation of Cell Viability.” *Gene* 574 (2). Elsevier B.V.: 193–203. doi:10.1016/j.gene.2015.08.009.

Stone, Vicki, Helinor Johnston, and Roel P F Schins. 2009. “Development of in Vitro Systems for Nanotoxicology: Methodological Considerations.” *Critical Reviews in Toxicology* 39 (7): 613–26. doi:10.1080/10408440903120975.

Tang, Ying, Fude Wang, Chan Jin, Hao Liang, Xinhua Zhong, and Yongji Yang. 2013. “Mitochondrial Injury Induced by Nanosized Titanium Dioxide in A549 Cells and Rats.” *Environmental Toxicology and Pharmacology* 36 (1). Elsevier B.V.: 66–72. doi:10.1016/j.etap.2013.03.006.

Tavares, Ana M., Henriqueta Louro, Susana Antunes, Stephanie Quarr??, Sophie Simar, Pieter Jan De Temmerman, Eveline Verleysen, et al. 2014. “Genotoxicity Evaluation of Nanosized Titanium Dioxide, Synthetic Amorphous Silica and Multi-Walled Carbon Nanotubes in Human Lymphocytes.” *Toxicology in Vitro* 28 (1). Elsevier Ltd: 60–69. doi:10.1016/j.tiv.2013.06.009.

Terradas, Mariona, Marta Martín, Laura Tusell, and Anna Genescà. 2010. “Genetic Activities in Micronuclei: Is the DNA Entrapped in Micronuclei Lost for the Cell?” *Mutation Research - Reviews in Mutation Research* 705: 60–67. doi:10.1016/j.mrrev.2010.03.004.

Tice, R R, E Agurell, D Anderson, B Burlinson, a Hartmann, H Kobayashi, Y Miyamae, E Rojas, J C Ryu, and Y F Sasaki. 2000. “Single Cell Gel / Comet Assay : Guidelines for In Vitro and In Vivo

Genetic Toxicology Testing." *Environmental and Molecular Mutagenesis* 35 (3): 206–21. doi:10.1002/(sici)1098-2280(2000)35:3<206::aid-em8>3.0.co;2-j.

Truffault, Laurianne, Minh Tri Ta, Thierry Devers, Konstantin Konstantinov, Val??rie Harel, Cyriaque Simmonard, Caroline Andreazza, et al. 2010. "Application of Nanostructured Ca Doped CeO2 for Ultraviolet Filtration." *Materials Research Bulletin* 45 (5): 527–35. doi:10.1016/j.materresbull.2010.02.008.

Vallabani, N V Srikanth, Ritesh K Shukla, Dinesh Konka, Ashutosh Kumar, Sanjay Singh, and Alok Dhawan. 2014. "TiO2 Nanoparticles Induced Micronucleus Formation in Human Liver (HepG2) Cells : Comparison of Conventional and Flow Cytometry Based Methods" 7 (Suppl 1): 2013–14. doi:10.1186/1755-8166-7-S1-P79.

Van Koetsem, Frederik, Simon Verstraete, Paul Van der Meeren, and Gijs Du Laing. 2015. "Stability of Engineered Nanomaterials in Complex Aqueous Matrices: Settling Behaviour of CeO<inf>2</inf> Nanoparticles in Natural Surface Waters." *Environmental Research* 142. Elsevier: 207–14. doi:10.1016/j.envres.2015.06.028.

Verstraelen, Sandra, Sylvie Remy, Eudald Casals, Patrick De Boever, Hilda Witters, Antonietta Gatti, Victor Puntes, and Inge Nelissen. 2014. "Gene Expression Profiles Reveal Distinct Immunological Responses of Cobalt and Cerium Dioxide Nanoparticles in Two in Vitro Lung Epithelial Cell Models." *Toxicology Letters* 228 (3). Elsevier Ireland Ltd: 157–69. doi:10.1016/j.toxlet.2014.05.006.

Wang, Lili, Wenchao Ai, Yanwu Zhai, Haishan Li, Kebin Zhou, and Huiming Chen. 2015. "Effects of Nano-CeO2 with Different Nanocrystal Morphologies on Cytotoxicity in HepG2 Cells." *International Journal of Environmental Research and Public Health* 12 (9): 10806–19. doi:10.3390/ijerph120910806.

Wang, Yurong, Haiyan Cui, Jiaping Zhou, and Fengjuan Li. 2015. "Cytotoxicity , DNA Damage , and Apoptosis Induced by Titanium Dioxide Nanoparticles in Human Non-Small Cell Lung Cancer A549 Cells," 5519–30. doi:10.1007/s11356-014-3717-7.

Warheit, David B. 2008. "How Meaningful Are the Results of Nanotoxicity Studies in the Absence of Adequate Material Characterization?" *Toxicological Sciences* 101 (2): 183–85. doi:10.1093/toxsci/kfm279.

Weyermann, Jörg, Dirk Lochmann, and Andreas Zimmer. 2005. "A Practical Note on the Use of Cytotoxicity Assays." *International Journal of Pharmaceutics* 288 (2): 369–76. doi:10.1016/j.ijpharm.2004.09.018.

Xia, T., M. Kovochich, M. Liong, M. Schowalter, A. Rosenauer, B. Gilbert, J. I. Zink, a. E. Nel, and L. Mädler. 2009. "Comparison of the Mechanism of Toxicity of Zinc Oxide and Cerium Oxide Nanoparticles Based on Dissolution and Oxidative Stress Properties." *Chemie Ingenieur Technik* 81 (8): 1167–1167. doi:10.1002/cite.200950629.

Xie, Shao-Hua, Ai-Lin Liu, Yan-Yan Chen, Li Zhang, Hui-Juan Zhang, Bang-Xiong Jin, Wen-Hong Lu, Xiao-Yan Li, and Wen-Qing Lu. 2010. "DNA Damage and Oxidative Stress in Human Liver Cell L-02 Caused by Surface Water Extracts during Drinking Water Treatment in a Waterworks in China." *Environmental and Molecular Mutagenesis* 51 (3): 229–35. doi:10.1002/em.

Xu, Can, and Xiaogang Qu. 2014. “Cerium Oxide Nanoparticle: A Remarkably Versatile Rare Earth Nanomaterial for Biological Applications.” *NPG Asia Materials* 6 (3). Nature Publishing Group: e90. doi:10.1038/am.2013.88.

Z. Qiang, H Li, M. Tang, and P. Yue. 2013. “ZnO, TiO2, SiO2, and Al2O3 Nanoparticles-Induced Toxic Effects on Human Fetal Lung Fibroblasts.” *Biomedical and Environmental Sciences : BES* 26 (1): 23–31. doi:10.3967/0895.

8. ANNEXES

ANNEX I - DLS Analysis

Table I.1 - Results from DLS analysis for NM-212 in the culture medium for concentrations 3.2, 32 and 240 µg/mL at 0, 24, 48 hours and 7 days.

	Concentration 3.2 µg/mL		Concentration 32 µg/mL		Concentration 240 µg/mL	
Time	PdI±SD	Z Average±SD	PdI±SD	Z Average±SD	PdI±SD	Z Average±SD
0 hours	0.71±0.01	125.48±1.01	0.23±0.03	288.15±2.19	0.17±0.01	293.2±23.33
24 hours	0.3±0.01	169.4±24.32	0.23±0	241.6±32.24	0.18±0.04	258.05±19.16
48 hours	0.23	167.1	0.19	222	0.15	250.7
7 days	ND	ND	0.37	298.7	0.41	462.5

ND- not done.

Table I.2 - Results from DLS analysis for NM-101 in the culture medium for concentrations 3.2, 32 and 240 µg/mL at 0, 24, 48 hours and 7 days.

	Concentration 3.2 µg/mL		Concentration 32 µg/mL		Concentration 240 µg/mL	
Time	PdI±SD	Z Average±SD	PdI±SD	Z Average±SD	PdI±SD	Z Average±SD
0 hours	0.6±0.11	277.95±117.05	0.4285±0.08	534.55±237.65	0.32±0.06	499,9±5.7
24 hours	0.94	64.09	0.42	179.1	0.19	188.5
48 hours	0.22	165.1	0.23	197	0.16	187.2
7 days	0.16	169.5	0.12	194.2	0.14	163.3

Table I.3 - Results from DLS analysis for NM-100 in the culture medium for concentrations 3.2, 32 and 240 µg/mL at 0, 24, 48 hours and 7 days.

	Concentration 3.2 µg/mL		Concentration 32 µg/mL		Concentration 240 µg/mL	
Time	PdI±SD	Z Average±SD	PdI±SD	Z Average±SD	PdI±SD	Z Average±SD
0 hours	0.39±0.08	225.2±29.9	0.21±0	319.45±2.55	0.20±0.04	320.57±30.97
24 hours	0.475±0.10	255.8±37.8	0.25±0.03	317.15±56.55	0.14±0.01	246.5±3.6
48 hours	0.44	267.9	0.25	250.07	0.22	291.5
7 days	0.51	367.8	0.58	363.8	0.21	247.4

Table I.4 - Results from DLS analysis for NM-220 in the culture medium for concentrations 3.2, 32 and 240 µg/mL at 0, 24, 48 hours and 7 days.

	Concentration 3.2 µg/mL		Concentration 32 µg/mL		Concentration 240 µg/mL	
Time	PdI±SD	Z Average±SD	PdI±SD	Z Average±SD	PdI±SD	Z Average±SD
0 hours	0.63±0.08	26.62±2.32	0.58±0.0	88.94±1.6	0.2±0.02	138.51±0.09
24 hours	0.70±0.12	28.54±4.95	0.42±0.17	145.95±56.75	0.19±0.01	139.2±1.8
48 hours	0.56	23.52	0.6	90.57	0.18	136.9
7 days	0.97	39.29	0.6	111.1	0.22	117.5

ANNEX II- Cytotoxic Assays

Table II.1 - Viability results obtained from MTT assay for NM-212, NM-101, NM-100 and NM-220.

	NM-212	NM-101	NM-100	NM-220
NM Concentration (µg/cm^2)	Mean±SD	Mean±SD	Mean±SD	Mean±SD
0	100	100	100	100
1	91.94±6.64	107.06±11.47	103.71 ± 7.39	95.24 ± 10.32
3	90.12±7.08	106.31±19.72	98.19 ± 7.63	95.24 ± 2.45
10	103,30±3,96	108.13±12.98	91.35 ± 6.92	92.07 ± 11.93
30	94.95±16.03	97.91±8.41	93.14 ± 25.62	88.94 ± 9.61
75	102.12±7.37	92.41±10.51	95.16 ± 27.85	87.72 ± 27.75
100	93.75±18.70	87.85±11.56	97.82 ± 10.96	91.69 ± 16.56
SDS 0.01%	34.72±2.59	16.12*±21.20	5.24* ± 1..30	5.38* ± 0.99

*- Significantly different (p≤ 0.05) from the negative control (Mann- Whitney U test)

Table II.2 - Cellular proliferation study from clonogenic assay for NM-212.

	NM-212
NM Concentration (µg/cm^2)	Mean±SD
0	1±0.15
1	0.84±0.11
3	0.76±0.09
10	0.77±0.2
30	0.69±0.1*
75	0.63±0.21*
100	0.56±0.28*
MMC 0.00425 µg/mL	0.16±0.16**

*-Significantly different (p≤ 0.05) from the negative control (Post-Hoc testes from One-Way ANOVA test); **- Significantly different (p≤ 0.05) from the negative control (t-Student test).

Table II.3 - Replication indexes (RI and CBPI) obtained from CBMN assay for NM-212, NM-100 and NM-220.

	NM-212		NM-100		NM-220	
	Mean±SD	Mean±SD	Mean±SD	Mean±SD	Mean±SD	Mean±SD
NM Concentration (µg/cm^2)	CBPI	RI	CBPI	RI	CBPI	RI
0	1.96±1.83	100±0	1.91±0.02	100±0	1.87±0.00	100±0.00
1	1.95±0.84	97.83±7.74	1.86±0.01	93.65±1.47	1.80±0.01	92.09±0.86
3	1.9±1.41	92.82±2.54	1.89±0.02	97.90±1.75	1.81±0.00	92.72±0.46
10	1.94±0.5	96.87±5.58	1.86±0.01	94.47±0,77	1.82±0.02	94.33±2.18
30	1.93±7.94	96.36±3.17	1.84±0.01	91.73±1.1	1.73±0.03	84.36±3.09
75	1.95±8.43	97.59±2.61	NA	NA	1.75±0.02	85.44±2.81
100	1.99±0.03	102.6±3.31	NA	NA	1.73±0.00	83.34±0.36
MMC 0.3 µg/ml	1.37±0.01*	38.59±1.02*	1.45±0.01	49.21±1.01	1.46±0.02	52.37±2.52

*- Significantly different (p≤0.05) from the negative control (Mann-Whitney U test); NA- not applicable.

ANNEX III- Genotoxicity Assays

Table III.1 - Results from CBMN assay for NM-212, NM-100 and NM-220.

	MNBNC/1000 BC		
	NM-212	NM-100	NM-220
NM Concentration ($\mu g/cm^2$)	Mean±SD	Mean±SD	Mean±SD
0	2.49±1.29	2.00±2.83	1.00±0.00
1	1.25±1.26	1.50±2.12	3.00±2.00
3	2.25±1.50	1.00±0.00	1.50±1.50
10	2.00±1.83	0.50±0.71	2.00±1.00
30	1.98±0.84	0.00±0.00	2.50±1.50
75	1.00±1.41	NA	1.00±1.00
100	0.25±0.50*	NA	2.00±0.00
MMC 0.3 µg/mL	21.96±8.43*	12.50±12.02*	14.67±1.38*

*- Significantly different ($p \leq 0.05$) from the negative control (Fisher's Excat Test).

Table III.2 - Results from comet assay, after 3 hours of exposure, with and without FPG, for NM-212, NM-101, NM-100 and NM-220.

	NM-212		NM-101		NM-100		NM-220	
	No FPG	FPG	No FPG	FPG	No FPG	FPG	No FPG	FPG
NM Concentration (µg/cm^2)	Mean±SD	Mean±SD	Mean±SD	Mean±SD	Mean±SD	Mean±SD	Mean±SD	Mean±SD
0	7.74±2.78	6.62±4.74	6.82±2.75	9.47±1.95	6.04±0.10	11.36±0.19	4.89±0.75	7.96±0.29
1	10.20±4.62	9.88±4.88	11.39±5.11	15.67±11.29	12.91±0.59	14.15±3.5	8.62±1.72	9.67±4.64
3	9.01±7.5	7.74±2.94	9.35±2.8	14.37±4.68	12.06±2.50	22.83±0.64	9.52±1.73	14.07±5.67
10	9.07±4.23	10.01±6.15	8.69±1.2	8.05±6.38	16.02±1.27	24.51±0.51*	6.86±1.23	13.95±2.03
30	10.59±4.95	9.68±8.58	14.07±4.63	30.97±5.42*	25.06±1.15*	31.2±6.96*	8.71±1.24	7.64±2.11
75	10.06±8.51	17.42±11.46	19.83±5.95*	41.31±3.98*	33.06±1.20*	30.5±4.53*	7.72±1.45	11.66±3.38
100	11.62±5.9	18.09±18.14	17.73±3.59*	46.45±7.23*	40.85±6.27*	42.72±0.14*	6.94±1.95	9.66±1.18
EMS	11.71±12.55	43.65±3.33**	28.19±5.66**	49.66**±4.41	44.71±3.48**	67.86±4.36**	39.6±7.36*	60.37±18.71

*- Significantly different from the negative control (Post Hoc from One-Way ANOVA test). **- Significantly different from the negative control (t-Student test).

Table III. 3- Results from comet assay, after 3 hours of exposure, with and without FPG and respective significant *p* values (control versus treated culture) for NM-101 and NM-100.

	NM-101		NM-101		NM-100		NM-100	
	No FPG	FPG	No FPG	FPG	No FPG	FPG	No FPG	FPG
NM Concentration (µg/cm^2)	Mean±SD	Mean±SD	*p* value	*p* value	Mean±SD	Mean±SD	*p* value	*p* value
0	6.82±2.75	9.47±1.95	NS	NS	6.04±0.10	11.36±0.19	NS	NS
1	11.39±5.11	15.67±11.29	NS	NS	12.91±0.59	14.15±3.5	NS	NS
3	9.35±2.8	14.37±4.68	NS	NS	12.06±2.50	22.83±0.64	NS	NS
10	8.69±1.2	8.05±6.38	NS	NS	16.02±1.27	24.51±0.51	NS	*p*<0.001
30	14.07±4.63	30.97±5.42	NS	*p*<0.001	25.06±1.15	31.2±6.96	*p*<0.001	*p*<0.001
75	19.83±5.95	41.31±3.98	*p*=0.003	*p*<0.001	33.06±1.20	30.5±4.53	*p*<0.001	*p*<0.001
100	17.73±3.59	46.45±7.23	*p*=0.014	*p*<0.001	40.85±6.27	42.72±0.14	*p*<0.001	*p*<0.001
EMS	28.19±5.66	49.66±4.41	*p*=0.001	*p*=0.064	44.71±3.48	67.86±4.36	*p*<0.001	*p*=0.001

NS- Concentrations without significant *p* values.

Table III.4 - Results from comet assay, after 24 hours of exposure, with and without FPG, for NM-212, NM-101, NM-100 and NM-220.

	NM-212		NM-101		NM-100		NM-220	
	No FPG	FPG	No FPG	FPG	No FPG	FPG	No FPG	FPG
NM Concentration (µg/cm^2)	Mean±SD	Mean±SD	Mean±SD	Mean±SD	Mean±SD	Mean±SD	Mean±SD	Mean±SD
0	7.38±4.43	5.87±3	6.17±2.93	11.13±1.21	6.42±2.4	8.55±1.34	6.77±1.05	8.97±1.31
1	10.55±4.47	8.46±1.31	7.25±3.2	13.02±8.53	11.16±4.63	12.04±1.44	11.74±1.92	11.03±1.83
3	6.04±2.48	9.05±4.72	7.69±1.46	11.83±5.05	11.62±0.64	12.78±2.32	11.31±6.92	13.55±2.87
10	9.69±4.72	9.2±4.98	9.02±4.12	13.66±6.12	18.11±3.09*	26.06±4.28*	12.31±2.39	18.98±4.17
30	12.89±7.81	8.82±4.72	12.15±2.79	28.17±6.12*	26.68±3.99*	30.95±2.18*	6.21±1.3	15.18±2.57
75	10.59±6.35	7.87±3.13	15.68±1.34*	39.46±5.5*	32.48±4.16*	36.63±4.89*	12.84±2.46	10.99±1.82
100	14.57±3.51	7.51±0.56	27.45±4.27*	39.13±8.42*	36.79±3.2*	38.11±7.68*	13.63±1.56	12.9±5.84
EMS	19,98**±6	37.83**±11.09	28.06±4.76**	49.66±4.41**	39.93±4.66**	67.86±4.36**	34.24±1.85	59.78±11.05

*- Significantly different from the negative control (Post Hoc from One-Way ANOVA test). **- Significantly different from the negative control (t-Student test)

Table III. 5- Results from comet assay, after 24 hours of exposure, with and without FPG and respective significant *p* values (control versus treated cultures) for NM-101 and NM-100.

	NM-101		NM-101		NM-100		NM-100	
	No FPG	FPG	No FPG	FPG	No FPG	FPG	No FPG	FPG
NM Concentration (µg/cm^2)	Mean±SD	Mean±SD	*p* value	*p* value	Mean±SD	Mean±SD	*p* value	*p* value
0	6.17±2.93	11.13±1.21	NS	NS	6.42±2.4	8.55±1.34	NS	NS
1	7.25±3.2	13.02±8.53	NS	NS	11.16±4.63	12.04±1.44	NS	NS
3	7.69±1.46	11.83±5.05	NS	NS	11.62±0.64	12.78±2.32	NS	NS
10	9.02±4.12	13.66±6.12	NS	NS	18.11±3.09	26.06±4.28	*p*=0.001	*p*<0.001
30	12.15±2.79	28.17±6.12	NS	*p*=0.012	26.68±3.99	30.95±2.18	*p*<0.001	*p*<0.001
75	15.68±1.34	39.46±5.5	*p*=0.004	*p*<0.001	32.48±4.16	36.63±4.89	*p*<0.001	*p*<0.001
100	27.45±4.27	39.13±8.42	*p*<0.001	*p*<0.001	36.79±3.2	38.11±7.68	*p*<0.001	*p*<0.001
EMS	28.06±4.76	49.66±4.41	*p*<0.001	*p*=0.003	39.93±4.66	67.86±4.36	*p*<0.001	*p*<0.001

NS- Concentrations without significant *p* values.

ANNEX IV- Clonogenic Assay

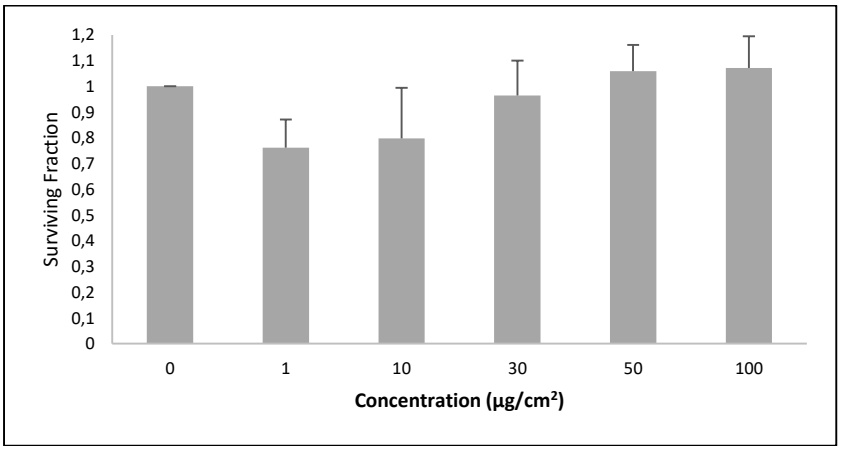

Figure IV. 1- Results of the clonogenic assay after 7 days cells exposure to NM-100.

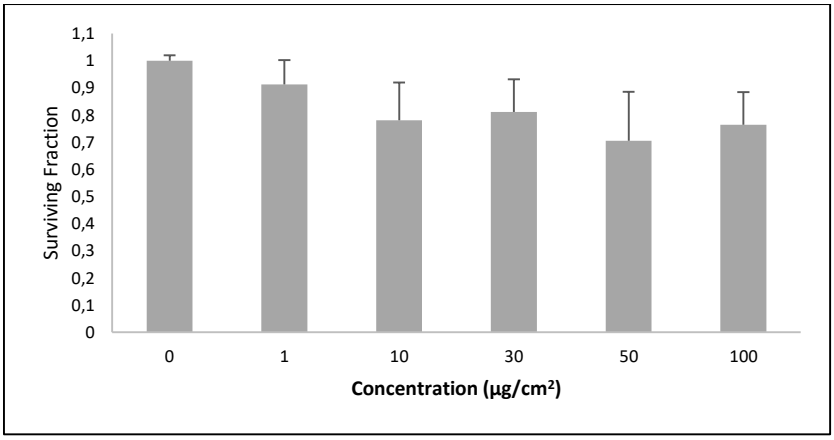

Figure IV. 2- Results of the clonogenic assay after 7 days cells exposure to NM-101 (Santos (2015)).